Self-Healing Strain Sensor for Biomedical Applications

Engr. Zubair Ibrahim

Registration No. 30-FET-PHDEE-F19

Supervisor: Dr. Gul Hassan

A dissertation submitted to IIUI in partial
Fulfillment of the requirements for the degree of

DOCTOR OF PHILOSOPHY (Ph.D)

Department of Electrical and Computer Engineering Faculty
of Engineering and Technology
INTERNATIONAL ISLAMIC UNIVERSITY, ISLAMABAD

2025

Copyright©2025 by Engr.Zubair Ibrahim

All rights are reserved. No section of this thesis under production by copyright pointed may be reproduced, copied, utilized and replicated in any form. Reproduction distributed and copy of this thesis in any form (Electronic or Mechanical media or Photocopying) is not allowed without approval of author.

DEDICATED TO

This thesis is dedicated to my great Almighty Allah which give me Strength, Skill, mind's power and healthy life, also to my Holy prophet Hazrat Muhammad (PBUH), Ehle-Bait, his Companions and his followers, My respected parents, My beloved wife, My sisters, My brother, My teachers and My friends who give me encouragement and advices for complication of my thesis work.

Acceptance by the Viva Voce Committee

Title of thesis Self-Healing Strain Sensor for Biomedical Applications

Name of Student Engr.Zubair Ibrahim

Registration No. 30-FET-PHDEE-F19

Accepted by the Faculty/Department of Electrical and Computer Engineering Faculty of Engineering and Technology INTERNATIONAL ISLAMIC UNIVERSITY ISLAMABAD, in partial fulfillment of the requirements for the Doctor of Philosophy Degree in Electrical Engineering with specialization in Advance Electronics.

Viva Voce committee

_____

Dean

_____

Chairman/Director/Head

_____

External Examiner

_____

Supervisor

(Day, Month, 2025)

ABSTRACT

This thesis investigates the development of wearable, self-healing strain sensors using two alternative fabrication techniques: hydrogel-based synthesis and inkjet printing. Each technique makes use of various composite materials and polymers. This study presents a novel strain sensor made of a polyurethane (PU) substrate combined with magnetic iron oxide nanoparticles (MIONPs) and silver flakes to address significant issues in existing strain sensor technologies, including low sensitivity, poor durability, and limited healing efficiency. With its high gauge factor of 271.4 at 35% strain, magnetic sensitivity of 0.0049 T^{-1}, and self-healing efficiency of 96.6% within 24 hours, the inkjet-printed sensor enhances its use in biomedical devices and soft robotics. The sensor is perfect for human motion detection because of its mobility, excellent skin adhesion, PU encapsulation that resists humidity, and moderate aging rate. Advanced methods like scanning electron microscopy (SEM) are used to completely evaluate mechanical and electrical properties, and testing is carried out utilizing a professional graded DIY testing setup. A self-supporting three-dimensional structure is created in the second phase using a hydrogel-based fabrication technique that combines copper electrodes, deposited via magnetron sputtering over the cross-linked polymeric network comprising of polyvinyl alcohol (PVA), Irgacure, glycerin, phosphoric acid (H_3 PO_4), and deionized water. Significant stretchability, self-adhesion, and electrical sensitivity are provided by this hydrogel-based sensor; SEM and EDS investigations show a homogeneous porous architecture that is essential for conductivity and flexibility. The sensor, which was developed by physical and chemical cross-linking, exhibits reliable performance and can sustain 100 stretching-releasing cycles with a strain limit of 110%. Electrical tests confirm a reliable inverse strain-current relationship, while LED glow tests validate a self-healing efficiency of 94%. The sensor's capacity for real-time monitoring is further supported by its response and recovery times of 600 ms and 730 ms, respectively. All things considered, this work marks a major advancement in the rapidly growing field of strain sensors that are flexible and self-healing. Recent developments in wearable sensing technologies have highlighted the need for gadgets that can withstand repeated mechanical stress and extended use in addition to being extremely sensitive and flexible. Conventional strain sensors frequently have restricted stretchability, low durability, and an inability to self-repair, which limits their practical use, particularly in biomedical monitoring and human–machine interfaces. By creating sensors with exceptional strain sensitivity, high healing efficiency, and outstanding mechanical robustness, our research overcomes such constraints. Faster recovery, increased flexibility, and more dependable signal

responsiveness are ensured by the incorporation of innovative materials including self-healing hydrogels and magnetic iron oxide nanoparticles. These developments could thereby significantly increase the functionality and longevity of wearable technology used for rehabilitation, motion tracking, and medical diagnostics. This technology establishes the groundwork for a new generation of intelligent, flexible sensors that meet the expanding needs of remote and personalized healthcare systems by merging multifunctionality with long-term stability.

PUBLICATIONS

- **Ibrahim, Z.,** Hassan, G., Alatawi, A. A., Alwageed, H. S., & Asif, A. (2025). Development of wearable self-healable strain sensor utilizing Nano-composite materials for advanced sensing applications. (**Journal of Materials Science: Material in Electronics) (Impact Factor:2.8)** DOI: 10.1007/s10854-024-14144-5

- **Ibrahim, Z.,** Asif, A., Hassan, G., & Shuja, A. (2025). Fabrication of UV-curable and self-adhesive strain sensor based on 2-hydroxy-4′-(2-hydroxyethoxy)-2-methylpropiophenone and PVA composite for biomedical applications.(**Sensors and Actuators A: Physical)(Impact Factor: 4.2)** DOI: 10.1016/j.sna.2025.116754

- Alam, S., Asif, A., Bibi, M., Hassan, G., Shuja, A., Shah, I., & **Ibrahim, Z.** (2025). Fabrication of Self-healing Strain Sensor Based on AgNWs and Fe_2O_3 Nanocomposite on Engineered Polyurethane Substrate. (**Journal of Materials Science & Processing: Applied Physics A) (Impact Factor:2.5)** DOI: 10.1007/s00339-025-08438-6

- Asif, A., Bibi, M., Hassan, G., Shuja, A., Ahmad, H., Alam, S., & **Ibrahim, Z.** (2024). Highly sensitive strain sensor based on ZnO nanofiber mat for medical applications. (**Journal of Materials Science: Material in Electronics) (Impact Factor:2.8)** DOI:10.1007/s10854-024-12964-z

ACKNOWLEDGEMENTS

In the name of Allah (SWT), the most merciful and the greatest benefactor, I am thankful to Allah Almighty for giving me the courage and showing me the path so that I can complete my research. I am truly indebted to my worthy supervisor Associate Prof. Dr. Gul Hassan, for his guidance, constant support, and knowledge feedback that gave me the hope and pathway to complete my research phase. His level of commitment towards research and wisdom has been an inspiration for me and others. I would like to extend my gratitude to the Centre of Advanced Electronics & Photo-Voltaic Engineering, its research associates and supporting staff especially Research Associate Engr. Arfa Asif, Research Associate Shah fahad, Research Associate Shoaib Alam and all the supporting members of CAEPE for their wonderful cooperation and technical supports throughout my research phase, for their profound cooperation and help throughout my research phase. My almighty Allah gives me this opportunity in the field of science as a part of my job is to find and discover in the field of science.

Engr. Zubair Ibrahim

TABLE OF CONTENTS

LIST OF TABLES

LIST OF FIGURES

LIST OF ABBREVIATIONS

TENGS	Harvesting Turboelectric Nano Generators
ITRS	International Technology Road Map of Semi-conductor
Fe_2O_3	Ferric Oxide
UF	Urea formaldehyde
ECG	Electro Cardio Graphy
CNTs	Carbon Nano Tubes
PDMS	Polydimethylsiloxanes
TPU	Thermoplastic Polyurethane
PEDOT	Poly (3, 4-ethylenedioxythiophene)
PSS	Polystyrene sulfonate
PDA	Polydopamine
CNFs	Cellulose Nano fibers
GN	Grephene Nano Complexes
GF	Gauge Factor
Zn	Zinc
MCNT	Multi-walled Carbon Nanotubes
PPy	Polypyrrole
RGO	Reduced Graphene Oxide
LED	Light Emitting Diode
NBR	Nitrile Butadiene Rubber
CB	Carbon Black
CNF	Cellulose nanofibril
PDA	Polydopamine
GI	Glycerol
Eg	Ethylene Glycol
DA	Diels Alder
PANI	Polyaniline
MPa	Mega Pascal
AAC	Crosslinking acrylic acid
FeNWs	Iron Nanowires
TA	Tannic Acid
PAA	Polyacrylic acid
TP	Tea Polyphenol
AA	Acrylic acid
PVP	Polyvinylpyrrolidone
WP	Wheat Protein
EG	Ethylene Glycol
CaCl	Calcium Chloride
$NaCO_3$	Sodium Carbonate
DNH	Double Network Hydrogel
AMPS	Acrylamido methylpropanesulfonic acid
ATR-FTIR	Attenuated Total Reflectance Fourier-Transform Infrared

B-PVA	Borax-Polyvinyl alcohol
kC	k- Carrageenan
Ag	Silver
H	Magnetic Field
E	Young's Modulus
Q	Volume of inkjet
A	Area of the droplet
V	Velocity of the droplet
D	Diameter of the droplet
F	Force
ms	Millisecond
DAPU	Diels-Alder Adducts
CFs	Carbon Fibers
NR	Natural Rubber
EVA	Ethylene-vinyl acetate
DLP	Digital light Processing
DIW	Direct Link Writing
PVA	Polyvinyl alcohol
PENGs	Piezoelectric Nano generators
TENGs	Turboelectric Nano generators
PSIW	Piezo Self-powered instantaneous wireless
PTUM	Polythiocurethane microspheres
CPCs	Conductive Polymer Composites
NaCl	Sodium chloride
CVD	Chemical Vapour Deposition
PVD	Plasma Vapour Deposition
SEM	Scanning Electron Microscopy
IV	Current Voltage
XRD	X-Ray Diffraction
APCVD	Atmospheric chemical Vapour Deposition
LPCVD	Low Pressure Chemical Vapour Deposition
UV	Ultra-Violet
MIONPs	Magnetic Iron Oxide Nanoparticles
FESD	Flexible Energy Storage Device
EHD	Electrohydrodynamic
AgNWs	Silver Nanowires
P	Polyols
I	Isocyanate
BD	Butanediol
pH	Potential of Hydrogen
RPM	Revolution per minute
GO	Graphene Oxide
$C_3H_8O_3$	Glycerin
FTIR	Fourier transform Infrared Spectroscopy
TGA	Thermogravimetric Analysis
EIS	Electrochemical Impedance Spectroscope

H_3PO_4	Phosphoric acid
R	Resistance
T	Tensile Strength
L	Length
EDS	Energy Dispersive X-rays Spectroscopy
PMMLI	Predictive Model and Machine Learning Integration

LIST OF SYMBOLS

$\boldsymbol{\beta 0}$	Signifying the interception
$\boldsymbol{\beta 1}$	The Slope of the Regression Line
$\boldsymbol{\sigma}$	Surface tension/tensile stress
$\boldsymbol{\rho}$	Density of the Ink
$\boldsymbol{\varepsilon}$	Strain
$\mathbf{S_m}$	Magnetic Sensitivity
$\boldsymbol{\eta}$	Efficiency
$\boldsymbol{\Delta}$	Change
$\boldsymbol{\Omega}$	Ohm
$\boldsymbol{\mu}$	Micro

FORWARDING SHEET

The Thesis entitled Self-Healing Strain Sensor for Biomedical Applications.

Submitted by Dr.Gul Hassan in partial fulfillment of PH.D degree in Electrical Engineering.

Engr.Zubair Ibrahim has been completed under my guidance and supervision. I am satisfied with the quality of the student's research work and allow him to submit this thesis for further process of as per IIU rules and regulations.

Date: _____ Signature: _____

Name: _____

Chapter 1

Introduction

Wearable devices are increasingly becoming more popular because they are light weight, meeting consumer's demands as traditional rigid electronics did not meet these applications of wearable devices [1]. These ultra-stretchable flexible devices have very high potential in healthcare applications specifically biomedical implants [2]. CNT Carbon based nano materials, elastomers and conductive polymers made these devices perform well even under significant deformation, improving the electric conductivity, longevity and mechanical properties [3]. Even in the field of Energy Harvesting Triboelectric Nano Generators [TENGS] and Piezo electric generators, as energy harvesters are used in smart wearables. Electrical energy is produced to power wearable electronics from mechanical energy of environmental sources and body movements for consumer's demands. Stylish and discrete wearables are made when these ultra-stretchable and flexible devices are integrated into items like jewelry, clothing, smart shoes and fitness apparels [4, 5]. Through ultra-feedback systems these flexible and ultra-stretchable wearable devices have improved the user's experience. These are also used in gaming, fitness tracking, balancing and navigation [6].

1.1. Scaling of Technology

Traditional rigid electronics devices are not compatible in the flexible arena, while flexible and ultrastrechable devices are comfortable to wear by any part of human body including areas that experience discomfort and movements [7]. These Flexible devices in field of biomedical wearable applications are durable, long lasting, and long running [8]. Self-healing properties of these devices made them automatically repair their microcracks and damage, so devices remain operational in challenging environment [9]. These devices provide continuous monitoring of healthcare parameters without invasion [10]. Biocompatibility of these devices made them comfortable when worn against skin [11]. These biomedical devices can interact with smart phones or other devices to send data to healthcare providers for health monitoring [12].

Semiconductor electronics technology is moving towards even smaller scales to surmount the barriers of physical dimensions imposed on us by nature, new approaches in the form of improved and strengthen materials, new structure and other such potential routines are realized and studied upon. This gives the world a new

hope to realize the "More than Moore's" approach owing to the even tougher requirements posed by International Technology Road Map of Semiconductor (ITRS). In the past, we have witnessed that the scalability was addressed using new and improved technologies and techniques [13]. The "More than Moore's" approach is the idea behind this industry shift as shown in Fig 1.1.

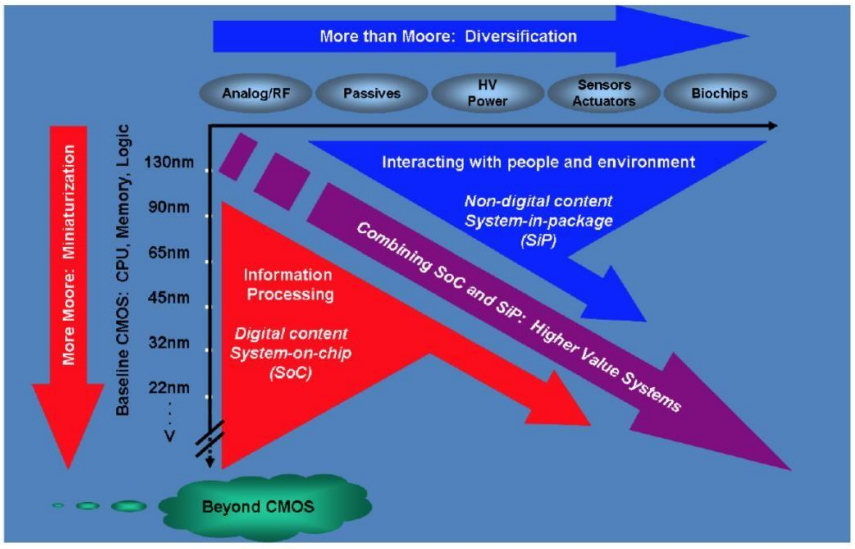

Fig 1.1: More than Moore's approach [13]

Moore's law is very important for communication systems, mobile phone, computer system etc. In Moore's law the size of the IC is improved, increasing energy power, increasing efficiency and decreasing the size. Now Moore's law is saturated, and latest technology moves toward organic materials which have excellent properties of flexibility, stretchability, self-healing and require lesser time for fabrication of the device with absolute temperature. This is also desirable to meet up with the International Technology Roadmap of semiconductors (ITRS) node requirements [14].

1.2. Self-healing Devices

These sensors have flexibility, stretchability, self-healing, biocompatibility, high sensitivity and durability [15]. Self-healing hydrogels are used for wearable sensors in biomedical applications as hydrogel is soft, biocompatible and self-repairing when damaged [16]. Polymers are utilized in biosensors as they combine stretchability and self-healing properties along with mechanical and electronic durability [17].

Elastomeric matrices such as PDMS, silicon, improve the flexibility and also stretchability of these sensors when combine with CNTs [18]. So, in field of implantable devices these self-healing flexible and ultrastrechable devices combine the properties including conductivity and ability to recover which make them ideal biosensors and neurostimulators [19]. These self-healing devices follow self-healing mechanisms due to dynamic covalent chemistry of cross linked networks which allow material to heal at room temperature or with minor heating after damage. Super molecular material like polymer based on hydrogen bonding, pi-pi interaction or host guest chemistry are also used for self-healing applications. Recently ionic and conductive hydrogels are also designed to be stretchable and self-healing [20].

Fig 1.2: Illustration of ultra-stretchable strain sensor properties [21]

A strain gauge is a sensor used to determine the strain of the object where resistance changes with respect to the applied force as shown in Fig 1.2. The deformation of the object occurs in the shape when we applied external force. When the object deforms either it becomes broader and narrower, or it becomes longer and shorter, changing its current carrying characteristics. Then strain of object is measured with respect to resistance change from end to end. The magnitude of induced stress can be determined by some factors that affect the stain gauge accuracy, i.e. temperature affects the resistance, high temperature less resistance, low temperature high resistance. This problem can be overcome by using ISO-elastic alloy during making of strain gauge [21, 22].

1.3. Industry of Ultra-stretchable and Self-Healing Wearable Sensors

The family of these sensors should be bio compatible, must have self-healing, and compatibility with the modern industry. Their application in the field of health monitoring, like heart rate and respiration muscles activity, help to manage chronic diseases like diabetes, neurological disorder and cardiac conditions. In the field of rehabilitation these strain sensors capture motion for rehabilitation therapies to provide data on joint analysis, muscles contraction and joints angles. Sensors improve the functionality of prosthetics when used in prosthetic limbs to provide feedback [23]. Smart sensors are used as energy harvesters and power solutions as electric signals produce from mechanical movement [24]. In modern wearable electronic industry, they are used as AR augmented reality and VR virtual reality of wearable Electronics [25]. These sensors have wide industry in biomedical application, as these meet consumer demand for stylish and discrete wearable sensors [26].

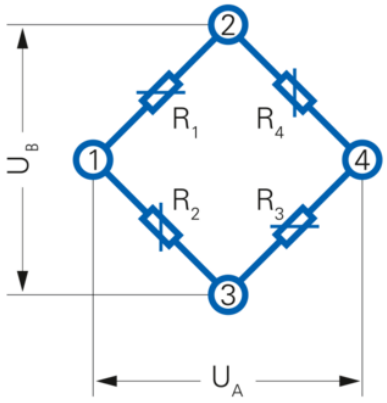

Fig 1.3: Illustration of Wheatstone bridge using Ultra-stretchable strain sensor [27]

In the Fig 1.3 above, strain sensor is used in Wheatstone bridge because of its high sensitivity due to which it measures dynamic strain and low frequency in typical four wire strain gauge. Output voltages are achieved by changing the resistance for this purpose. Wheat stone bridge is used for better results [27].

Strain sensors have achieved great interest in the research community in the past decades. Structural changes detection that occurs in surroundings, human body's internal activities and damage detection are main application [28]. Continuous monitoring of its status is required to prevent failure of structure, and damage in real

time. Conventional sensors (metal and semiconductor strain gauges) have high sensitivity and can be low in cost. However, they have disadvantages, and most of such strain sensors have fixed direction, thus in a particular direction strain can only be measured. These sensors have low resolution at the nanoscale and cannot be used in structural materials as shown in Fig 1.4 [29].

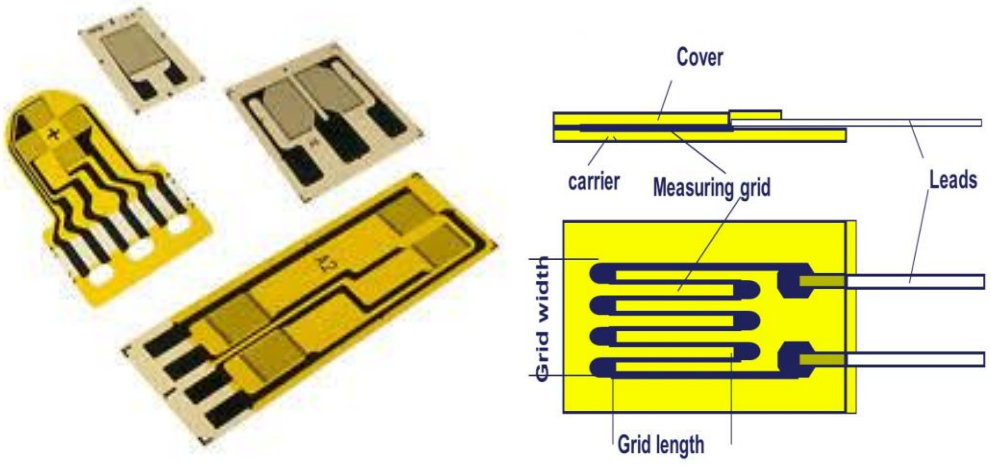

Fig 1.4: Semiconductor strain gauges [30]

To manufacture a smart strain sensor as shown in Fig 1.5 researchers are in search of materials that can show optimal flexibility and reaction to a minimal-applied strain. To make the device flexible and stretchable based on nano materials such as Graphene [30], conductive polymer [31], micro fluidic [32], nanotubes [33], nanoparticles [34] and nanowires [35] used along with PDMS, or polyurethane substrate effectively. There is now a growing demand in developing flexible and stretchable smart strain sensors to play a vital role in intelligent robotics, biomedical, wearable Electronics and safety equipment [36-38].

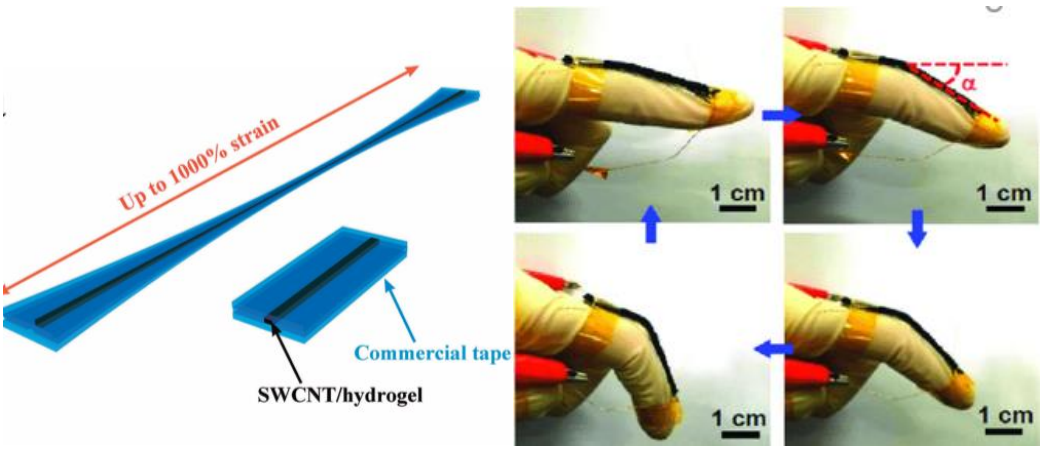

Fig 1.5: Strain sensor detected human finger motion [37]

1.4. Application of Strain Sensor

Strain sensors are becoming an integrated part of today's wearable systems. As they are used in textile, inkjet printers, physiological signals monitoring [39]. Strain sensors can be resistive or capacitive depending on changes that occur in electrical resistance or dielectric properties when stress is applied. To improve self-healing property of these self-healing strain sensor polymers (polyurethane etc.) are used in these sensors for stretchability and for electrical conductivity CNT carbon-based material are used in addition. Elastomeric matrices such as PDMS, silicon, and TPU improve flexibility and stretchability, and hydrogels give softness and improve self-healing after damage [40]. These sensors are used in the following field of biomedical: Health monitoring activities like muscles action, joint motion, Respiratory Rate, diagnostics, rehabilitation and fitness tracking are the main fields of health monitoring in which self-healing flexible strain sensors are main building blocks. Biomedical movements to adjust prosthetics for better performance is another field of application of these sensors as these sensors are crucial for prosthetics. Smart clothing [wearable clothes contain these sensors] are used to provide monitoring of healthcare, physiological signal and muscles activity [41].

However, such stretchable strain sensors which have structural problems give poor electric signal response. This structural problem occurs due to inefficient interfacial bonding between polymer matrix and conductive fillers. It is very difficult to restore the mechanical scratches of conductive network. Therefore, due to the instability of output signal the whole component breaks up. To improve their performance, an ideal

strain sensor is required to incorporate repeatable self-healing properties while preserving their sensitivity after cutting and healing cycles. Self-healing property of the strain sensor improved stability for a long time due to which the durability increased, and the cost of strain sensor automatically reduced.

Different types of self-healing mechanism have been reported over the last few decades which include intrinsic and extrinsic self-healing. Intrinsic self-healing adventures the chemical and physical crosslinking (reversible covalent and non-covalent bond) [42]. External healing agent triggers the extrinsic self-healing inserted into the material in the form of vascular or capsule network [43]. The container is broken when the crack is formed automatically at the time the healing agent releases and heals the container. Thus, to provide the required self-healing capabilities for strain sensors a mass of reversible bonds e.g. hydrogen bonding [44], dynamic covalent bond [45], π−π stacking [46], and host−guest recognition [47] is targeted. In literature many researchers explain various underlying and classifications of chemistries. Now after comprehensive literature review in self-healing materials it is realized that self-healing property is very useful in electrical applications. Therefore, the self-healing sensors with conductive links-based optoelectronics and transistor applications are as shown in Fig 1.6 [48-50].

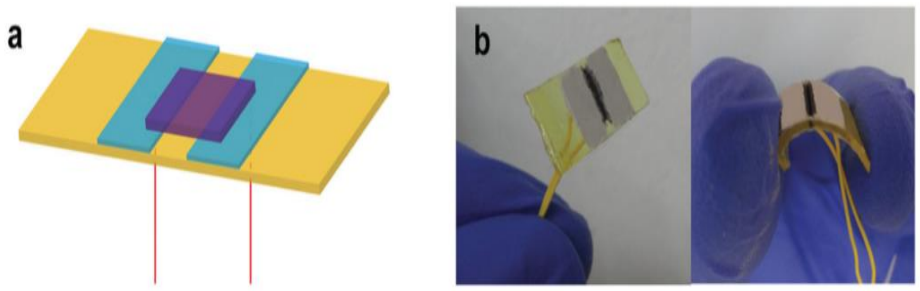

Fig 1.6: In figure a) and b) Yellowish transparent Chemi resistor with self-healing property consist of two electrodes [49]

Mostly, In the strain sensor reversible bonding exists due to which it has very good self-healing but having poor mechanical properties due to weak bonds [51]. Therefore, to improve its mechanical properties covalently cross-linked network is used. Now after improvement in mechanical properties the rate of self-healing is improved [52]. Recently all these improvements in self-healing materials remain a great challenge to balance the conflict between self-healing and mechanical properties. Table 1.1 shows

the comparison of studies related to highly stretchable and self-healing strain sensors in electro-conductive hydrogel matrices.

Table 1.1: Highly Stretchable and Self-Healing Strain Sensors in Electro-Conductive Hydrogel Matrices

Author	Techniques	Methodology	Results	Limitations
[53]	Synergistic triple network hydrogel	Synthesis of skin-inspired strain sensors	High sensitivity, human-motion detection	Biological compatibility concerns
[54]	3D printing	Intrinsically self-healing sensor production	High stretchability, 3D print compatibility	-
[55]	Gellan gum hybrid hydrogel	Development of stretchable strain sensors	High stretchability, self-healing properties	Limited material versatility
[56]	Cellulose nanofibers-reinforced polyacrylic acid	Preparation of self-healing strain sensors	Enhanced durability, self-repair capability	Limited stretchability in certain conditions
[57]	Conductive hydrogel fibers	Creation of stretchable conductive materials	Triboelectric energy harvesting capabilities	Limited scalability for industrial use
[58]	Review of conductive hydrogels	Analysis of conductive hydrogel properties	Comprehensive overview of hydrogel types	Lack of specific experimental data
[59]	Polyaniline nanoparticle-based hydrogels	Self-healing flexible sensor development	Fast self-healing, sensitivity	-
[60]	MXene-composited hydrogel	Flexible strain sensor fabrication	High stretchability, sensitivity, durability	-
[61]	Nanocellulose-supported graphene hydrogels	Fabrication of highly stretchable sensors	Enhanced flexibility, self-healing ability	Potential degradation over time

1.5. Analysis and Issues

Self-healing flexible ultrastrechable wearable sensors face several challenges and issues in their application and development. Limitation of materials is the main issue as traditional materials may lack significant self-healing and high stretchability needed for the best performance. So, advanced materials like hydrogels are required for better performance [62]. Self-healing efficiency of materials is also a barrier in practical application, as self-healing capabilities of many materials are not rapid. Durability of these sensors while maintaining sensitivity and functionality is also a big challenge [63]. These sensors provide accurate data on a lab scale, but its real-world performance is affected by variability in sensitivity, especially in health monitoring. In existing

electronic system incorporation of these self-healing sensors is complex so addressing compatibility with current wearable technologies is needed [64].

1.6. Problem Statement

In recent years, for future wearable electronic devices like health care, human motion detection, intelligent robotics, wearable electronics and safety equipment in a flexible strain sensor is good choice. However, inefficient interfacial bonding between polymer matrix and conductive fillers is cause of poor mechanical stability and electric signal reliabilities under repeated stretching and bending is problem with such flexible strain sensors. In addition, under repeated deformation mechanical fractures and micro cracks occurred very easily in strain sensors. Structure damage is caused by low performance of sensors, and this damage may cause functionality loss. Self-healing property in strain sensor is very important to have a long life and will not lose its functionality after damage. Nano-composite containing materials such as Fe_2O_3,Graphene and Urea formaldehyde (UF) on self-healable polyurethane substrate having Ag-flacks is introduced to produce high stretchable and cut-able strain sensor. Excellent high mechanical fracture recovery, high sensitivity and self-healing property is achieved. New opportunities in smart wearable biomedical applications are opened for this designed ultra-stretchable self-healing device.

1.7. Objectives of Research

This work could be helpful for Flexible and Ultra-Stretchable wearable smart electronic devices industry to provide efficient work assessment for process engineers. The foundations and possible solutions to the stated problem will be carried out as follows approaches.

- **Objective 1:** The detailed study of self-healing and flexible strain sensors will be investigated by using different fundamental theories, graphs and equations. Which will be very useful for biomedical application. Flexible and good quality materials will be used for fabrication of strain sensors.
- **Objective 2:** The best technique is adopted for fabrication of proposed senior i-e (Inkjet printer) to get the best outcomes. The proposed strain sensor efficiency in this research will be durable and will sustain their characteristics for a long time period.

1.8. Significance of Research

Stain sensor stability is the key feature to get the ideal and optimized output results. However, mechanical damage, harsh environment and scratches reduce the durability of the strain sensors. To meet their practical applications, self-healing and mechanical strength are vital to play role in highly stretchable and sensitive strain sensors. However, it is still a great challenge to match these two key performance parameters. It would be imperative to improve the stretchability and strain limits of the device, and to work on gauge factors, response time and interact with the medical applications like human body movement detections, progressive reports on pulse rates should be tackled and can be challenging as well. Through our persistent efforts, we sincerely hope to firmly hold this opportunity to fill up the process and technique specific blanks to devise our own core technology/process strategy for the next generation energy harvesting systems.

1.9. Methodology of Research

The methodology of the current research is as follows.

- Literature review of strain sensors based on Ag-flacks, Fe_2O_3 self-healing material and UV curable polyurethane substrate.
- Current-Voltage analysis
- Producing scanning electron microscope (SEM) based analysis to cross verify the polymer chain linkages.
- Stretching, bending and healing after cutting can be observed.

Different footsteps are followed for designing, fabrication and characterization of proposed wearable flexible self-healing strain sensor their comprehensive infrastructure is illustrated in Fig 1.7.

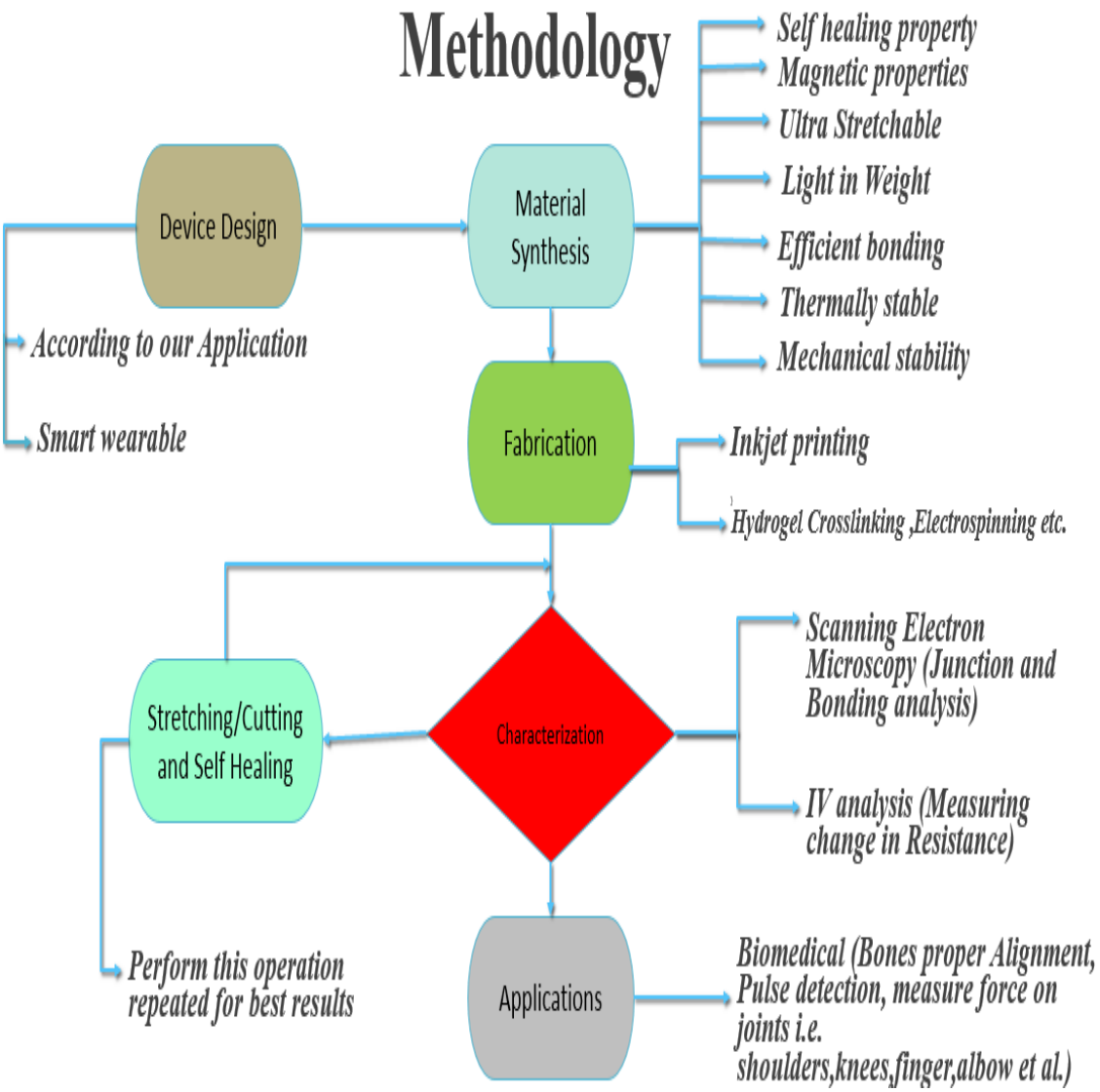

Fig 1.7: Overall research flow chart from the device's synthesis to fabrication and respective characterization

1.10. Thesis outline

Thesis is divided into 6 chapters symmetrically. An elementary introduction which explains the formation, fabrication and characterization of stretchable strain sensors for application (wearable biomedical) is provided in chapter 1. Chapter 2 explains and clarifies the background theory which is related to ideas that are important for the basis of the current research problem. Literature review about the fabrication and characteristics of stretchable self-healing for biomedical application of strain sensors are enlisted in chapter 3. Chapter 4 gives information about the experimental technique used in this work. In chapter 5, a proposed strain sensor based on Fe_2O_3, Ag flakes (nanocomposite material), and PU materials is comprehensively experimented, and

their respective results are properly defined. Similarly, the Polyvinyl Alcohol (PVA) Hydrogel-Based Strain Sensor experimental work and outcomes are deeply explained. In chapter 6, the futuristic approach about strain sensors technology has been projected.

Chapter 2

Background Theory

2.1. Introduction

This chapter explains the main sensing and self-healing mechanism of the self-healing strain sensor. The chapter explains the factors that affect the design, optimization of the factors and problems faced during the development of these self-healing strain sensors.

2.2. Sensing Mechanism

Self-healing strain sensors monitor mechanical deformation i.e. stretching, bending or compressing and can repair itself after damage as shown in Fig 2.1 [65]. These sensors work by detecting deformation in a material. The main mechanisms include (Piezo resistive mechanism) in which the strain produces changes in electrical resistance. Another sensing mechanism in which the strain changes the area or distance between two electrodes is called capacitive sensing [67]. Optical sensing is a mechanism in which strain produces changes in optical properties like reflection and light absorption. Stretching and compression of conductive composite that changes conductive path which changes electrical properties of sensors [66].

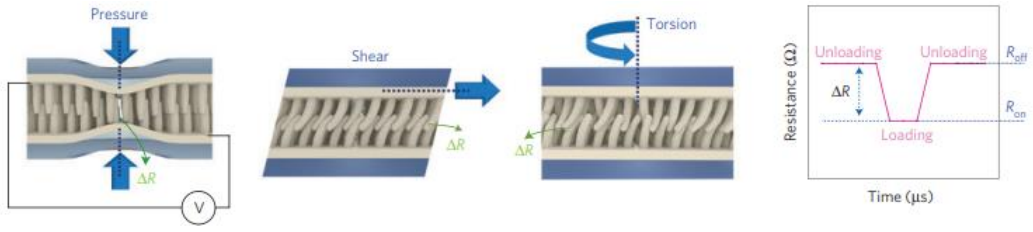

Fig 2.1: Strain sensor sensing mechanism [71]

2.3. Self-Healing Mechanism

The self-healing mechanisms of strain sensors are due to polymeric material with dynamic covalent bonds that enables the material to heal cracks and breaks when pressure or heat is applied [66]. Microcapsules containing healing agents are embedded in these sensors which show healing properties when sensor got damage [68]. Super molecular chemistry makes interaction reversible and allows sensors to achieve their original properties after damage as illustrated in Fig 2.2[69]. The shape memory polymer matrix can return its original shape after deformation [70].

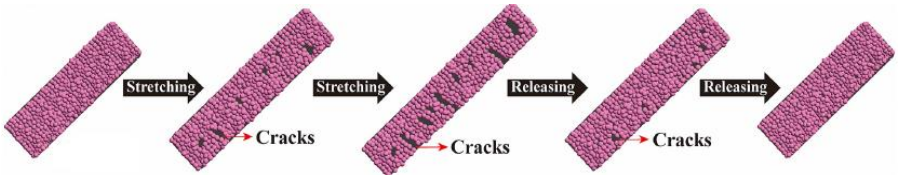

Fig 2.2: Self-healing mechanism of strain sensor

2.4. Flexibility of Strain Sensor

Self-healing strain sensors have high flexibility and tunable mechanical properties like toughness, stretchability and resilience as shown in Fig 2.3. These properties combined with self-healing enhance the functionality and durability of the sensor [72]. Self-healing strain sensors are made from composites materials that maintain their mechanical properties after damage which made them suitable for wearable health monitoring devices. The development of these flexible sensors supports the growth of flexible electronics [73]. Sensors having a combination of self-healing properties with flexibility and softness in structure make it reliable even while working under challenging environment [74].

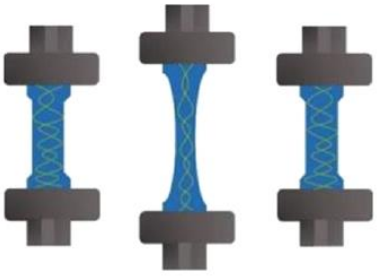

Fig 2.3: Flexible and stretchable strain sensor

2.5. Durability and Longevity

Strain sensors having self-healing properties recover from minor cracks and mechanical damage that make them durable and increase their lifespan [75]. Self-healing property reduces the need for frequent replacement and repairing as show in Fig 2.4. Longevity made it important in long term monitoring application [76].

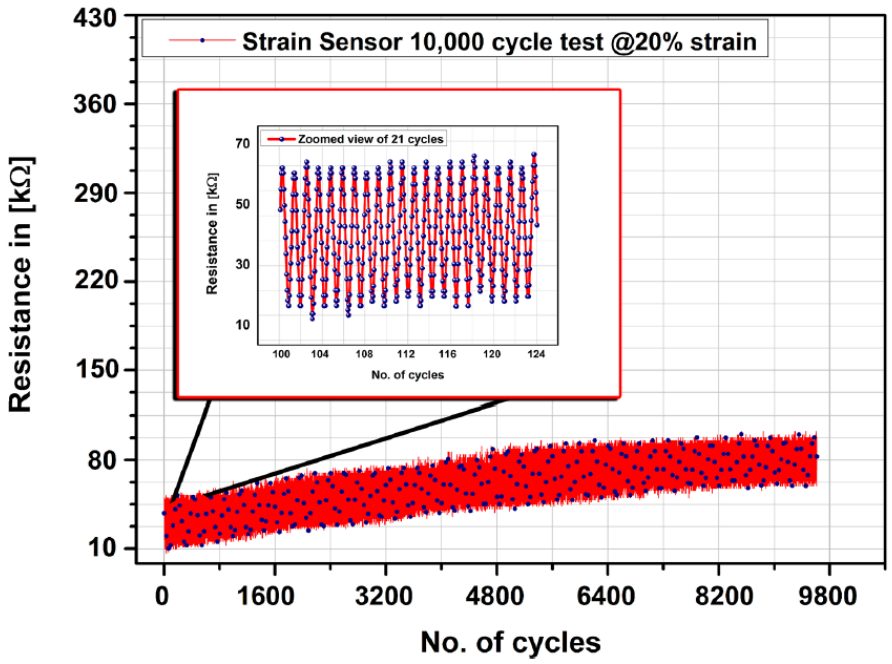

Fig 2.4: Strain sensor retain longevity and durability over 10000 cycles at 20% Strain [77]

2.6. Different Types of Strain Sensor

The common type of self-healing strain sensors with details are as given below:

2.6.1. Polymeric self-Healing Strain Sensors

Polymer based self-healing strain sensors contain polymer with dynamic covalent bonds or super molecular interaction having flexibility and self-healing properties as shown in Fig 2.5 [78]. Healing material is filled within microcapsules of polyurethane used in self-healing strain sensors. These healing materials are released when sensors get damaged [84]. Super molecular polymers network is used with hydrogen bonding or pi-pi stacking which provides flexibility and self-healing property to the sensor [78].

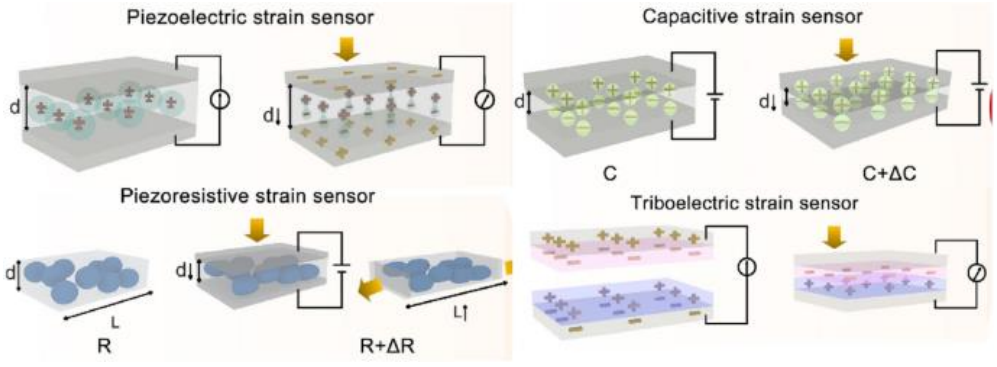

Fig 2.5: Polymer based strain sensor used in various formation [78]

2.6.2. Self-Healing Strain Sensor Based on Hydrogel

Hydrogel based self-healing strain sensors are another type of strain sensors in which hydrogel is present giving it stretchability, flexibility and self-healing after mechanical damage. Dynamic physical networks such as hydrogen bonds or ionic interaction give self-healing property to these hydrogel-based sensors as shown in Fig 2.6 [79]. Hydrogels with ions are used which allows them to conduct electricity. Ionic network of these hydrogel self-heal using water absorption and reorganization. PVA hydrogel when exposed to humidity and water self-heal itself [85]. Chitosan based hydrogels are used in sensors which recover their mechanical and electrical properties after rehydration [85].

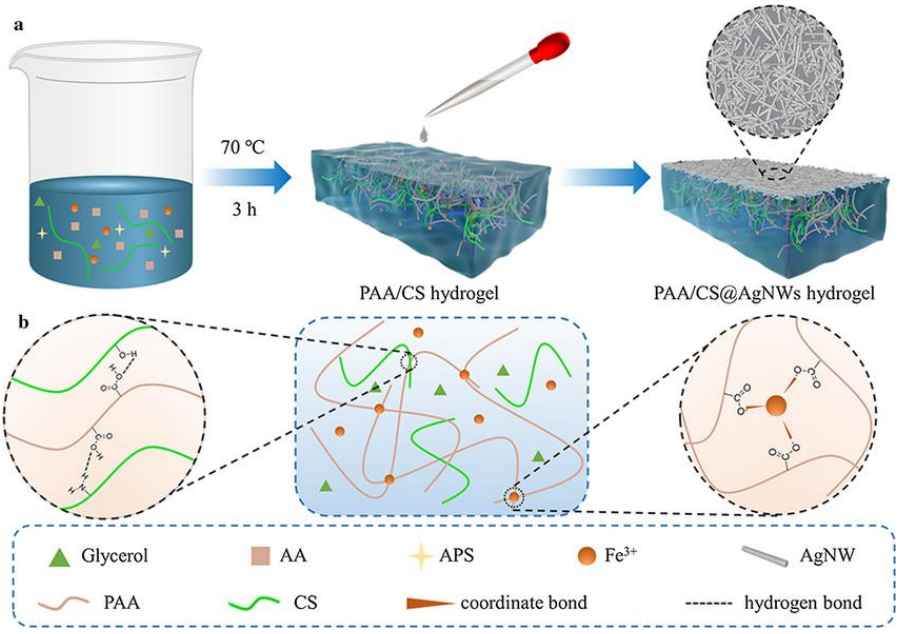

Fig 2.6: Hydrogel based strain sensor [79]

2.6.3. Self-Healing Strain Sensor Based on Carbon

Conductive carbon-based self-healing sensors have CNTs, graphene or carbon black due to excellent mechanical strength and electrical conductivity [80]. Graphene oxide based self-healing sensor restores its electrical conductivity after damage by using light or heat to trigger a chemical reaction between healing agent and graphene oxide as shown in Fig 2.7 [80].

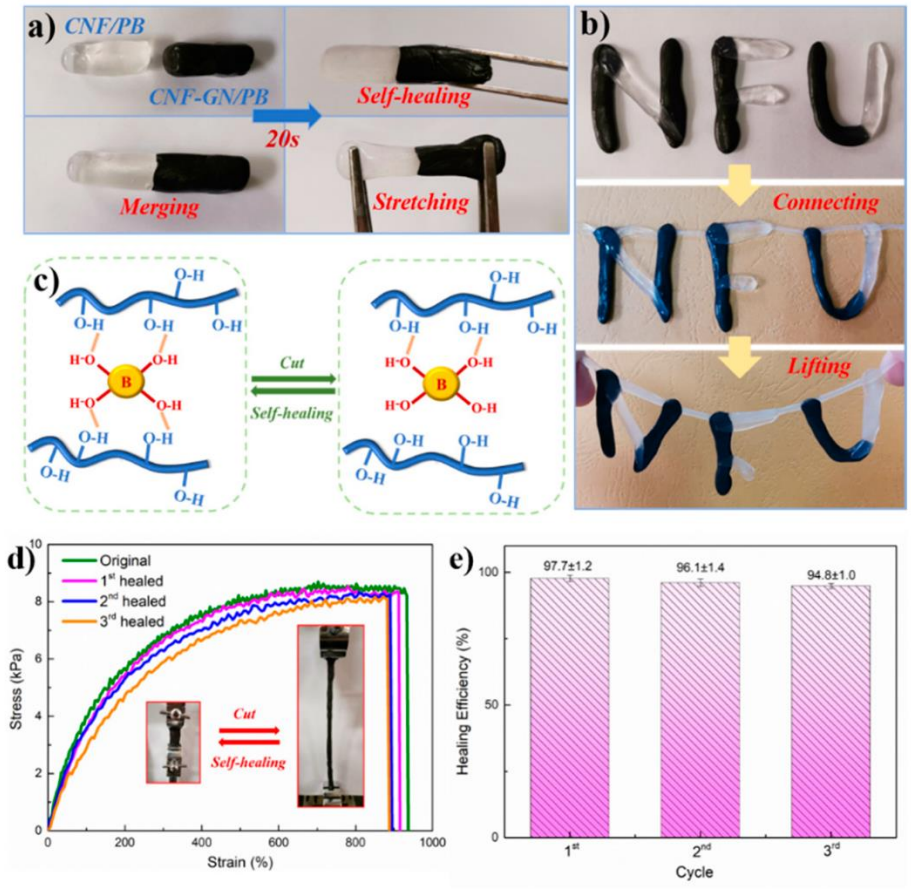

Fig 2.7: Graphene oxide based strain sensor [80]

2.6.4. Self-Healing Strain Sensor Based on Ionic Liquids

Ionic liquids (salts present in liquid state) at room temperature are also used in sensors called ionic liquid based self-healing strain sensors as shown in Fig 2.8. These ionic liquids are used along with polymers which give self-healing property and ionic conductivity and are suitable for flexible strain sensors [81]. Polymer /ionic liquid composite-based sensor when exposed to mechanical damage recovers its functionality by reorganizing the polymer chain and ionic interaction [81].

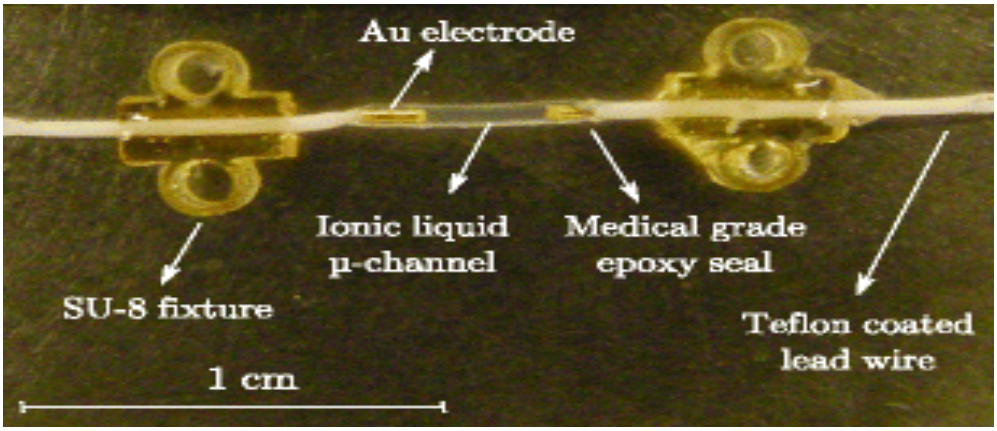

Fig 2.8: Ionic liquid based strain sensor [81]

2.6.5. Self-Healing Strain Sensor Based on Metals

Metal oxides or metallic strain sensors are another type of strain sensors as shown in Fig 2.9. Metals are combined with flexible substrates which provide stretchability and self-healing properties and have the capability to restore its functionality under critical condition [82]. Metal polymer hybrid-based sensor when expose to heat or external stimulus the silver and copper embedded in flexible polymer matrix will self-heal the sensor [82].

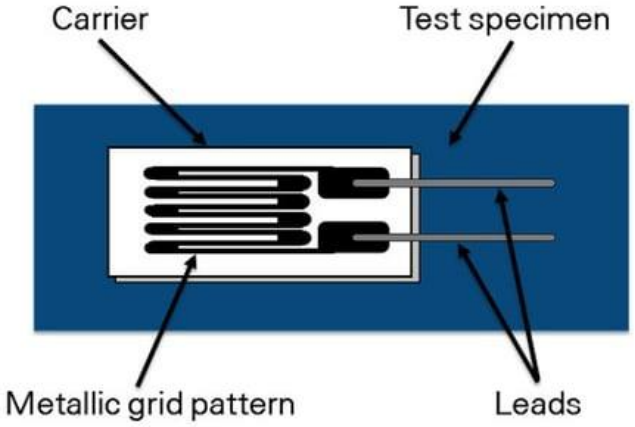

Fig 2.9: Metal based strain sensor [82]

2.6.6. Self-Healing Strain Sensor with Microcapsules or Vascular Network

Microcapsules or Vascular Network are used in strain sensors creating another type of sensor as shown in Fig 2.10. These materials have healing agents like liquid rubber or adhesives which are released and give self-healing action when experiencing mechanical damage [83]. Microcapsules containing self-healing/polymer healing agent filled which got released after damage [83].

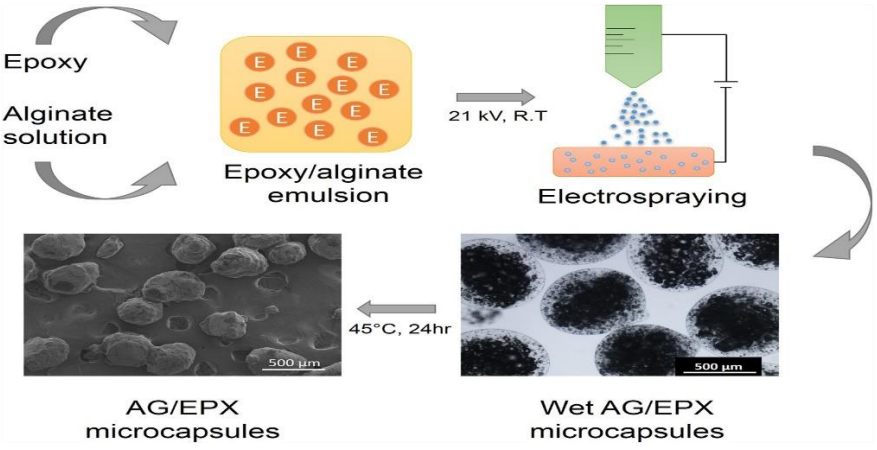

Fig 2.10: Microcapsules technology based strain sensor [83]

2.7. Electrodes for Self-Healing Strain Sensor

Strain sensors contain electrodes that are stretchable, conductive and durable [86]. Electrodes are used to retrieve the electrical and mechanical properties of proposed strain sensor as shown in Fig 2.11.

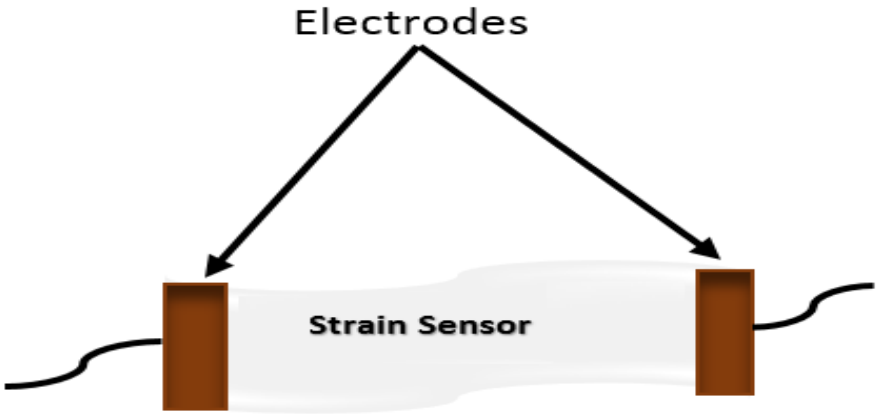

Fig 2.11: Electrodes of strain sensor

The following materials are used for fabrication of electrodes in self-healable strain sensor. Conductive polymers such as poly3-4ethylenedioxy-thiophene polystyrene sulfate (PEDOT) are used in electrodes of strain sensors due to flexible nature and easy fabrication [87].The next material used as electrodes are carbon-based materials as these materials combine their mechanical properties with high electrical conductivity [88].Metal nanowires like silver nanowires and copper nanowires creating mesh like structures are also used in electrodes of strain sensors as they are extremely stretchable and highly conductive [89].The recent material used as an electrode of strain sensors are hydrogels made from polyaniline or Polypyrrole because these create self-healing ultrastretchable electrodes [90].

2.8. Modeling and Design of Strain Sensor

In strain sensor to improve the performance for various applications, modeling and design of these sensors is important. The key parameters in design of strain sensors are as given below:

2.8.1. Range

The maximum strain that sensors measure unless its response fails is called ‘range’ that is expressed as a percentage of strain [90].The strain sensor show different ranges according to their respective strain.

Strain=ΔL/L ×100%

Where:

- ΔL is the change in length
- L is the original length

Strain ranges of strain sensor varies from moderately stretchable upto 50% strain to highly stretchable 50 to 100%strain and more advanced ultra-stretchable over 100% strain as shown in Fig 2.12. Optimization strategy used is extend the range of strain sensors composite materials with large elastic moduli are used, for example optical fiber with resistive strain gauge increases the range of these sensors [91].

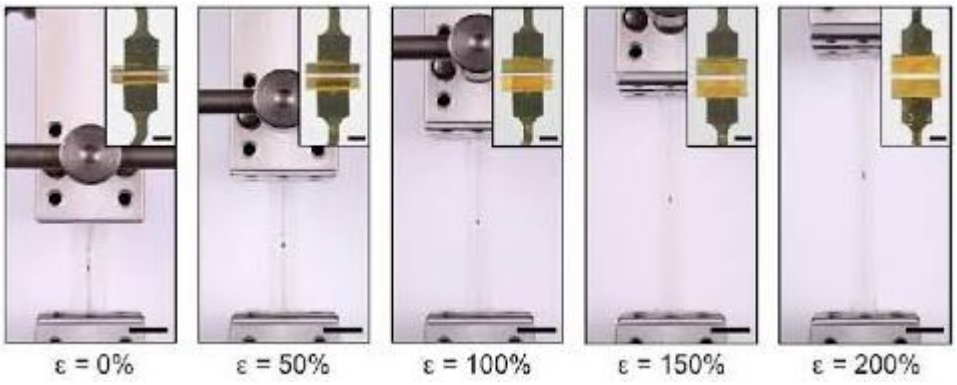

Fig 2.12: Range of strain sensor at different strain level [90]

2.8.2. Sensitivity

The ratio of electrical output to the change in input is called sensitivity [92].The sensitivity is typically measured using gauge factor. In the Fig 2.13 illustrated various ranges of gauge factor.

Gauge Factor (GF) =ΔR/R / ε

Where:

- ΔR = change in resistance
- R = original resistance
- ε = strain (relative change in length)

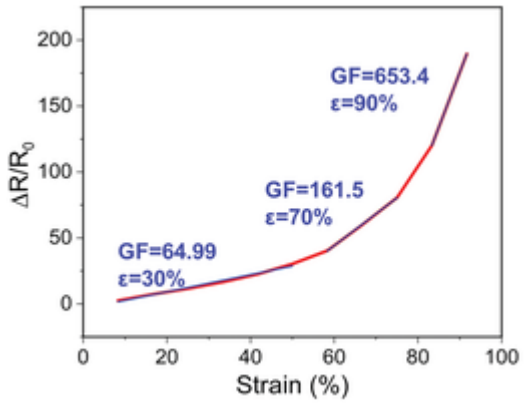

Fig 2.13: Gauge factor (GF) define sensor sensitivity [92]

Sensitivity of strain sensor is mainly affected by composition of materials, sensor geometry, microstructure and strechability so, to improve the sensitivity of sensors the material with high resistive nature such as carbon nanotubes, conductive polymers, graphene are used. Other factors increasing the sensitivity are strain gauges with optimal geometries [92].

2.8.3. Linearity

The correspondence of sensors output to applied strain in measurement range [93].The accuracy, predictability, and easy interpretation of readings depends upon linearity of sensor. The straight line relationship between strain and output signal is shown in perfect linear sensor in Fig 2.14.

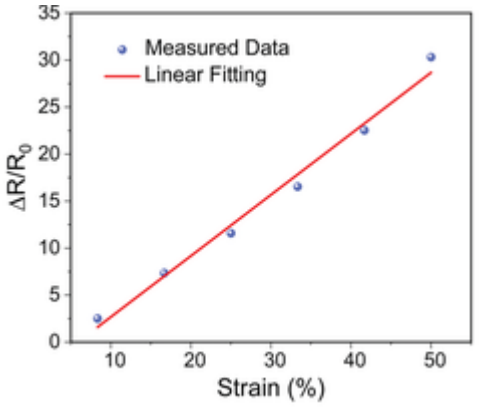

Fig 2.14: Linearity in stretchable strain sensor [93]

Factors that affect the linearity of sensor are properties of material, structure of sensor and fabrication techniques. Optimization strategy for linearity is to *use* material with consistent electrical and mechanical properties over wide range of strain and circuit compensation method increase the linearity [93].

2.8.4. Resolution

The smallest measurable strain that sensor measures is called resolution [94]. Sensor with high resolution can measure very small changes in strain [94].It is typically expressed in units like % strain as shown in Fig 2.15.

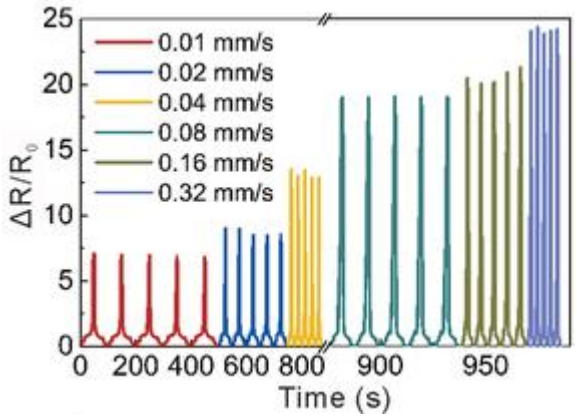

Fig 2.15: Resolution of strain sensor [94]

High resolution of strain sensors are important because of its application in medical field like heart monitoring and in soft robotics. Resolution of sensor is affected by factors like sensitivity, Gauge factor, Noise level and Rate of sampling. To improve the resolution of sensor nanomaterials are used due to their high surface area and excellent conductivity [94].

2.8.5. Hysteresis

The strain sensors output differs depending on the increase and decrease of strain is shown in Fig 2.16.Then hysteresis occurs for accurate measurement and should be minimum [95].The hysteresis of strain sensor are of three types Mechanical hysteresis, Electrical Hysteresis, and Contact Hysteresis. Hysteresis affect cyclic and dynamic application of sensor reduced its accuracy and repeatability.so therefore optimization is important for sensors application. Hysteresis is optimized by choosing material with minimum plastic deformation and minimum internal friction and viscoelasticity to reduce hysteresis [95].

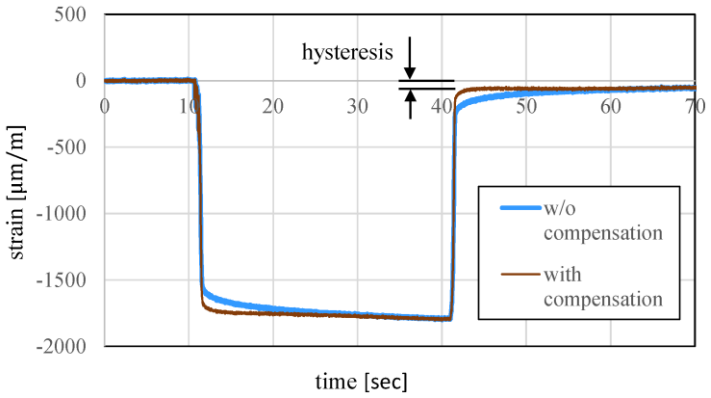

Fig 2.16: Hysteresis of strain sensor [95]

2.8.6. Power Consumption

For battery operated strain sensor low power consumption is needed as shown in Fig 2.17.The power consumption rate is typically in microwatt to milliwatt depending on Microcontroller used and sampling rate [96].Material with minimum power needed for proper operation or sensor with low power consumption electronics is needed to reduce power consumption [96].

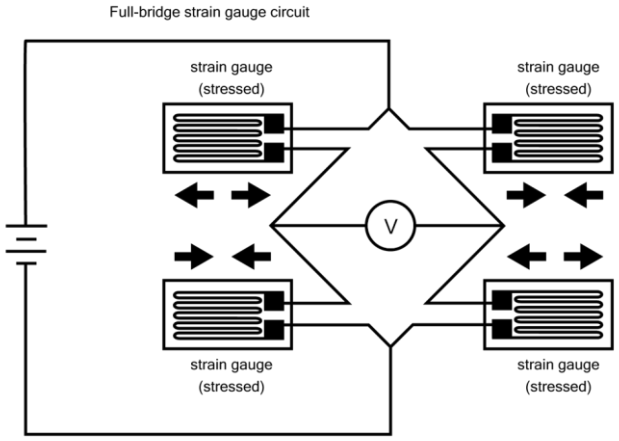

Fig 2.17: Biased strain sensor [96]

2.8.7. Temperature Sensitivity

Temperature can affect the performance of strain sensors as shown in Fig 2.18. Strain sensors are sensitive to temperature changes and produce errors in measurement [97].Temperature mainly effect the material resistance, thermal expansion challenging accuracy and signal ambiguity of sensor. Using material with low thermal expansion coefficient to correctly measure temperature drift and improve accuracy and using dual sensing designs and signal processing to optimize temperature sensitivity [97].

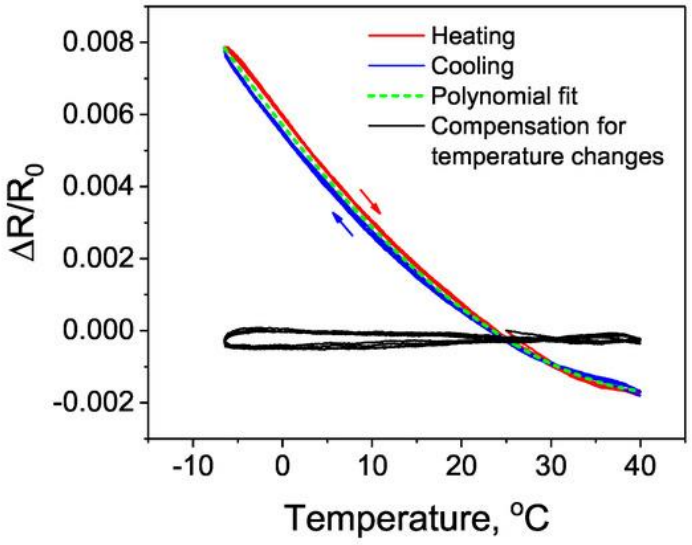

Fig 2.18: Temperature sensitivity of strain sensor [97]

2.8.8. Response Time

The time strain sensor takes to reach a stable output after a strain is applied is called response time [98]. Effectiveness of strain sensor is dependent on response time as shown in Fig 2.19. Factors affecting Response time are Properties of material, sensing mechanism, geometry, and Environmental conditions. Lightweight materials reduce the mechanical inertia, increase frequency and faster up response time of strain sensor [98].

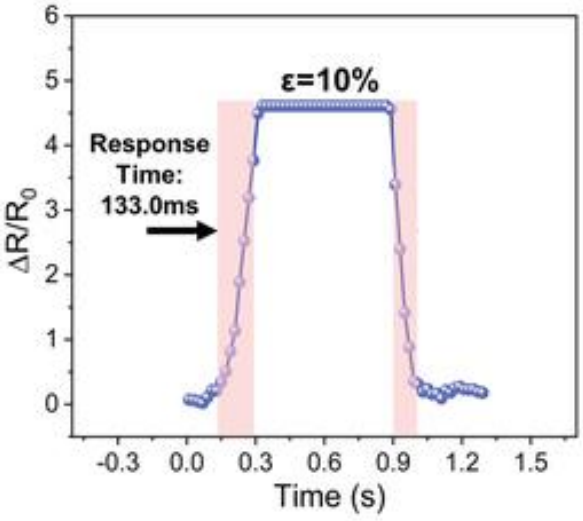

Fig 2.19: Response time of strain sensor [98]

2.9. Design Methods

The following factors play a vital role in the designing of self-healing strain sensors, the details of which are as follows:

- Material with high young modulus and low hysteresis are selected for precise measurement of strain sensors. Nano materials improve performance of strain sensors [99].
- The ability of strain sensor depends upon its Geometry. Multilayer design or composite structure improves performance of strain sensors because thinner and longer material used can lead to failure after excessive strain [100].
- Microcontrollers can enhance sensor performance by enabling noise filtration, real time data processing and Calibration [101].
- 3D Printing, microfabrication and nanolithography like advanced fabrication method improve precision of strain sensor with tailored properties and complex geometries [102].

2.10. Defects of Self-Healing Strain Sensor

Researchers face a lot of challenges while developing and using strain sensors due to structural defects, some of these defects are following.

- Sensors heal themselves after damage, but sometimes the healing process takes a lot of time and is not immediate or in some cases self-healing efficiency is limited as material may not fully recover itself after damage [103].
- Inconsistency in healing occurs when the mechanical and electrical properties of healed region change after healing. Malfunctioning may result in variability of healing across different regions of material. So, healing of physical damage may not be uniform which leads to inconsistency [104].
- Lifetime of sensor reduces because material may lose its ability of self-repair with time and repeated cycles of damage and healing. The structure integrity and function of the sensor is disturbed with repeated self-healing cycles [105].
- Integration of self-healing material with flexible base effect the performance of the sensor. The self-healing process is negatively affected by elastic deformation required for flexibility. So, under strain or stretching the self-healing mechanism may not function properly [106].

- Harmful chemicals are released during healing process of self-healing sensors based on material like polymer or other solvents. Toxic material which could pose health and safety risk when released during healing process [107].
- Self-healing material needed for flexible strain sensors are complex and expensive. Commercial viability of material used is limited by special technique and synthesis associated cost. Self-healing composite and polymers are expensive raw materials and manufacturing of these sensors also increase the cost [108].
- Environmental conditions such as high humidity, temperature fluctuation or exposure to chemical effect the performance of a strain sensor. The self-healing property is compromised under harsh conditions which limit the sensor functionality [109].

2.11. Summary

The self-healing strain sensor follows different types of sensing mechanism like change in resistance, change in the distance between electrodes or change in optical properties with strain. These sensors have flexibility, durability and self-healing properties. These sensors are of various types depending upon the base material. Electrodes of different types like polymer, carbon containing compounds, nanowires and hydrogel etc. are used in these sensors. Basically, self-healing strain sensors have two types of healing, intrinsic healing and extrinsic healing. In intrinsic healing the healing process is done by chemical bonding recovery (i.e. hydrogen bonding) and in extrinsic healing metallic liquids are used to fill the cracks and retrain the self-healing property of the sensor. To design and model these sensors different parameters are optimized like Range, sensitivity, linearity, hysteresis, power consumption and geometrical design etc. Some challenges faced by the researchers when developing these sensors are healing speed and efficiency inconsistency in results, decreasing durability, compatibility and high cost.

Chapter 3

Literature Review

In this chapter extensive literature related to different fabrication techniques of wearable flexible self-healing strain sensors are reviewed. Where different characterizations of wearable flexible self-healing strain sensors are explored by using different materials. This section gives an overview of past developments in wearable flexible self-healing strain sensors.

3.1. Fabrication through Hydrogel Method

Skin inspired ultra-flexible and stretchable strain sensors consist of a tough layer, adhesive layer and conductive hydrogel. Polymerization of nuclei is used to prepare bilayers in ultra-flexible wearable hydrogel-based strain sensors driven adhesive hydrogels on surface of conductive tough hydrogels that are cross-linked by hydrophobic association. Skin inspired example is shown in Fig 3.1[110].

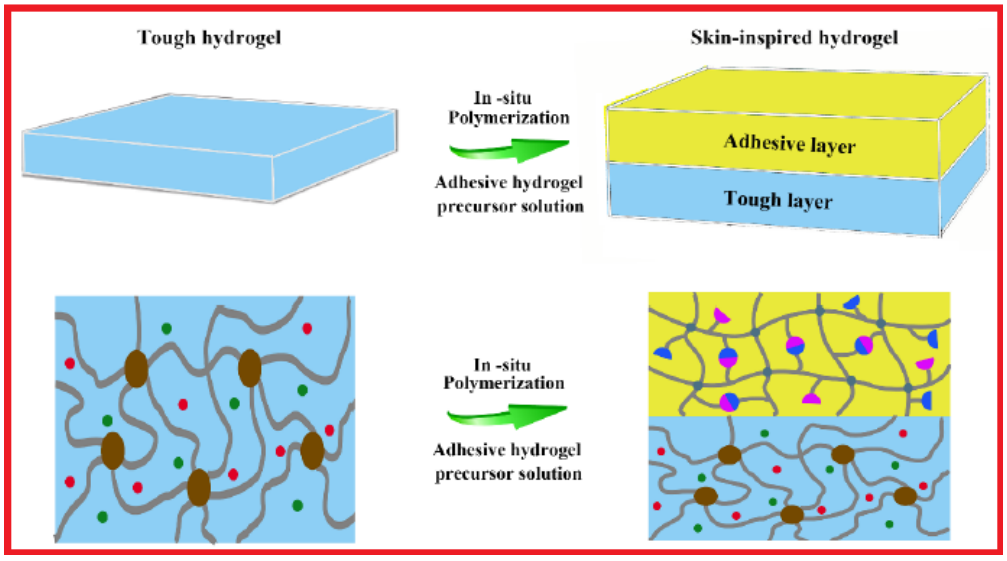

Fig. 3.1: Fabrication of bilayer hydrogels [110]

Shuqi Liu and his colleagues reported a compliant, self-adhesive and self-healing epidermal strain sensor. Self-healing, low-modulus polyvinyl alcohol hydrogel (PVA) hydrogel was selected as the base material for obtaining a compliant and self-adhesive epidermal strain sensor. To enhance skin adhesion Polydopamine (PDA) was introduced. They successfully prepared highly stretchable PVA/PDA hydrogel by mixing the aqueous solutions of PVA, PDA and sodium tetraborate. Their fabricated epidermal strain sensor can detect ultra-low strain up to 0.1% and due to the excellent

stretchability of the hydrogel can detect very high strain up to 500% of the human body. In addition, the hydrogel has super self-healing ability due to the reversible boron ester bond. They observed the self-healing time of the sensor which was 250 ms at ambient temperature (25 ℃) which makes their sensors more humanoid as shown in Fig 3.2 [111].

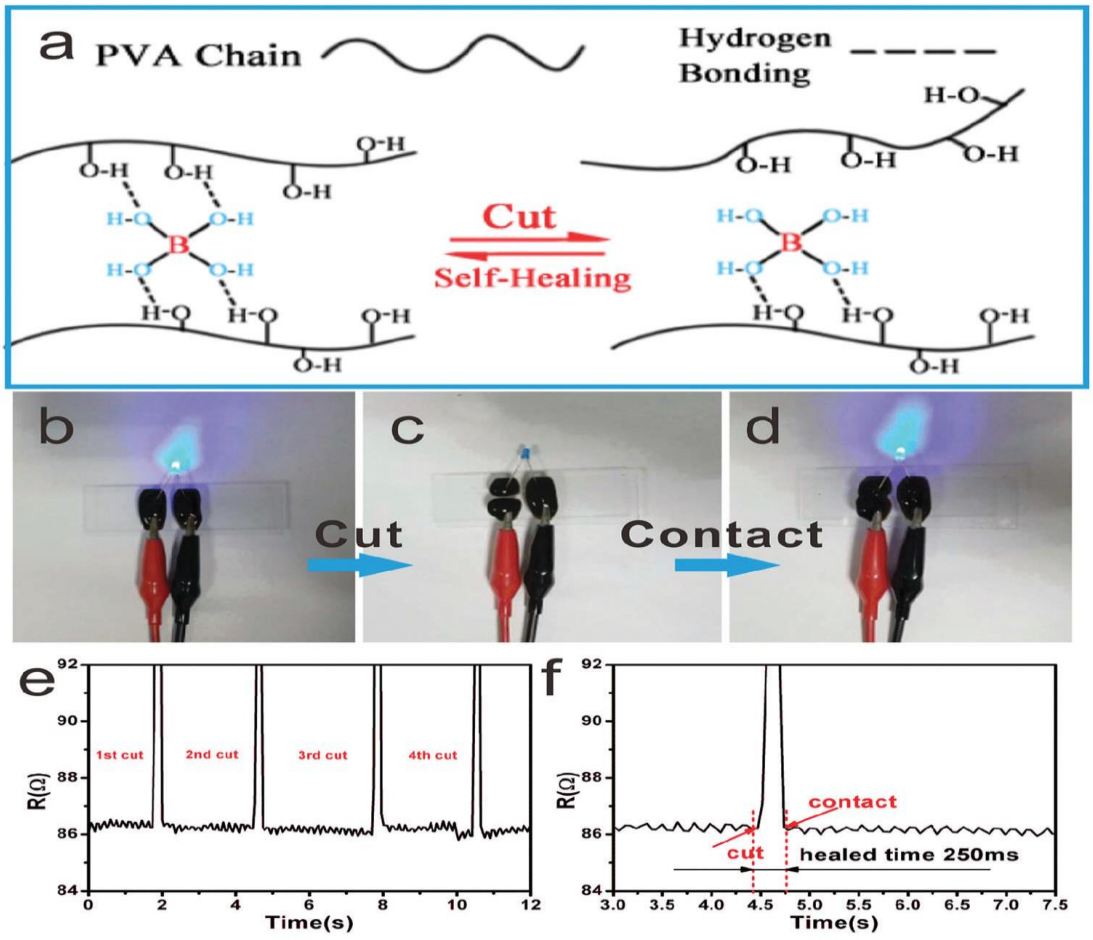

Fig 3.2: (a) Hydrogel having mechanism of self-healing (b) Hydrogel in series circuit (LED ON) (c) Cut hydrogel (LED OFF) (d) After healed (LED ON) (e and f) Shows resistance (R) after cutting and self-healing cycles [111]

Chunxiao Zheng at all introduced a new class of highly stretchable and self-healing strain sensors based on graphene, assisted by Nano cellulose distributed in electro-conductive hydrogels. They combine cellulose nano fibers (CNFs) and graphene (GN) to form GN-CNF Nano complexes. CNFs were used as a suitable nano carrier to promote GN distribution in aqueous medium, creating the interlinked conductive pathways. In the strain sensor homogeneously dispersed combine cellulose Nano fibers (CNFs) and graphene (GN) nano complexes are used as active material spread over the

polyvinyl alcohol polymer substrate network to create the 3D conducting pathway GN-CNF@PVA hydrogel. Their prepared composite gel shows high stretchability (up to 1000 %), excellent viscoelasticity (up to 3.7 kPa), fast self-healing ability (self-healed in 20 s) and high healing ability (97.7±0.1%).In this paper strain sensor dominant electrical pathways are obtained by GN-CNF Nano complexes, the device has excellent sensitivity, flexibility and stability efficiently track and recognize the various human movements with a gauge factor (GF) of about 3.8, showing great potential in the field of sensing devices as shown in Fig 3.3 [112].

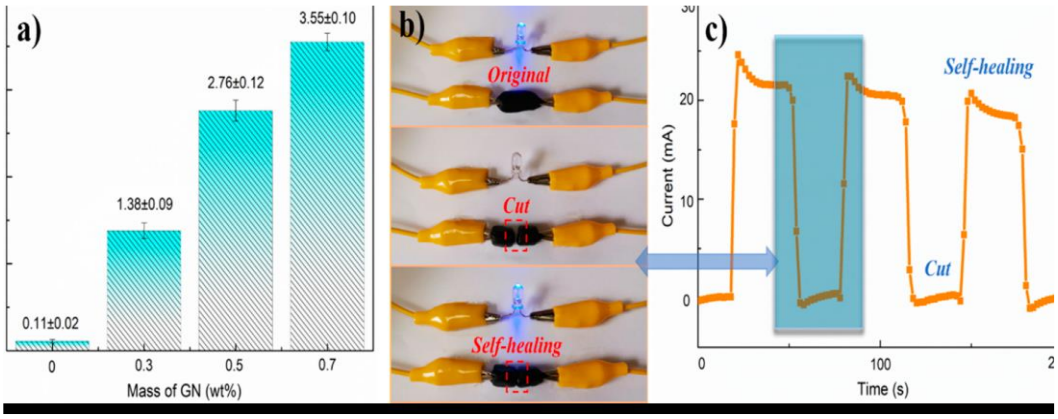

Fig 3.3. (a) Conductivity variation of gels by increasing amount of GN (b) circuit shows self-healing ability of conducting network in gels (c) shows changes in current during multiple cutting/healing of the gels [112]

Self-healing, conductive, magnetic (ZnFe2O4/MCNT/PPy ternary composite hydrogels based on PVA) properties show that these composite hydrogels expected to be needed in advance application. Application includes drug delivery, electronic skin and electromagnetic interference shielding. It is also a good candidate for 3D printing techniques of synthetic human organs due to easy remolding and bio compatibility as shown in Fig 3.4[113].

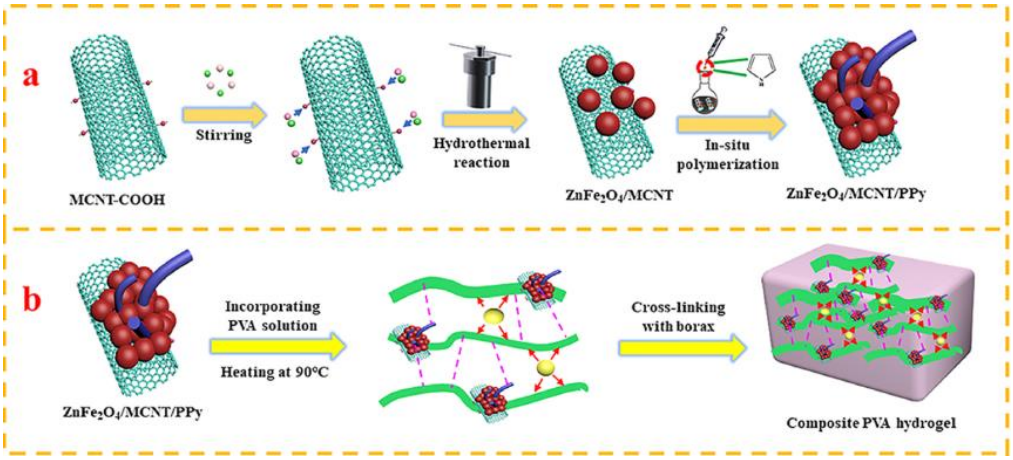

Fig 3.4: Fabrication process of the composite hydrogels and ternary composites [113]

Man Wang et al. documented and developed a novel approach by facilitating the preparation of quick PVA-PDA-pRGO conductive self-healing strain sensor nano composite hydrogel. Reversible diol-borate easter bonds is used to find the ability of rapid self-healing of that nano hydrogel. Recovery trials like electrical, rheological and mechanical stresses are used to demonstrate that diol-borate easter bond strength. Design hydrogel shows outstanding healable performance in seconds (92.89% in 60s). The rapid self-healing output was also observed in electrical and rheological healing cycle testing. They recorded 96.7 ± 2% of original resistance within 4.2s as shown in Fig 3.5. In comparison with PVA hydrogel, this nano composite hydrogel shows greater performance in rheological, mechanical and swelling test, due to physical association formed by functional group of oxygen. Strain sensitivity is tested by LED test by the obtained hydrogel. Therefore, to detect human activities design hydrogel is used to prepare soft strain sensor [114].

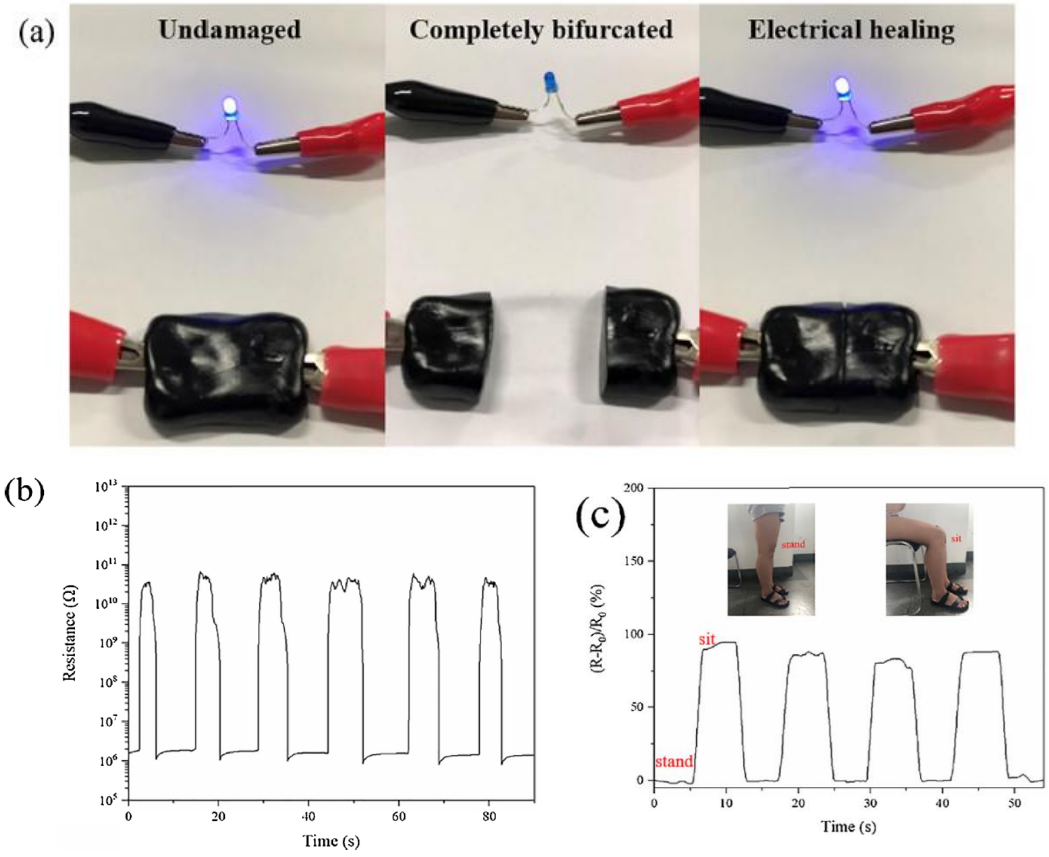

Fig 3.5: (a) Hydrogel conductive self-healing behavior showed by LED (b) The resistance change of hydrogel during cutting-healing cycles. (c) Strain sensor resistance varies according to knee joint motion [114]

In the current research the high sensitivity, ultrahigh stretchable and flexible strain sensor based on nitrile butadiene rubber (NBR) and conductive Carbon black (CB) was presented as shown in Fig 3.6. Three different coating times with two organic solvents during the coating process were observed. The degradation temperature and morphology of all the NBR/CB compound films were investigated and elongated at breaking lengths, the tensile strength as well as the dissipated energy and young's modulus for all the case were disclosed. In the strain sensing test NBR/CB film possess good sensitivity which maximum gauge factors 24.9 and 681% strain ultra-high sensitivity. Simmons mathematical model used for further investigation of strain sensitivity. Overall low-cost strain sensors are fabricated which have great strain-sensing performance due to its flexible nature [115].

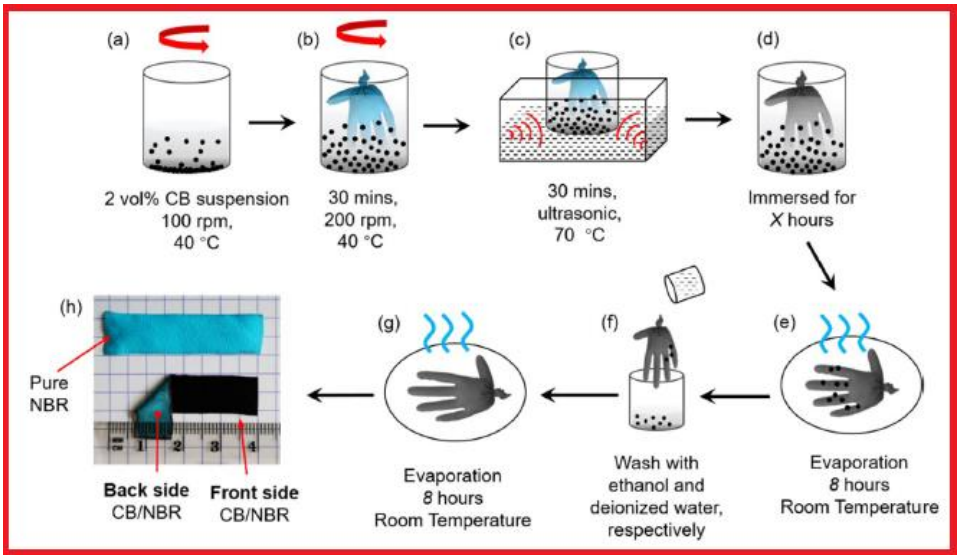

Fig 3.6: Illustration of fabrication of NBR/CB Composite film [115]

Flexible strain sensors that utilize conductive hydrogels are reviewed here for tissue engineering and bio sensing self-recover. Hydrogel is an important material because of bio compatibility and high stretchability, strong adhesion and excellent self-healing. The chemical, physical and fast healing properties of such conductive hydrogel materials make it more suitable to application in the field of human machine interface, health monitoring and human motion [116].

Polyvinyl alcohol/cellulose nanofibril (PVA/CNF) hydrogel strain sensor is presented for sensing and motion detection. This sensor is sensitive to very small pressure like droplets of water. Electronics skin. Human monitoring, wearable devices and personal health care are potential fields of introduced strain sensor [117].

Serpentine shaped composite films based highly sensitive and stretchable strain for flexible electronics skin application is introduced in literature. Fabrication of serpentine shaped sensing layer occurs by engineering graphene nano plates/carboxyl-functionalized multiwall carbon nanotubes/silicone rubber in addition with synergistic effects of three-dimension hybrid conductance network to create new flexible strain sensors with high sensitivity, stretchability and excellent response characteristics. These strain sensors are applicable in monitoring real time human body motion. [118].

Ultra-stretchable wearable strain sensor is made by using casein sodium salt and PDA inspired by mussels introduced on poly acrylamide hydrogel system fabrication. High

stretching capability, self-healing and superb fatigue resistance that make it flexible strain sensor for the direct monitoring human motions [119].

Ion intercalated graphene nano sheets and interfacial coordination-based sensors are also introduced in some recent literature. This nano composite shows desirable mechanical properties in comparison to the sample without interfacial coordination. This elaborated design makes it applicable for fields like artificial skin, smart robotics and other electronic devices [120].

Strain sensor ultra-stretchable conductive polymer with repeatable autonomous self-healing is mentioned in various domains. Regenerative polymer complex as skin like electronic device is introduced. This type of strain sensor provides excellent linear responses to Omni directional tensile strain and bending deformation. The materials are scalable and environmentally friendly [121].

Wavy patterned based low hysteresis and tremendous elastic ultra-flexible strain sensors are studied for human activities monitoring. This type of strain sensor shows excellent mechanical compliance and has been successfully applied in distinct monitoring of human activities and robotics [122].

In the soft electronics ionic hydrogel, conductive and stretchable material are mostly used. However, the easy drying and freezing of water-based hydrogels notably restrict their long-term stability. Therefore, a facile solvent replacement method is introduced to fabricate glycerol (GI)/ethylene glycol (Eg) water anti-drying and anti-freezing organ hydrogels for sensitive and ultra-stretchable strain sensing within a high temperature domain. Due to this strong formation of hydrogen bonds between water molecules and Eg/GI, the organ hydrogels gain exceptional drying and freezing patience with retained deformability, self-healing and conductibility even tolerate at high temperature for a long time as shown in Fig 3.7. Thus, the fabricated strain sensor has gauge factor 6, which is much higher compared to previously investigated value for hydrogel-based strain sensors. Furthermore at - 18°C this strain sensor has relatively wide strain range (0.5- 950%). In the temperature - 18° to 25°C different human motion with various strain conditions is observed by the strain sensor with outstanding stability. This work investigates novel insight into the manufacturing of ultrasensitive, ultra-stretchable and stable strain sensors using organ hydrogel which is chemically modified for emerging wearable electronics [123].

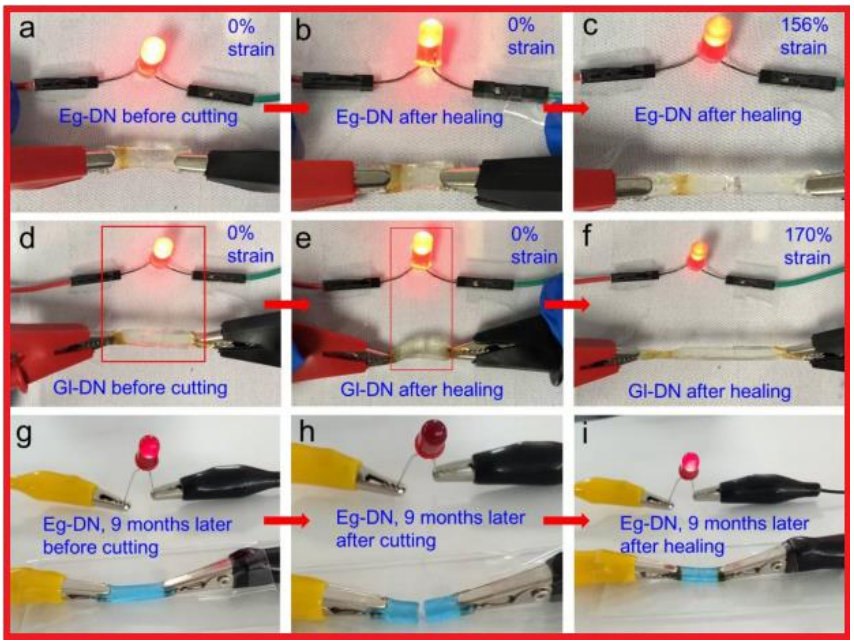

Fig 3.7: Demonstration of GI-DN cutting strain sensor after and before healing [123]

In recent years flexible and stretchable electronics have been investigated as they have great potential applications in soft robotics, healthcare technology, artificial skin and energy storage etc. Herein Diels Alder (DA) based polyurethane substrate (PU-DA-1), and polyaniline conductive polymer (PANI) composite is used for formation of strain sensor as shown in Fig 3.8. The strain sensor has 1.1 MPa tensile strength young's modulus, composition of strain sensor gives outstanding conductivity of 7.5 S$m^{-1}$and its physical motion represented gauge factor 2.9. Moreover, the conductivity and mechanical performance which could be self-healed by rearrangement of polymer chains, enabled by the hydrogen bonds and reversible covalent bond [124].

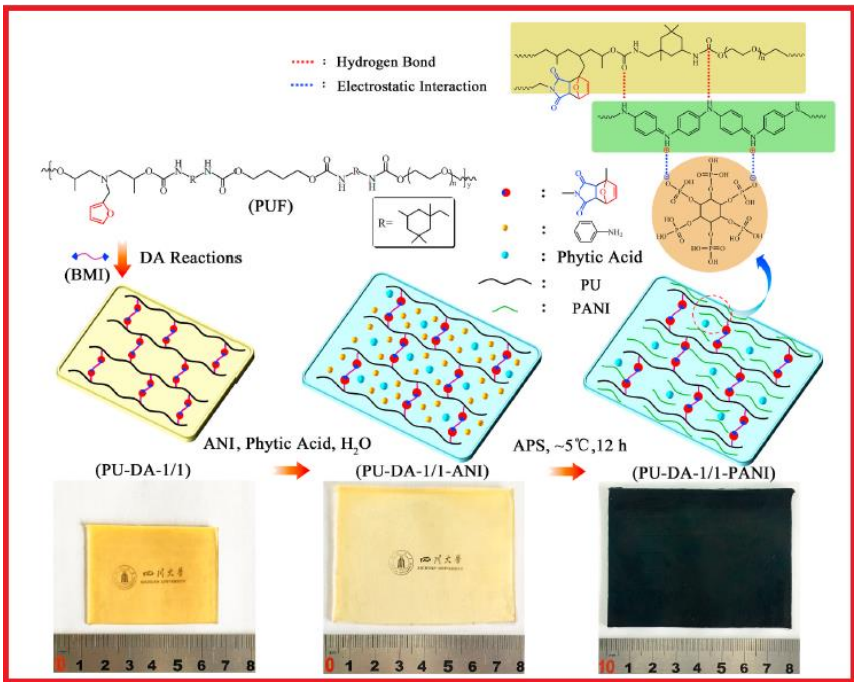

Fig 3.8: Preparation of PU-DA-1/1-PANI composite strain sensor [124]

Ultrastrechable double network hydrogel for flexible strain sensors are also considered with properties like insufficient energy dissipation and weak mechanical properties in intrinsic structure of hydrogel. This DN hydrogel is developed by an ironically crosslinking agar network and covalently crosslinking acrylic acid (AAC) network. Dynamic and reversible ionic cross-linked coordination is made between AAC and Fe^{+3} ion. Regeneration property of reversible AAC and Fe^{+3} interaction after stress relief increase toughness of the material. The break strains up to 3174.3% are developed in this DN hydrogel. Gauge factor of strain sensitivity is 0.83 under strain of 1000% while 3D printability property is present. These sensors are a good option for fabricating strain sensors, electronic skin and soft robotics as illustrated in Fig 3.9[125].

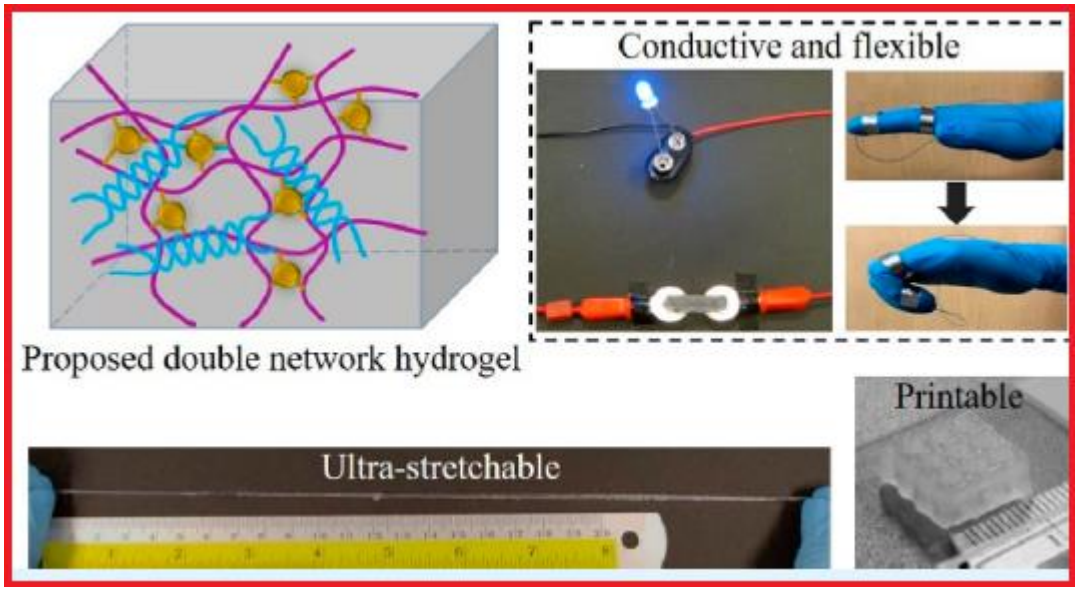

Fig 3.9: Preparation of double network hydrogel flexible strain sensor [125]

stretchable strain sensor and flexibility based on FeNWs/Graphene/PEDOT; PSS with porous structure is introduced for investigation to get better performance metrics. High linearity of 98% is achieved via these sensors. Stability of 3500 times at 80% strain and that is due to 3D network structure of Polyurethane combined with electrically conductive FeNWs. Stabilizing effect of PEDOT: PSS and Bridging effect of Graphene is shown in Fig 3.10. This stabilizing effect creates adhering property and makes it 3D network stable. These sensors can be used in smart robotics and intelligence applications [126].

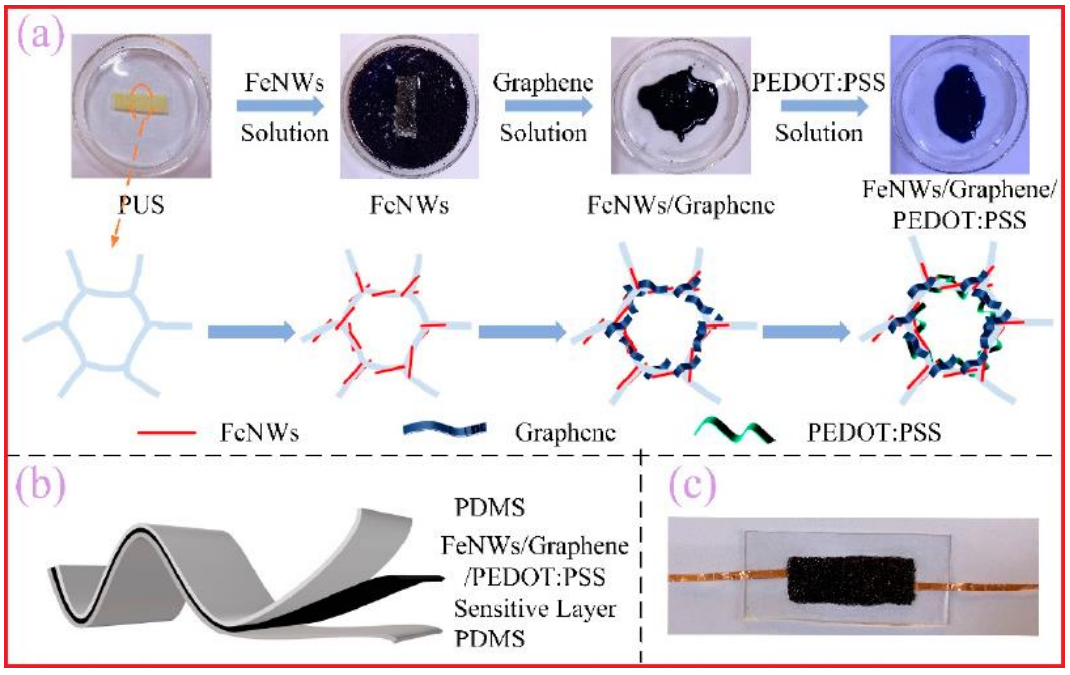

Fig 3.10: Demonstration of FeNWs/Graphene/PEDOT: PSS strain sensor [126]

High stretchable, tough, self-healing and ultrasensitive ionic hydrogel is used to create strain sensors in the next literature work presented next. Ionic crosslinking of Al^{3+} with Chitosan (CS), Tannic Acid (TA) and Polyacrylic acid (PAA). This gives adhesive conductive property to hydrogel as illustrated in Fig 3.11. High stretchability and rapid recovery are obtained due to hydrogen and coordination bonding. Durable and repeatable adhesiveness is obtained due to the utilization of ionic gel. Adhere to human skin without residual and inflammatory effects due to presence of catechol group from Tannic Acid (TA). Broad strain window of up 0 to 1400%, gauge factor12.2, make it suitable for plication in electronic skin, healthcare monitoring, and medical electrodes [127].

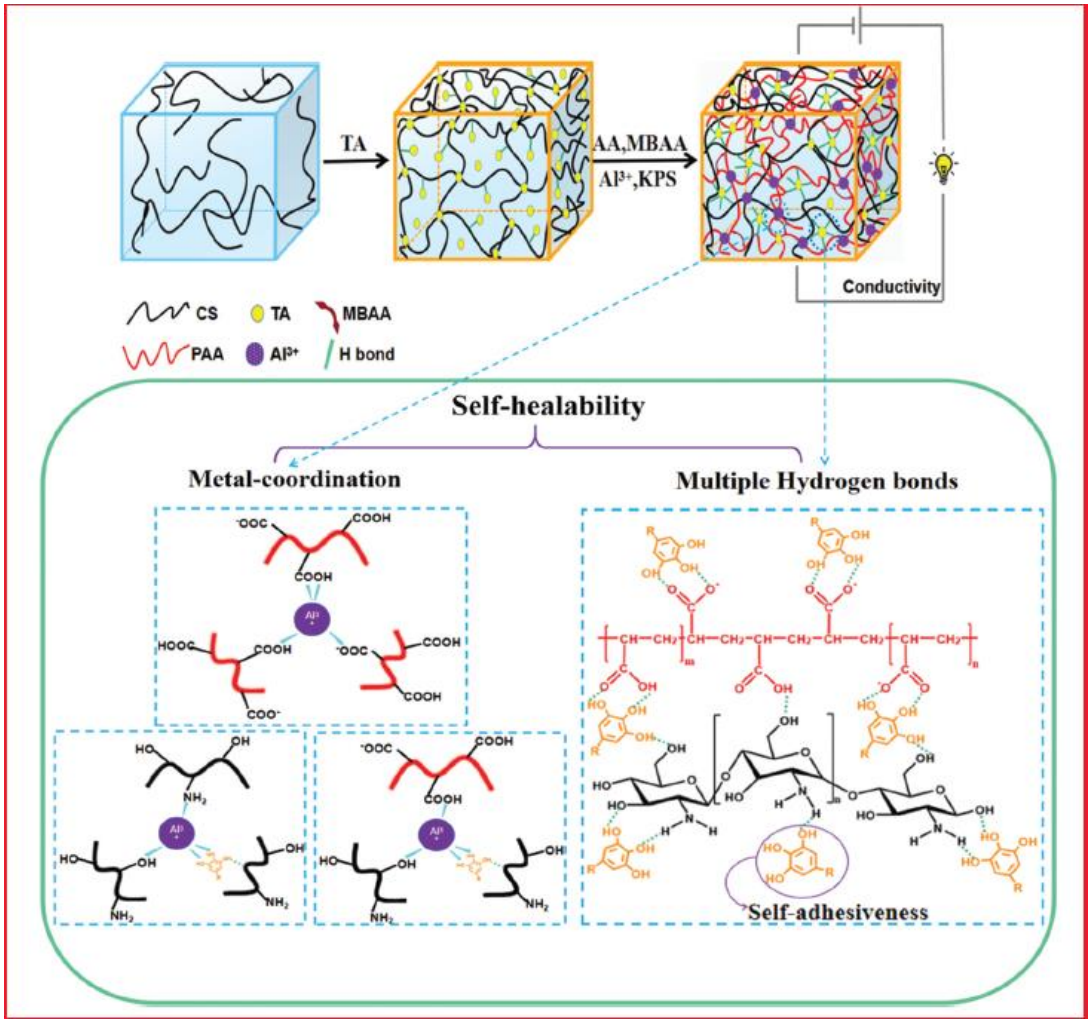

Fig 3.11: Multiple hydrogen bonding and metal coordination having self-healing property [127]

Rapid self-healable, self-adhesive anti-freezing/moisturizing, anti-bacterial and multi stimuli responsive strain sensor is introduced based on Tea polyphenol (TP)/ polyvinyl alcohol (PVA) in some recent literature reports. This self-healing strain sensor works in altered environment (Low temperature (-20℃), in the air and underwater). Completing starch is used to create Starch based composite conductive organo hydrogel based on borate ester bond formed. PBSTCE organohydrogel is produced by Tea polyphenol (TP), polyvinyl alcohol (PVA) with borax and multiple hydrogen bond interaction among PVA. Starch, TP and EG (Ethylene Glycol) silver nanoparticles Ag-NPs reduced and stabilized by TP and multi-walled carbon nanotubes (MWCNTs) were introduced into cross linking network .This hydrogel contain properties of antibacterial, conductivity, self-healing efficiency of 96.7% , self-adhesion both in air and water ,stretchability of 814% (Gauge Factor(GF)=6.85) ,anti-freezing -20 ℃ and moisture retention as shown in Fig 3.12 [128].

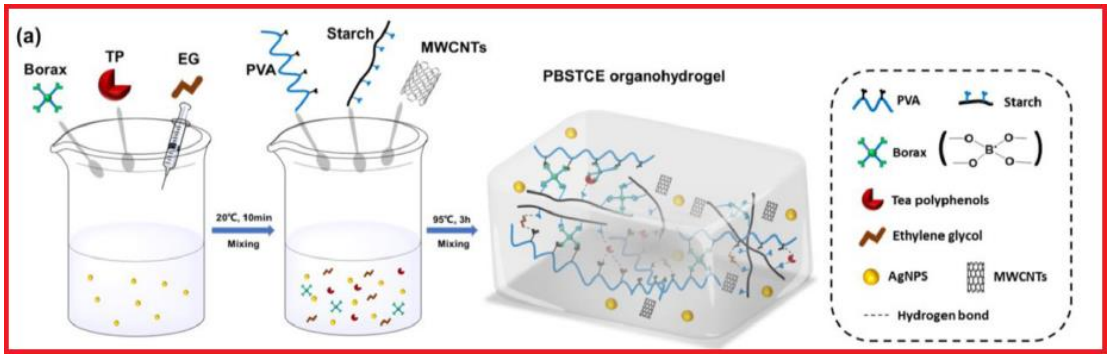

Fig 3.12: Fabrication of PBSTCE organohydrogel base flexible strain sensor [128]

Enke Feng at all developed freezing tolerant and self-healing strain sensors. Soft robotics, artificial medical organizations and electronic skins manufacturers use smart hydrogels which have tremendous healing performance. Herein, introducing acrylic acid (AA), acrylamide (AAm) and polyvinylpyrolidone (PVP) into dimethylsulfoxide/water binary solvent system for preparation of multifunctional organohydrogel. With the help of chemical cross-linked P(AA-co-AAm) chains and PVP provide self-healing and excellent mechanical property (1554% strain) as shown in Fig 3.13. Similarly, super low temperature tolerance (-40 ℃) achieves by using organohydrogel [129].

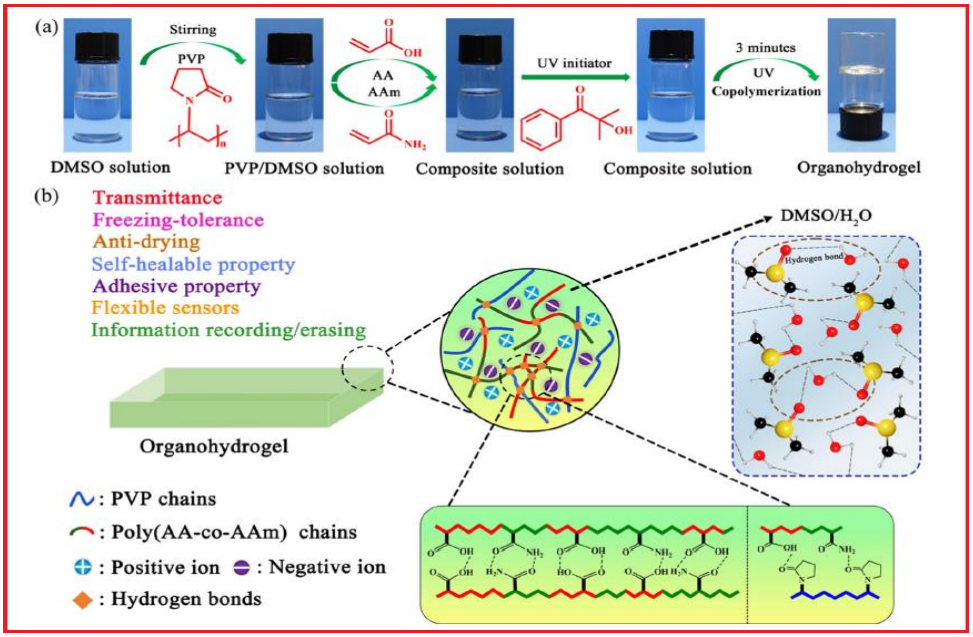

Fig 3.13: Illustration of multifunctional PVP/P (AA-co-AAm)/DMSO Organohydrogel strain sensor [129]

Ramin at all have used polyvinyl alcohol (PVA), branched chain starch (Amy), wheat protein (WP), ethylene glycol (EG) with saline is traditional food that give inspiration for creating this hydrogel-based sensor along with High toughness, electrical conductivity, low cost of Amy/PVA/EG/WP/S (APEWS). Issue arises with degradability, low mechanical properties and freezing resistance which make it less practical as shown in Fig 3.14 [130].

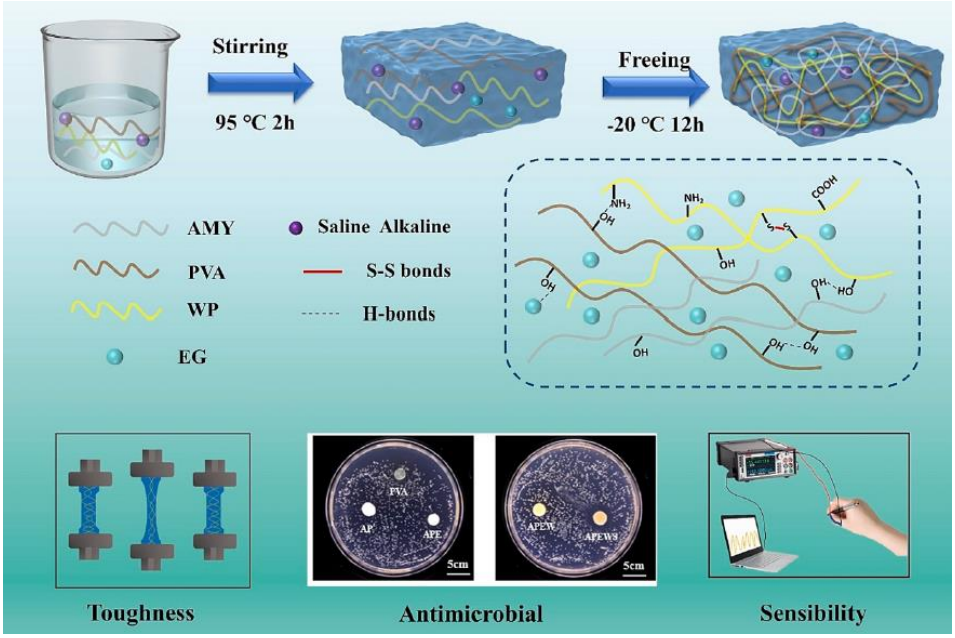

Fig 3.14: Fabrication of strain sensor (APEWS) [130]

PVA hydrogel embedded with CNT based sensor is designed tans is used for multimodal sensing skin which can recognize touch position and pressure simultaneously without any construction. This superior sensing performance made it suitable for practical application [131].

Biomineralization and salting-out synergistic effects were introduced in $CaCl_2$ doped soy protein isolate/poly (vinyl alcohol)/dimethyl sulfoxide (SPI/ PVA/DMSO) hydrogel. The hydrogel is immersed in $Na_2CO_3$and Na_3Cit solution, $Ca^{2+}$and CO^{2-}_3 perform biomineralization, and both NaCl and Na_3Cit it give salting out effect that enhance the electrical and mechanical properties of SPI/PVA/DMSO hydrogel [132].
SPETC organohydrogel-based sensor is designed by fully physical crosslinking of non-covalent interaction that is hydrogen bonding and ligand bonding, so this gives good recyclability to gel. This hydrogel gives high mechanical properties and shows excellent environmental stability to sensor [133].
Reports are present on biocompatible, antimicrobial stable, anti-freezing, and anti-fatigue property hydrogel designed and developed using polyvinyl alcohol, phytic acid, and glycerol. Physically cross-linking of Phytic acid and PVA formed hydrogen bonds improve the fatigue resistance and toughness of the hydrogel. This hydrogel has antimicrobial property and biocompatibility [134].

A novel approach in literature is Acid etching and PDA-mediated co-precipitation methods used to create magnetic and conductive two-dimensional nano-hybrid material (PDA-Fe_3O_4-MXene). Secondly, a magnetic field-induced orientation strategy was used to create the oriented arrangement of PDA-Fe_3O_4-MXene within a dual-network polyvinyl alcohol/polyacrylamide (PAAm/PVA) hydrogel high-strength anisotropic MXene-based conductive hydrogels were created. These hydrogels gave high conductivity, isotropic mechanical performance and sensing characteristic as illustrated in Fig 3.15 [135].

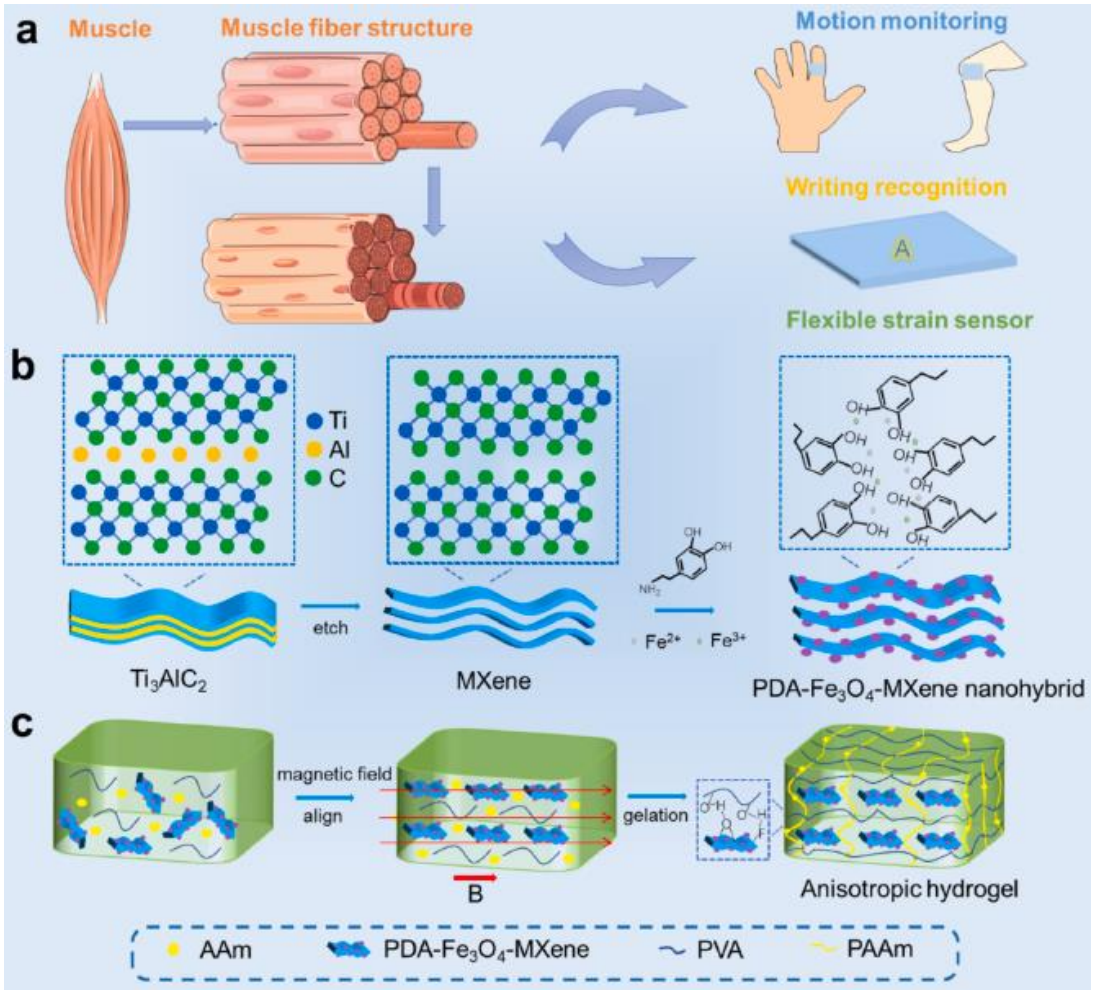

Fig 3.15: Preparation of stepwise hydrogel-based strain sensor [135]

Modified-κ-Carrageenan (κ-Car)/polyvinyl alcohol (PVA) double network hydrogel (DNH) membranes using Facile method are also utilized in literature. Five ionomeric DNHs are prepared by different grafting ratios of Material (acrylic acid (AA) and/or 2-Acrylamido-2-methylpropane sulfonic acid (AMPS))-grafted κ-Car/PVA. Fabrication technique used is solution casting method to fabricate ionomeric DNH membranes and sandwiched between two metal-free Vulcan carbon/functionalized multi-walled carbon nanotubes (V/*f*-M) electrodes using hot pressing to prepare ionic soft actuators. Physical-chemo-mechanical properties of the prepared DHN membranes are evaluated by ATR-FTIR and XRD spectroscopy, and thermal, mechanical, and electrochemical measurements are also studied [136].

Excellent combination of injective ability, conductivity, and sensing characteristics achievement in sensor are the main issues. To achieve these properties, suitable 3D printing inks are required. To create hydrogels with the desired morphological and functional characteristics. Composited thermosensitive kC with PVA using cross-

linking agent borax and a source of conductive ions (Na+) creating borax cross-linked PVA and kC conductive hydrogel inks. And then, their thermal response behavior and freeze-thaw method as illustrated in Fig 3.16is used to prepare the corresponding conductive hydrogels (B-PVA/kC) [137].

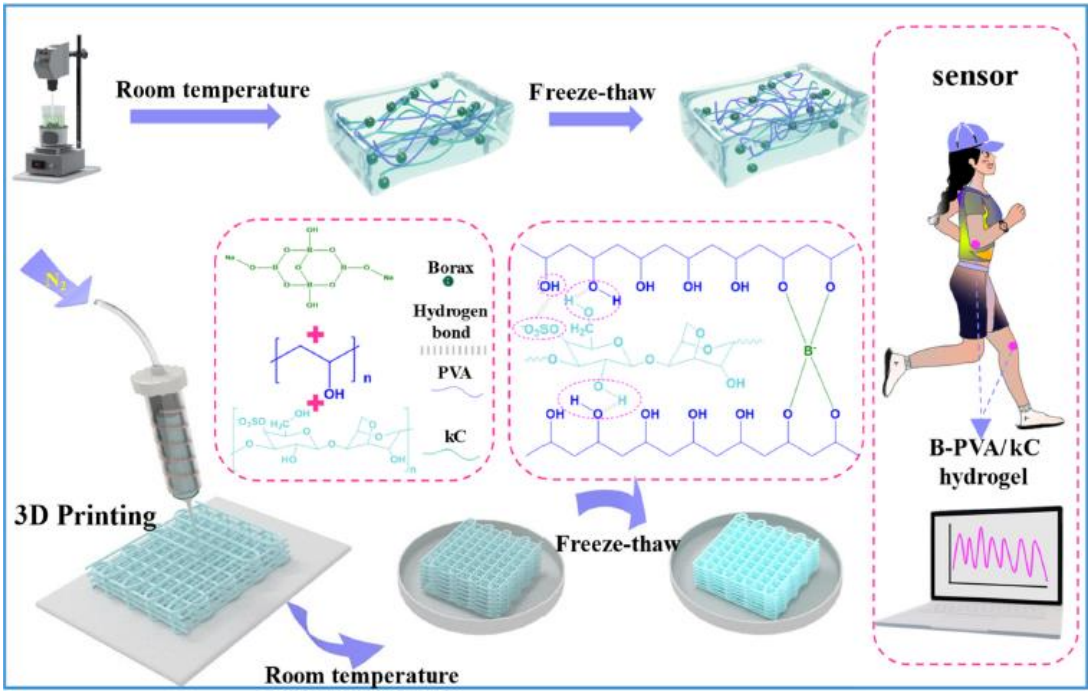

Fig 3.16: Preparation of 3D printing ink-based Strain Sensor [137]

3.2. Various Fabrication Methods for Strain Sensor

Human activities monitoring Ag/PDMs based sensitive multidimensional flexible strain gauge sensor is used along with liquid PDMs, mixed with grinded silver particles as shown in Fig 3.17. By using this sensor, human dynamic monitoring has been proved. These strain sensors show great potential in soft robotics, motion recognition and haptic perception [138].

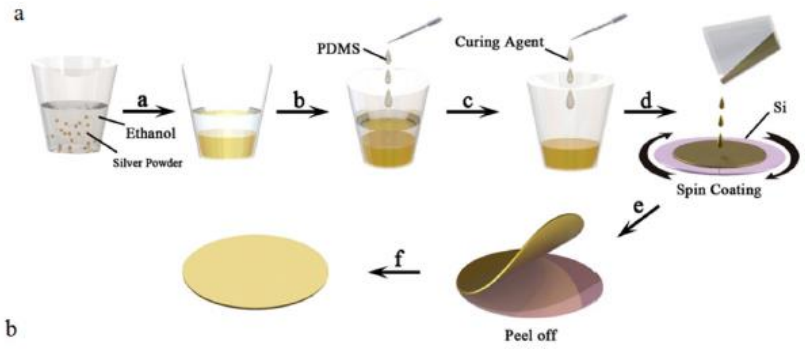

Fig 3.17: Demonstration of fabrication of Ag/PDMS [138]

Feng Liu at al. reported the fabrication of self-healing strain sensors by applied water-assisted and facile vacuum filtration transfer technique. Whereas polyurethane (PU) is used as substrate and silver nanowires (AgNWs) network is used as an active material. They prepared the percolation network of the AgNWs by using vacuum filtration method. This AgNWs intercalates between two polyurethane layers by Diels-Alders adducts (DAPU) with the help of the membrane AgNWs network is transfer to DAPU surface. The composite of PU/AgNWs/PU are obtained after one hour drying process. This composite of (PU/AgNWs/PU) is a very strong agent of piezo resistivity activity. The sensing and integrating performance have been improved by thermal therapy to recover damage. Its gauge factor was 15 at strain 11% as shown in Fig 3.18 [139].

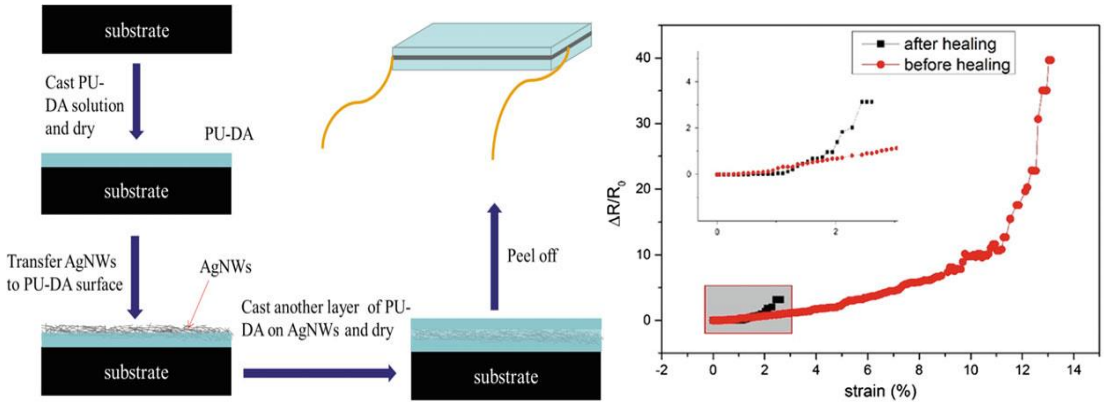

Fig 3.18: Fabrication process of strain sensor using material PU–AgNWs–PU [139]

Dawei Jiang and his coworker fabricated highly flexible 3D structures by sandwiching a sheet of self-healing polymer decorated with AgNWs between two layers of polydimethylsiloxane, showing good durability, self-healing and stretch ability as shown in Fig 3.19. For better mechanical properties, they use carbon fibers (CFs) to strengthen the self-healing polymer. The sensor shows tremendous ability to recover electrical and mechanical damage based on AgNWs and conductive grid of self-healing polymer. Now including 9% carbon fiber in sensor its crack tensile stress of reinforcing self-healing polymer enhanced to 10.3MPa with a break elongation of 8% as compare to that of pure polymer 1.0MPa with break elongation of 0.3%.In the dynamic and static loads

the sensor release response has a high sensitivity, superb performance, wide sensing array (ε = 60%) and incredible stability [140].

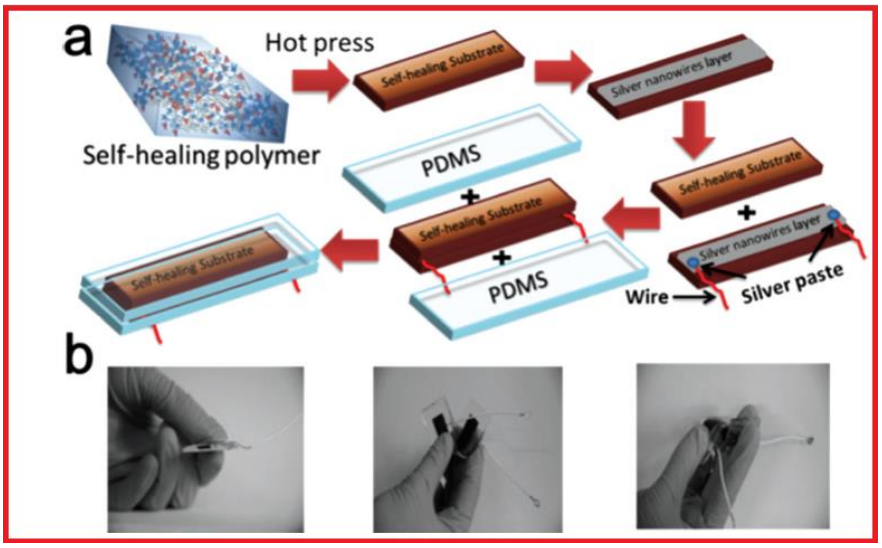

Fig 3.19: a) Fabrication of strain sensor using silver paste/ PDMS.) Demonstration of physical flexibility of Strain sensor [140]

Flexible strain sensor advancement in self-healing composite elastomers such as polyurethane (PU), natural rubber (NR) and polydimethylsiloxane (PDMS) are comprehensively reviewed for high performance of flexible strain sensor. Self-healing composite elastomer is used as shown in Fig 3.20 [141].

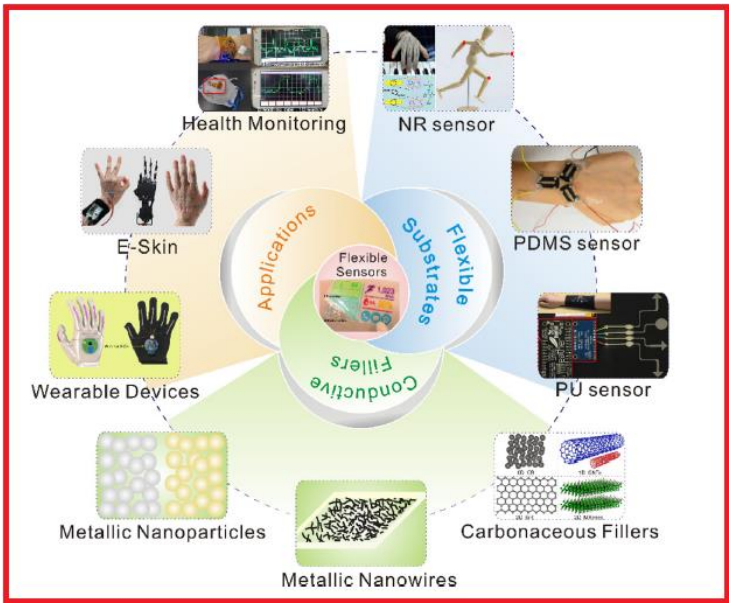

Fig 3.20: Demonstration of flexible Strain sensor with essential elements [141]

For human body monitoring strain sensors are made by embedding the CNTs (Carbon nanotubes) in the surface of swollen shape memory EVA (Ethylene vinyl acetate) fiber via ultrasonic methods showed significant results in fields like heath monitoring [142].

Strain sensors based on nanomaterials, graphene and carbon nanomaterials are good choice for strain sensor development due to their unique thermal, electrical and mechanical properties. Industrial applications such as pressure sensor; human body monitoring and structure health monitoring of graphene have been reported in various literature reports [143].

In some specific cases 3D printing is used to produce highly stretchable and intrinsically self-healing strain sensors. 3D printing technology of DLP (Digital light processing) is utilized for such purposes. Some glimpse of Strain sensor fabricated through N-acryloylmorpholine, and carboxyl multi-walled carbon nanotubes are shown in Fig 3.21. It is concluded that these sensors have shown tremendous response in applications like wearable electronics and personal health care [144].

Fig 3.21: Strain sensor nano-composite shows healing and stretching property [144]

In the latest technology arena, the development of wearable and stretchable strain sensors is discussed in current review. Capacitor type sensors perform outstanding linearity, stretchability and minor hysteresis but have low sensitivity. With the help of structural engineering and advanced material the stretchability and sensitivity of resistor type sensors can be improved. These stretchable and wearable strain sensors have some drawbacks, relatively slow response time, poor long-term durability and efficiency problems. Therefore, several problems related with design of high performance, breathable, skin conformal integrated wearable strain sensor and multi directional strain sensor should be further addressed [145].

In some cases, innovative cutting self-healing flexible strain sensors are proposed using Fe_3O_4, and graphene nano composites. Whereas polyurethane is used as substrate for fabrication process. Inkjet printers need to deposit the material and produce strain sensors for stretchability purposes. It was proposed that versatile self-healing electronics

devices could be created using the printing method as shown in Fig 3.22. Bending cycle on human fingers is used to maintain operating sensitivity of sensors. After cutting the sensor in half and upon rejoining the operating sensitivity about 94% recovered. Stretchability of strain sensor is about 54.5% but after cutting this decrease to it value drops to 32.5% [146].

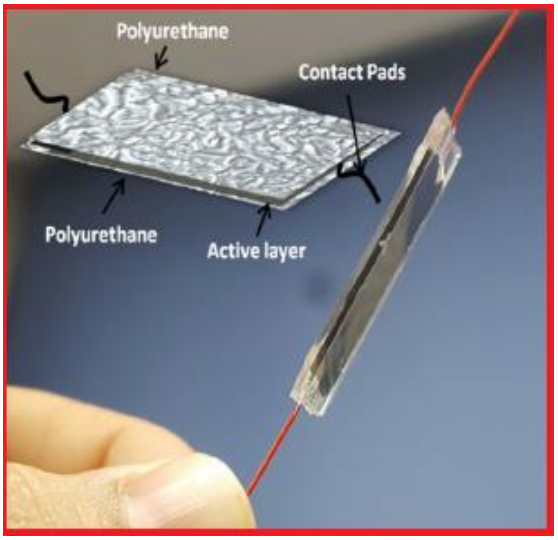

Fig 3.22: Demonstration of fabrication of the Strain sensor Nano composite of magnetic iron oxide and graphene [146]

Wearable electronics and high mechanical strength mulberry paper-based strain sensors are studied in some recent literature. This strain sensor shows high tear strength, degradability and suitable coating processability that shows its potential for next generation flexible electronics and medical applications [147].

The graphene quantum dot offers the strongest fluorescence emission under visible light excitation. Folic acid, histidine and serine functionalized, and boron-doped graphene quantum dot are the main contenders. Polyvinyl alcohol and polyglycerol introduction leads to improved fluorescence behavior. The luminescent film exhibits excellent mechanical flexibility, antibacterial and anti-ultraviolet characteristics. The luminescent film was used as an intelligent pH-sensor for detection of pH in human sweat [148].

Conductive hydrogel electrodes have remarkable stretchability and self-healing capabilities. For such purposes a self-powered strain sensing system was developed using conductive hydrogel electrodes. Complex internal structure within the electrode is also constructed. These strain sensors are used for remote human motion detection.

Achieving high-precision DIW (Direct Ink Writing) printing method was employed using conductive ink for fabricating glutaraldehyde (GA), polyvinyl alcohol (PVA), and cellulose nanocrystals CNC. Self-powered sensing system is prepared by large area printing using DIW printing as illustrated in Fig 3.23[149].

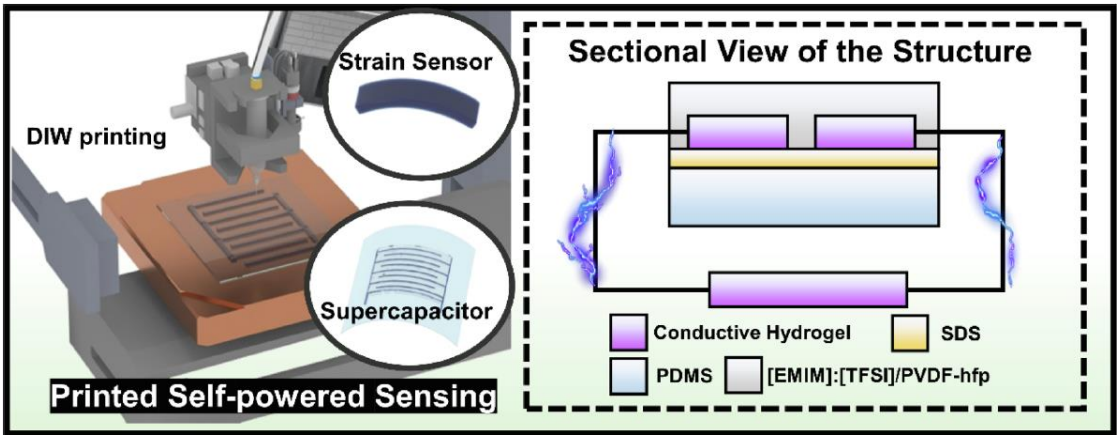

Fig 3.23: Preparation of Direct Ink Writing based strain sensor [149]

Comparative analysis of micropatterned PBMS based piezo resistive pressure sensors with multifunctional monitoring applications are also a choice of interest. Four different micropatterned physical polydimethylsiloxane PDMs based devices are used to develop cost effective high performing sensors for both pressure and strain sensing. PDMS is poured into four types of different micropatterned surfaces. So is then used for gesture detection [150].

Flexible capacitive pressure sensors with dual layer microstructure for health monitoring are introduced in some cases. Double layered microstructure flexible capacitive pressure sensors were prepared with simple structure, excellent linearity, low cost and high sensitivity. Identifying pressure distribution technique is used for sensors to detect sound signals, throat movement and human sitting posture. Porous silica gel membrane elasticity is used for protection of microstructure [151].

Piezoelectric nanogenerators (PENGs) have smaller dimensions compared with turboelectric nanogenerators (TENGs), making it easier to integrate into ICs, performing broader applications. For this purpose, a self-powered, instantaneous wireless (PSIW) sensor system is presented in some cases based on PENG structure. Integrating PENG with an RLC sensing circuit is used for spontaneous generation of oscillating signals with encoded sensing information to address the high internal impedance issue with PENGs. Ensuring a piezoelectric voltage, a driven electronic

switch is used. That ensures the stability of the oscillating signal's frequency and amplitude. The signal frequency is investigated in detail with varying input variables [152].

Green synthesis of the carbon-based filler, recyclability of the ink and material selection for the ink composition from biopolymer binder, solvent and additives are presented for eco-friendly environment as shown in Fig 3.24. To discuss performances of the carbon-based conductive ink, forming conductive pathway in microscopic level having stretched and relaxing phenomena for printed strain sensor applications, percolation theory and tunneling effect is used. Environmentally friendly and renewable bipolar binders are used with natural precursors for green synthesis of carbon and incorporated bipolar binder conductive ink. [153].

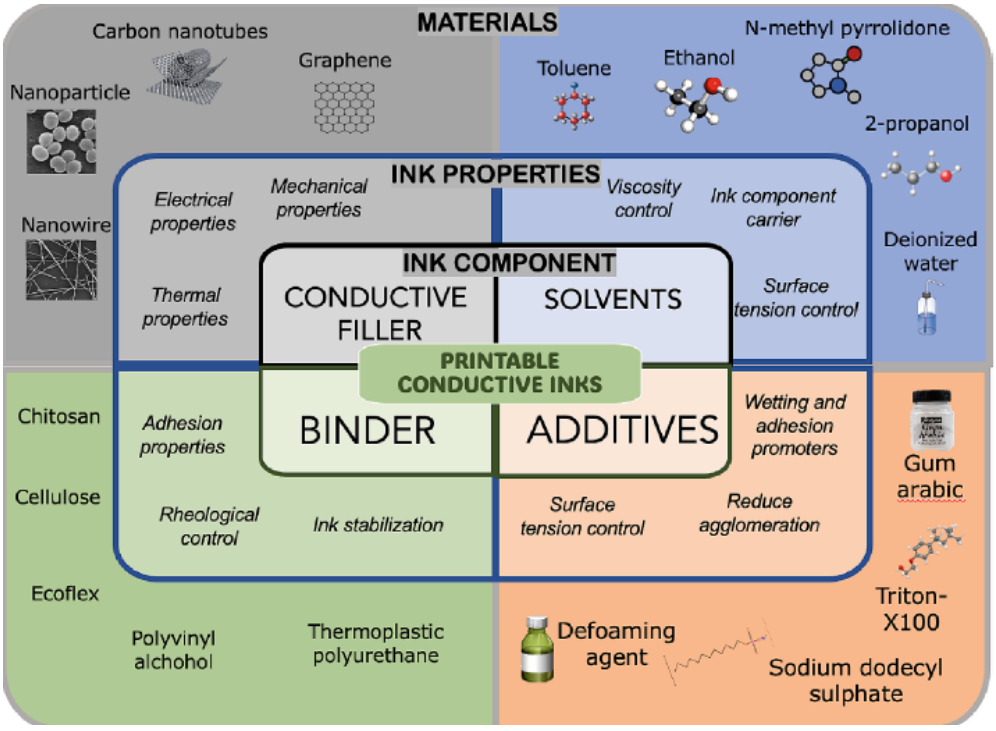

Fig 3.24: Various materials are used as ink for printable fabricated Strain Sensor [153]

PVA /graphene oxide composite film was developed for strain sensor applications. These sensors' mechanical properties and morphology were studied in detail. This sensor possesses exceptional sensing properties. Results show that PVA nano composite films are promising candidates for strain sensor and energy storage devices [154].

Polythiourethane microspheres based dynamic cross-linked are synthesized and designed the special mixing technique where the growth temperature is higher than melting temperature of PTUM soft segments to create carbon nano tubes CNTs that

adhere to surface of cross-linked PTUM for compact conductive network. This CNT/ PTUM network exhibits good healing properties, electrical and recycling properties. That are important for wearable electronics [155].

3.3. Summary

The self-healing wearable strain sensors are used in different bio-medical applications i.e. wrist, leg, forehead and elbow movement detection etc. Such strain sensors are also used in self-powered wireless systems and in electrical vehicles. These strain sensors are smart and can be easily placed on the human body's different parts. These flexible strain sensors are improving efficiency day by day using different organic and inorganic materials like graphene, PVA.PU, PVP, NaCl, and CaCl etc. Similarly various methods are used for fabrication of strain sensors to enhance their durability like hydrogel, ink jet printer, chemical vapour deposition (CVD), Epitaxial growth and carbon nano tube (CNT) methods etc. These strain sensors can be used at different temperatures even in under water. They retrain their electrical and mechanical properties under various pressure (before cutting and after healing).Table 3.1 enlisted all fabrication methods advantages and disadvantages used in this chapter.

Table 3.1: Advantages and disadvantages of fabrication methods of strain sensor

Fabrication Method	Advantages	Disadvantages
Spin coating	Low cost and simple Good for composites	Poor drop casting Adhesion issues
Electrospining	Lightweight Breathable	Poor mechanical strength Humidity friendly
Sputtering	Controlled films Uniform films	Not good for flexible materials Need vacuum equipment
3D printing	Rapid prototyping Difficult shapes possible	Poor resolution Limited conductive materials
Inkjet printing	No mask requirement Good choice for flexible Electronics	Nozzle freezing Slow for large areas
Screen printing	Support flexible substrate Simple process	Low durability Spreading ink
Photolithography	Precision pattering Used for MEMS-scale integration	High cost Not friendly for flexible substrate
Chemical vapor deposition (CVD)	Good conductivity Produce high quality thin film	High temperature need Required vacuum
Solution casting (Hydrogel based)	Good for polymer blends Low cost and simple	Poor control over microstructure Scalability lagging

Chapter 4

Experimental Techniques

In this chapter various synthesis and characterization tolls along with their fundamental working principles used for the flexible self-healing strain sensors are explained with details. These machines are utilized to characterize the proposed strain sensor mechanical, electrical and its self-healing efficiency, which actively demonstrates that scope of proposed strain sensor in biomedical and advanced sensing applications.

4.1. Magnetron Sputtering

A magnetron sputtering is an advanced deposition technique where deposition rate is high as compared to the other sputtering. Magnets are used with the help of which percentage of electrons ionization efficiency is increased which maximize the growth rate.

Magnetron sputtering is a versatile technique used to deposit metals, alloys and compound layering on wide range material under high-rate vacuum. The thickness of 5 pm can be achieved using the current technique. This technique has wide applications in microelectronics manufacturing, device electrodes and decorative coating.

Plasma vapour deposition (PVD) is the main procedure followed in Magnetron sputtering. In this procedure an electric field is used to accelerate positively charged plasma, which is first formed during the excitation process. Electric field superimposition is done on “target” or negatively charged electrode as in Fig 4.1.

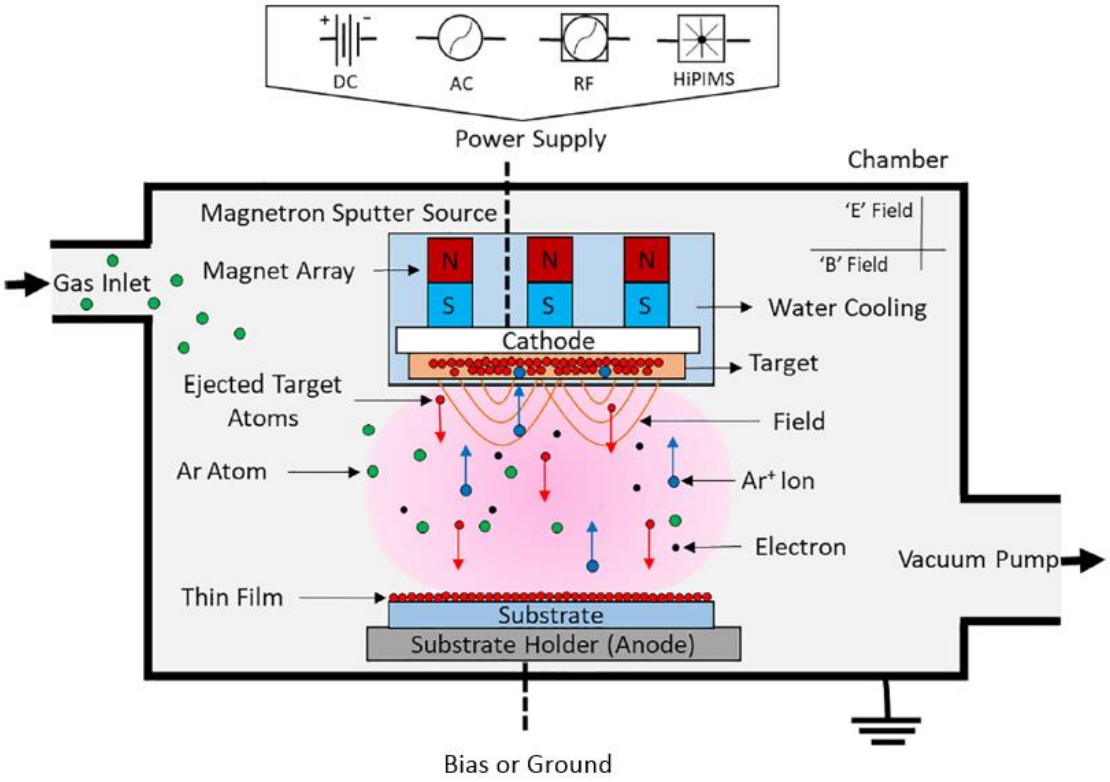

Fig 4.1: Image shows magnetron sputtering process [156]

4.2. Spin Coater

Spin coating is a method in which flat substrate is deposited by uniform thin film to the middle of substratum, which is spinning at constant speed, so the material spread uniformly according to achieve desire coating. Spin coaters use centrifugal force to rotate substratum at very high speed to spread coating material. The mechanism of the spin coating is shown in Fig 4.2.

Till the desired film thickness is achieved rotation continues to spin off the fluid from substratum edges. During this process the solvent may evaporate due solvent instability. The tinning of filling is proportional to high spinning angular velocity. Viscosity, concentration and solvent are main factors on which film thickness depends.

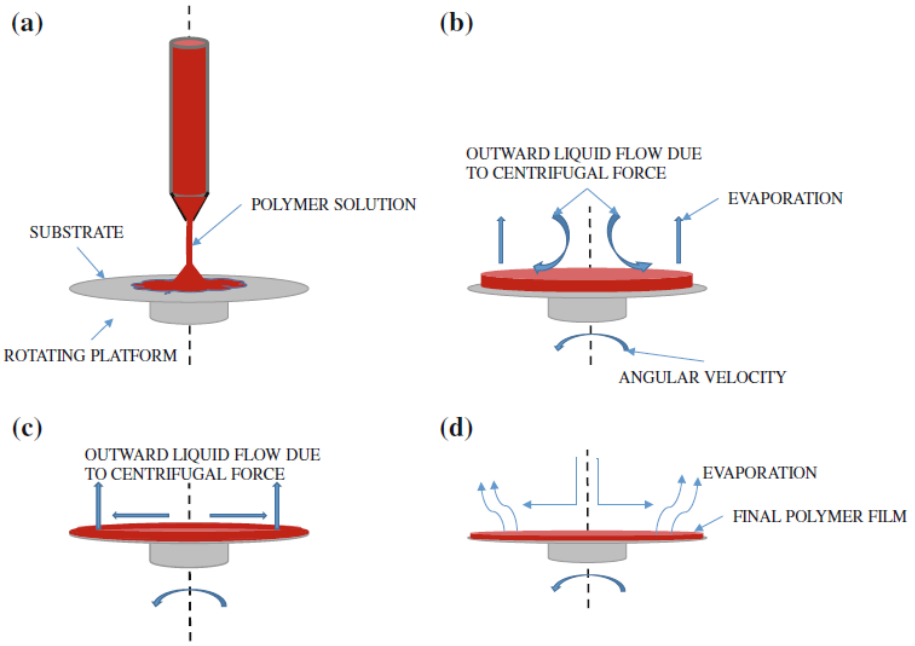

Fig 4.2: Illustration of spin coating process [157]

4.3. Scanning Electron Microscope (SEM)

The Scanning Electron Microscope (SEM) is one of the most fascinating examination methods for material surface morphology and internal arrangement of material nanoparticles visualization. With the help of the electron beam used for scanning we generate the high-quality sample image. Information about the topography of the surface and the sample composition is achieved by signals produced when the atom is interacted by electron beam in the sample. The image is created when the intensity of detected signals and beam's position is combined by scanning electron beam in raster scan. The Scanning Electron Microscope (SEM) consists of generally following parts column for electron beam generation, electron gun, anode, condenser lens, objective lens, X-ray detector, secondary detector, specimen chamber, vacuum pump, monitor and control panels. A high energy electron beam is produced by an electron gun. The electron gun required almost 20kV energy to produce electron beam. The beam is focused by a spot of about 100 Angstrom diameter and made to scan the surface of the specimen. The vacuum pump is used in SEM to create the vacuum, so no air particle can interact with sample. The Raster scan generator is used for deflecting electron beams to scan entire sample. As the electrons are used to scan all the specimens, that is why it is called Scanning Electron Microscope (SEM). The scintillator collects the

secondary or scattered electrons and converts them into light signals. Backscatter electrons reflect of the surface and deeper from the specimen it's also known as reflected electrons. The basic principle of SEM is to detect secondary electrons and use them to build-up images. A positively biased grill is placed in front of the detected grill attracts the secondary electrons and leaves them to SE detector (collect secondary electrons) of which magnified images are generated. Many recorded secondary electrons lead to bright image points; few electrons lead to gray image points. Remember primary electrons reach the surface of the sample knockout electrons of specific material. These are secondary electrons used for image information in samples. In the Scanning Electron Microscope (SEM) the materials are quantified by their different wavelengths of secondary electrons. SEM is used to investigate different virus structures, 3-D tissue image, Biological and non-Biological objects. Remember SEM cannot be used to visualize the image of living cells because first the sample is dehydrating before it's characterized. The Scanning Electron Microscope (SEM) can generate an in-depth and high-quality resolution image of the sample. In the most common SEM mode, secondary electrons are released when electron beam is used to excite atoms which are detected by secondary electron detectors (Everhart-Thornley detector) as shown in Fig 4.3.

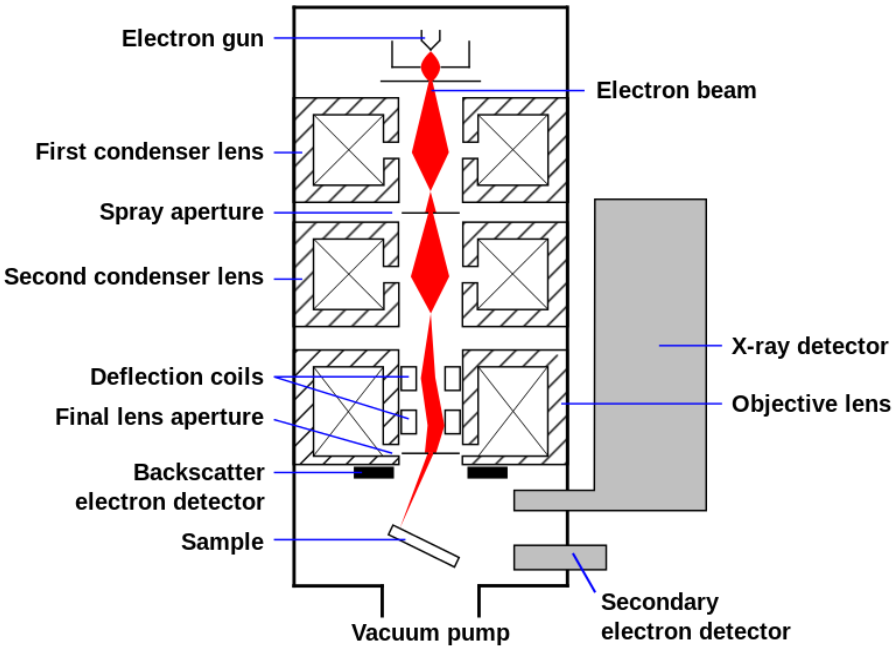

Fig 4.3: Schematic illustration of Scanning Electron Microscope (SEM) [158]

4.4. Current Voltage (IV) Technique

The two-point probing is a simple method for measuring electrical resistance of a material or a device. In the two-point probing voltage and current are the parameters for measuring the resistance. For resistivity and sheet resistance measurement two-point probing is not a preparable method therefore to overcome this problem four-point probing is used. The four-point probe method is used to measure resistivity in semiconductor samples. In the four-point probing method two current probes are used outward and two voltages probes are used inward. So, the sheet resistance is also measured by a four-point probing method. Sheet resistance and other fundamental properties such as carrier concentration can also be found out with the help of 4 point probing. The strain sensor resistance changes with stretching as a result current characteristics of the sensor changes [159-160].IV-characterization is very important to determine whether the device is in working condition under electrical analysis. In this research I-V characteristics of a strain sensor will be used for finding the current voltage relationship of the simples as shown in Fig 4.4.

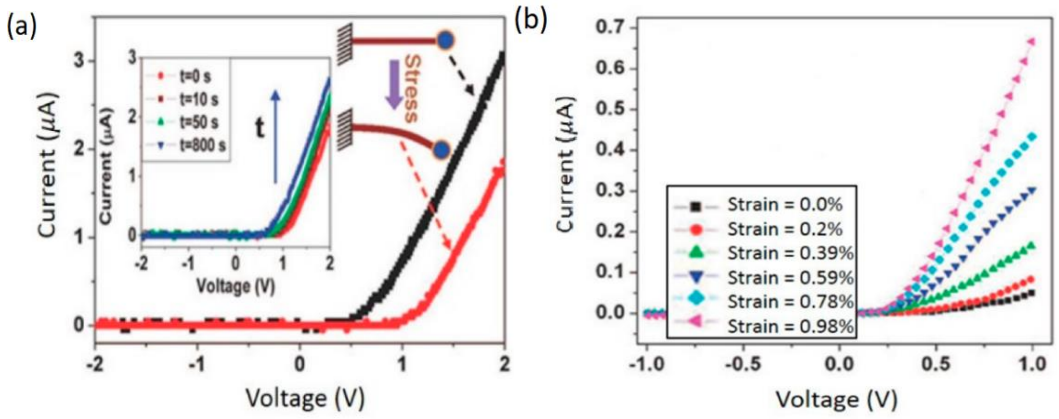

Fig 4.4: (a, b) Strain sensor I-V curves at various strain values [159, 160]

4.5. X-Ray Diffraction System

X-ray diffraction (XRD) is a fundamental and non-destructive technique widely used for the structural characterization of crystalline materials, and its working principle is based on the interaction of incident X-rays with the periodic atomic planes within a crystal. When a monochromatic X-ray beam is directed at a crystalline sample, the atoms within the crystal lattice act as scattering centers. These atoms are arranged regularly, repeating patterns that cause the X-rays to diffract in specific directions.

According to Bragg's Law, given by the equation $n\lambda=2d\sin\theta$, constructive interference occurs only when the path difference between rays scattered from adjacent planes of atoms equals an integer multiple of the X-ray wavelength. Here, n is the order of reflection, λ is the wavelength of the incident X-ray, d is the interplanar spacing in the crystal, and θ is the angle of incidence. At certain angles, the reflected X-rays reinforce one another, producing a detectable diffraction peak. The instrumentation of an XRD system generally comprises several key components: an X-ray source (commonly a copper target that generates Cu Kα radiation of approximately 1.54 Å), a sample holder to securely position the specimen, a goniometer that precisely rotates the sample and detector in a synchronized manner to scan different angles, slits for beam conditioning, and a high-sensitivity detector to measure the intensity of diffracted X-rays at various angles. During a typical scan, the instrument varies the angle of incidence and detects the corresponding diffracted intensity, generating a diffraction pattern, which is a plot of intensity versus the 2θ angle. The analysis of this pattern provides a wealth of structural information: the position of peaks indicates the interplanar spacings, allowing for the determination of lattice constants and identification of crystal systems and symmetry. The relative intensities of the peaks give insight into the atomic arrangement and preferred orientations (texture), while the full width at half maximum (FWHM) of peaks can be used to estimate crystallite size through the Scherrer equation and detect microstrain or lattice distortions. In addition to phase identification by comparing experimental patterns with standard databases like the ICDD Powder Diffraction File (PDF), quantitative phase analysis and even amorphous content estimation can be performed. Advanced techniques such as Rietveld refinement further enable precise determination of atomic positions, occupancies, and thermal vibrations. Therefore, XRD remains an indispensable tool in a broad range of scientific and industrial applications, including materials science, nanotechnology, solid-state physics, metallurgy, geology, and pharmaceutical research, offering detailed insights into the internal structure of crystalline materials without damaging the sample.

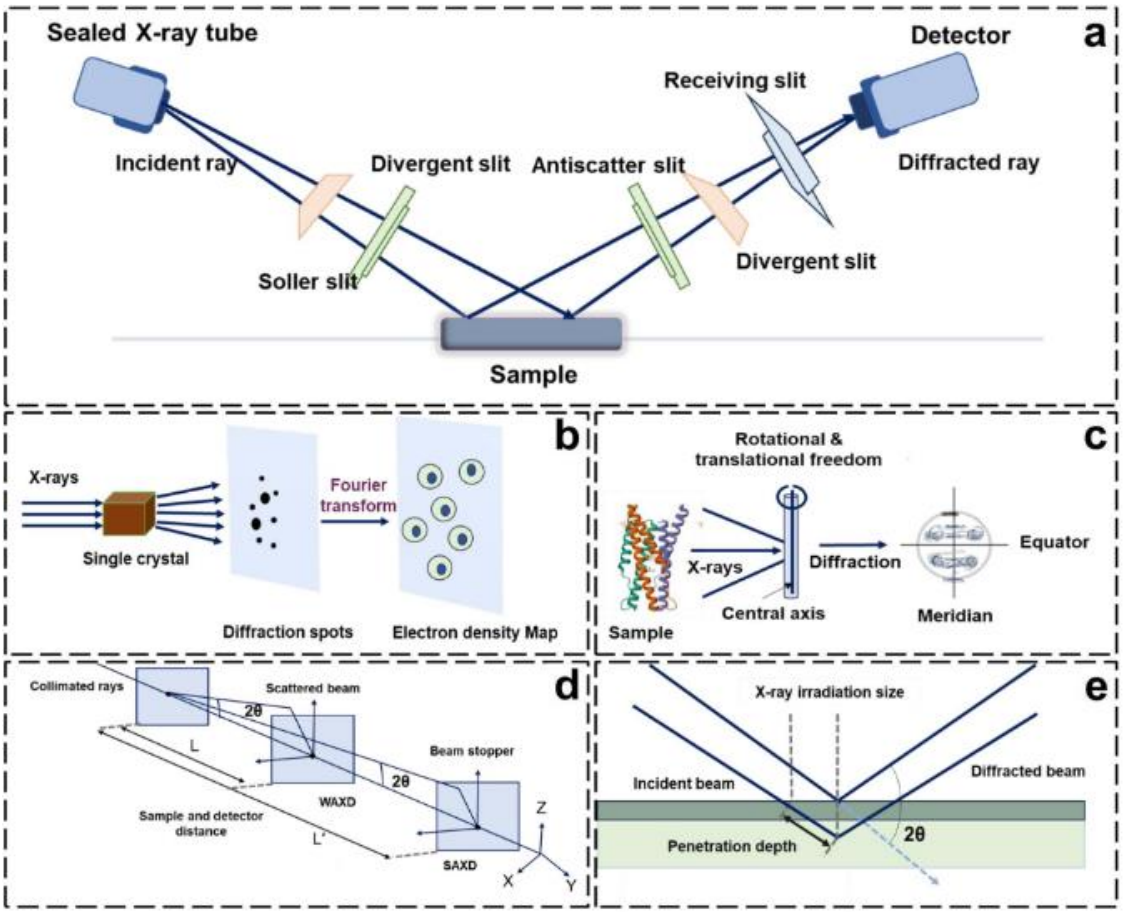

Fig 4.5: X-ray diffraction (XRD) machine and technique illustration [161]

4.6. Digital Magnetic Stirrer System

A digital ceramic hotplate stirrer is an advanced laboratory device designed to efficiently dissolve or mix material components through controlled heating and magnetic stirring. The instrument features two control knobs—typically located on the front panel—where the left knob regulates the heating element, and the right knob adjusts the rotational speed (RPM) of the magnetic stirrer, as illustrated in Fig. 4.7. The stirring mechanism operates via a magnetic field generated between a rotating magnetic field beneath the ceramic plate and a magnetic stir bar placed inside a beaker containing the sample. As the magnetic field interacts with the stir bar, it induces rotational motion, thereby promoting uniform mixing. The speed of this rotation can be precisely modulated using the stirrer control knob. This dual-action system of thermal and magnetic agitation facilitates the dissolution of most substances, except those with extremely high viscosity, which may require specialized equipment. The hotplate can reach a maximum temperature of 380 °C, while the stirring speed ranges from 200 to 2000 RPM. The heating control knob modulates the surface temperature of the ceramic

plate, and the stirrer knob adjusts the speed of the magnetic field to suit experimental requirements, as depicted in Fig. 4.7. The unit supports a maximum working volume of 5000 mL and features a ceramic plate with dimensions of 190 × 190 mm. It delivers a heating power of 600 watts, providing robust and consistent thermal energy for a variety of chemical and materials processing applications.

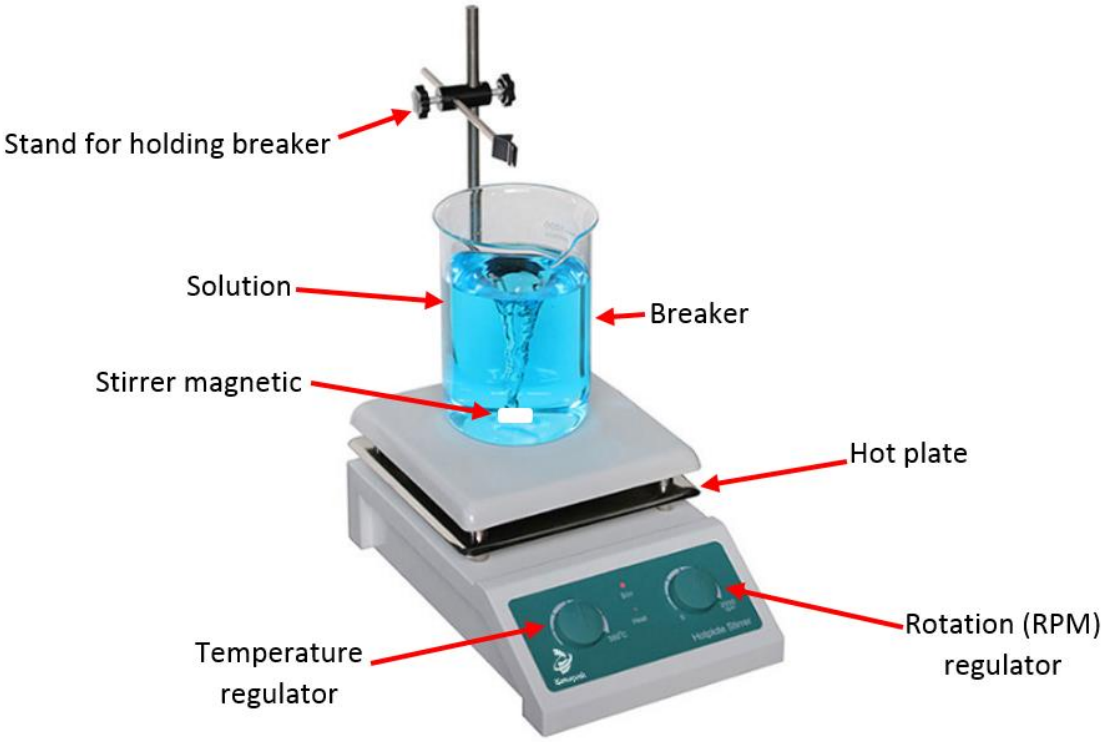

Fig 4.6: Illustration of ceramic hotplate stirrer system

4.7. Inkjet Printing

An inkjet printer is a precise and efficient tool for fabricating strain sensors by depositing functional inks—comprising solvents, nanoparticles, and auxiliary agents—onto insulating substrates to form sensor grids. This technique offers high spatial resolution, rapid processing, and minimal material waste compared to traditional methods like hydrogel fabrication or chemical vapor deposition (CVD). Successful implementation requires careful consideration of experimental parameters such as tensile testing, the use of conductive UV-curable resins, and controlled material

application [162]. Inkjet-based fabrication systems are mainly categorized into Direct Ink Writing (DIW) and embedded 3D Printing. DIW employs conductive inks to pattern sensor structures directly, while embedded 3D Printing enables one-step fabrication of flexible strain sensors by embedding conductive materials within a soft matrix, as shown in Fig. 4.8. This method supports efficient, accurate, and scalable production of wearable and stretchable sensing devices.

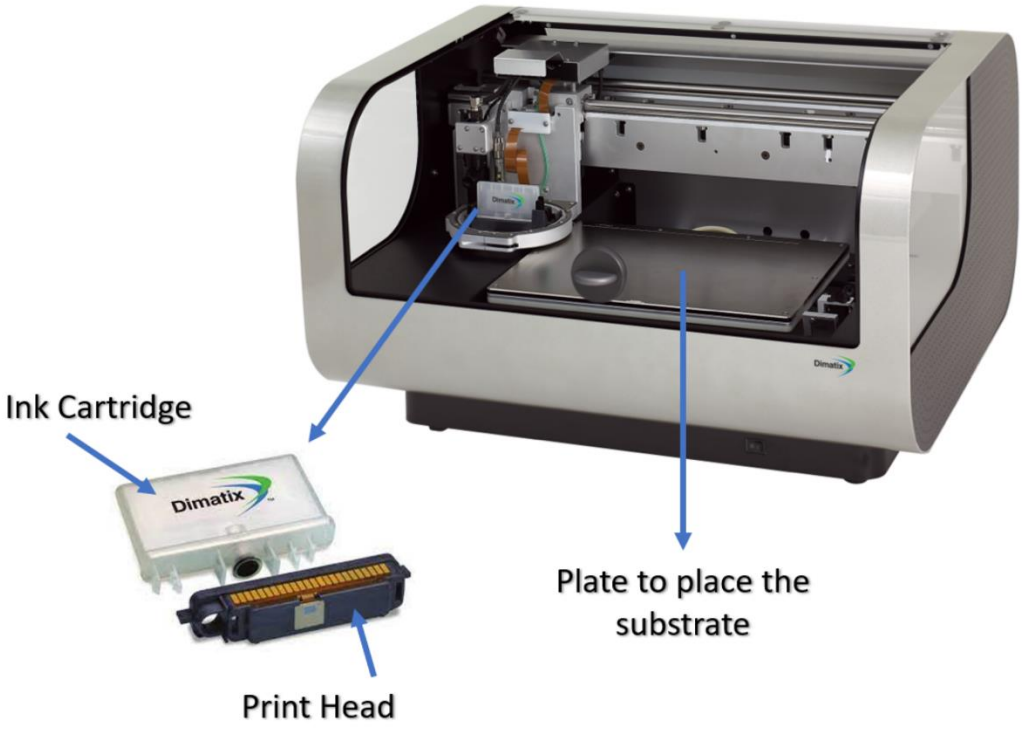

Fig 4.7: Illustration of inkjet printer [162]

4.8. Extensometer (Indigenously Developed)

The Centre of Advanced Electronics and Photovoltaic Engineering (CAEPE) houses a custom-built mechanical testing assembly specifically designed to evaluate the stretching and bending performance of the proposed strain sensor. This locally developed setup features a precision stretching machine, where the sensor is mounted between two clamps—one fixed to hold one end of the sensor and the other movable to apply controlled stretching to the opposite end. The movement of the adjustable clamp is precisely regulated by an Arduino UNO microcontroller, enabling smooth and accurate displacement on a millimeter scale. An H-bridge circuit is integrated to manage the operation of a stepper motor that drives the movable clamp. For visual inspection of strain during testing, a magnifying glass is employed to observe the

sensor's deformation. Additionally, a touch-enabled LED display is incorporated into the system, allowing users to select and execute various test protocols, including cyclic stretching and releasing tests (e.g., 100–300 cycles), response and recovery time measurements, mechanical durability, stability assessments, and open-circuit evaluations. This mechanical setup provides a comprehensive platform for assessing the functional and structural integrity of the proposed strain sensor under diverse mechanical stress conditions, as illustrated in Fig. 4.9.

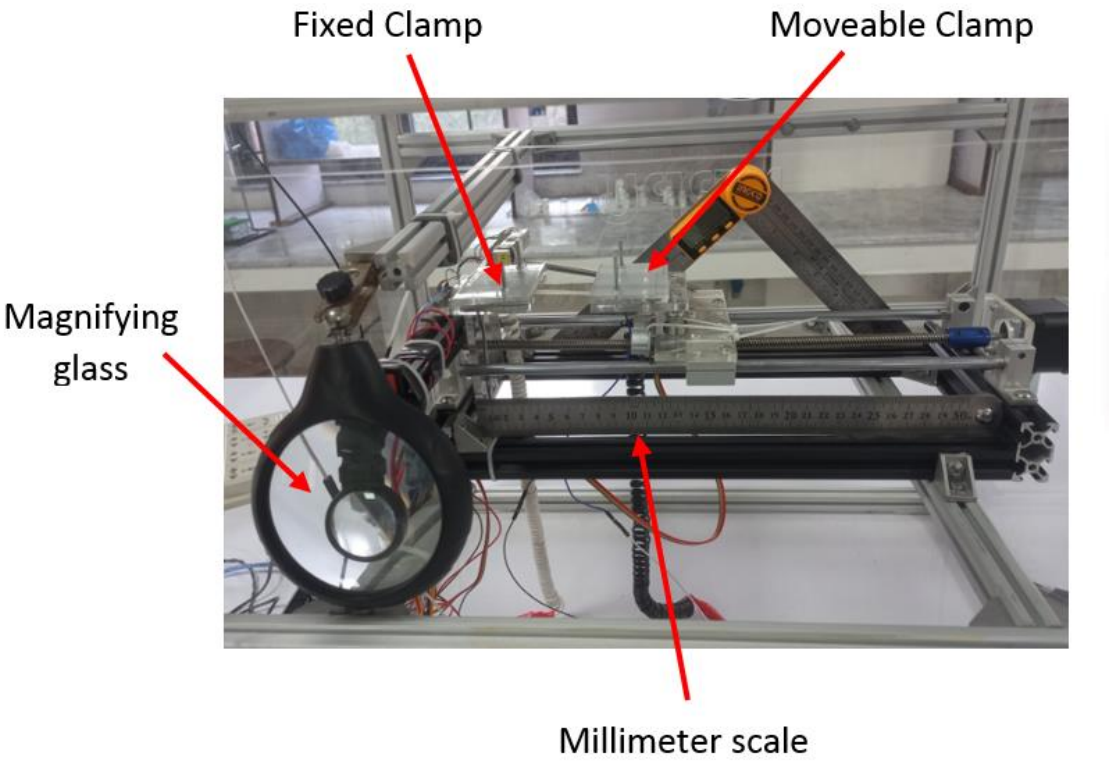

Fig 4.8: Indigenously developed mechanical assembly setup used for stretching/releasing the proposed strain sensor

4.9. Summary

The fabrication of flexible self-healing strain sensors is carried out using inkjet printing technology, with careful attention given to sample geometry and material composition through detailed analytical evaluation (ultimate analysis). To enable mechanical and electrical characterization, it is essential that strain sensors are equipped with conductive contacts. For this purpose, magnetron sputtering is employed to deposit copper electrodes onto the fabricated flexible sensors, ensuring reliable interfacing with external testing systems. At the Centre of Advanced Electronics and Photovoltaic Engineering (CAEPE), a dedicated experimental assembly has been developed for

comprehensive evaluation of the strain sensor's performance, including mechanical properties such as cutting resistance, self-healing behavior, and stretchability, as well as electrical responsiveness. Furthermore, Scanning Electron Microscopy (SEM) is utilized to investigate the surface morphology and assess the nanoparticle distribution within the sensor material. SEM imaging plays a critical role in analyzing the bonding quality before and after self-healing, offering in-depth insights into the nanoscale structural integrity and functional recovery of the sensor. Table 4.1 provided the all experimental techniques used in my research advantages and disadvantages as given below.

Table 4.1: Enlist experimental techniques advantages and disadvantages

Experimental Techniques	**Advantages**	**Disadvantages**
Spin coater	Fast process Less material used	Suitable for low viscosity solutions Limited to small substrate
Scanning electron microscope (SEM)	Good resolution imaging Extract surface morphology	Required vacuum Expensive
Current voltage (IV) technique	Provide electrical parameters Simple Implement	Doesn't give surface morphology data Limited to electrical parameters
Digital magnetic stirrer system	Uniform mixing Compact	Stirring volume is limited Not recommended for high viscosity fluids
Extensometer	Extract multiple mechanical and electrical property of strain sensor Compact and high accuracy	Complex circuit sensitive
X-Ray Diffraction (XRD) system	In lattice spacing high accuracy Non-destructive	Not recommended for amorphous materials Costly Equipment

Chapter 5

Experiments, Results and Discussion

5.1.1. Fe_2O_3/Ag flakes and polyurethane sensors

- **Materials**

Strain sensors have become indispensable components in a wide range of emerging technologies, particularly in wearable electronics, soft robotics, and biomedical systems. Their ability to convert mechanical deformation into readable electrical signals makes them crucial for applications such as health monitoring, motion tracking, prosthetics, and human-machine interfaces. Despite the tremendous potential, most conventional strain sensors face several unresolved challenges, including poor mechanical robustness, inadequate tolerance to environmental conditions such as freezing, fragile conductive pathways, and lack of multifunctionality such as self-healing or responsiveness to magnetic fields. These limitations restrict the sensors' durability and usability in long-term, real-world applications, especially in dynamic or unpredictable environments.

To address these critical shortcomings, the present study proposes a novel design that integrates ferric oxide (Fe_2 O_3) and silver (Ag) flakes as the active nanocomposite sensing layer, embedded on a polyurethane (PU) substrate, with an outer PU encapsulation. The resulting sensor architecture is lightweight, flexible, self-healable, and magnetically responsive, tailored to endure repeated deformation and mechanical damage while maintaining high sensitivity. Now, the process of creating self-healing strain sensors is still in its infancy, so new materials and preparation approaches are required to boost the sensitivity, stamina, and capability of these sensors to self-heal [163,164]. In the making of a self-healing strain sensor, the various layered as well as intercalated materials-based sensors are widely studied, comprising conductive polymers, carbon nanomaterial and magnetic nanoparticles [165,166]. PU is well known for its exceptional elasticity, mechanical durability, and biocompatibility, making it a go-to material for applications that require consistent performance under strain [167,168]. Additionally, PU can be engineered for enhanced functionality by incorporating additives such as crosslinking agents, reinforcing fillers, and healing agents, allowing precise control over its mechanical behavior and healing capabilities [169,170]. A key innovation in this sensor design is the incorporation of magnetic iron oxide nanoparticles (MIONPs) into the PU matrix. These particles contribute

significantly to the sensor's self-healing properties by enabling magnetically-induced molecular alignment during damage recovery. When an external magnetic field is applied, the MIONPs facilitate the reorientation and reconnection of polymer chains, accelerating the healing process and restoring electrical pathways a mechanism supported by prior literature on magnetic self-healing composites [171,172]. This magneto-responsive behavior not only enhances reliability and longevity but also adds an intelligent feature to the sensor for remotely triggered repair or real-time control.

To establish the necessary electrical conductivity, the sensor leverages a hybrid combination of graphene oxide (GO) and silver nanoparticles (AgNPs). GO provides a highly flexible, percolative network structure that ensures mechanical compliance with the substrate, while AgNPs offer superior electron mobility and conductivity, thereby forming an integrated conductive pathway that is highly sensitive to strain. This dual-phase conductive layer dynamically responds to applied mechanical forces, resulting in significant and detectable changes in resistance an essential property for high-performance strain sensors [164].

Overall, the synergistic integration of PU, MIONPs, GO, and Ag flakes results in a strain sensor that overcomes multiple limitations of existing technologies. Table 5.1 provides a comparative overview of materials, their quantities, and roles based on recent literature, reinforcing the rationale behind the material selection for the current study.

Table 5.1: Overview of Polymer Materials used in Previous Studies for Self-Healing and Sensing Applications

Reference	Material	Quantity of Material	Self-Healing Application	Sensor
[163]	Polyurethane	10 g	Substrate for self-healing sensor	Yes
[163]	Magnetic iron oxide nanoparticles	2 g	Embedded in polyurethane for magnetic self-healing	Yes
[164]	Graphene oxide	0.1 g	Conductive material for sensor	Yes
[164]	Silver nanoparticles	0.05 g	Conductive material for sensor	Yes
[165]	Gelatin	5 g	Self-healing hydrogel for biomedical application	No
[165]	Chitosan	2 g	Crosslinking agent for gelatin hydrogel	No
[166]	Polyvinyl alcohol	10 g	Self-healing polymer for drug delivery	No
[166]	Borax	0.1 g	Crosslinking agent for polyvinyl alcohol	No
This Work	PU + Fe_2O_3+Ag Flakes	5g+1g+0.5g	Self-healable strain sensor for Biomedical applications	Yes

- **Fabrication**

The fabrication process of the proposed flexible self-healable strain sensor involves a multi-step procedure designed to ensure uniform dispersion of functional materials and to maximize mechanical integrity, electrical conductivity, and healing efficiency. The process begins with the homogenization of polyurethane (PU) serving as the primary matrix—with magnetic iron oxide nanoparticles (MIONPs) and conductive nanomaterials such as silver (Ag) flakes and graphene oxide (GO). This homogenization is carried out using mechanical stirring followed by sonication to ensure uniform dispersion of nanoparticles and prevent agglomeration, which is crucial for maintaining consistent sensing performance throughout the sensor's surface.

Once a stable nanocomposite solution is prepared, it is then cast into molds or onto planar substrates to form thin films. These films are cured thermally under controlled temperature and humidity conditions to allow crosslinking and solidification of the PU matrix. Curing not only solidifies the sensor geometry but also ensures the mechanical bonding between PU chains and embedded nanoparticles, thereby enhancing the elastic recovery and self-healing capability of the sensor. Post-curing, the sensor film is patterned or laser-cut into the desired geometry, allowing for integration into various wearable or structural configurations.

To enhance environmental resilience, the fabricated strain-sensitive layer is fully encapsulated with an additional PU layer, forming a sandwich structure. This encapsulation not only protects the sensor from humidity, oxidation, and mechanical abrasion but also preserves its flexibility and stretchability, which are essential for dynamic applications such as human motion tracking.

A distinguishing feature of this fabrication process is the use of Electrohydrodynamic (EHD) jet printing for forming high-resolution conductive mesh structures. This technique employs conductive inks—specifically silver nanowires (AgNWs)—to print patterns with resolutions as fine as 5 micrometers [173]. EHD printing relies on the precise control of electric field strength, ink flow rate, nozzle-to-substrate distance, and stage velocity, each of which is carefully optimized to achieve high pattern fidelity. Following printing, the printed layers undergo plasma surface treatment, which significantly enhances the adhesion of AgNWs to the elastomeric PU substrate. This treatment improves the mechanical interlocking between nanowires and polymer

chains, resulting in greater long-term mechanical durability under cyclic strain conditions.

The combined use of solution casting, nanoparticle dispersion, EHD printing, plasma treatment, and encapsulation results in a multifunctional sensor that is not only mechanically robust and flexible, but also exhibits long-term reliability, high resolution, and resistance to environmental stressors [174-176]. This comprehensive fabrication approach enables the realization of next-generation self-healable strain sensors for smart wearables and adaptive electronics.

Polymer composites, with their desirable properties and the availability of natural and synthetic reinforcements, are quickly emerging as a critical class of materials for various industrial uses. Fabricating polymer composites traditionally requires expensive equipment, time-consuming handwork, and a higher price tag [177-179]. As a result of this study [180], 3D printing technologies have gained popularity across disciplines and industries to mass-produce high-precision composite components that meet demanding design and processing criteria. Scientists are striving to improve the performance and durability of 3D printed materials by adding reinforcements and self-healing characteristics to counteract the effects of poor interfacial adhesion between printed layers. As a technique to boost the mechanical characteristics and durability of polymer materials, 3D printing of polymer composites is gaining popularity. A critical takeaway from this research is understanding the range of materials available for 3D printing polymer composites. Soft robotics and the 3D printing of flexible energy-storage devices (FESD) such as batteries and supercapacitors are also covered. Several polymer materials are employed in 3D printing for bioengineering and earth science [181-186].

- **Experiment**

The fabricated sensor was evaluated for electrical, mechanical, magnetic, and healing properties. Real-time motion detection was tested by attaching sensors to various body parts (forehead, knee, elbow, fingers), tested data is given in table 5.2.

Table 5.2: Various human bodies are tested through proposed strain sensor

Parameters	Details
Number of participants	15
Age Range	18-50 years
Gender segregation	10 Males and 5 Females
Examination parts	Fingers,Knee,Forehead and Elbow
Observations	Stable Mechanical and Electrical Signals reliability across all age of groups

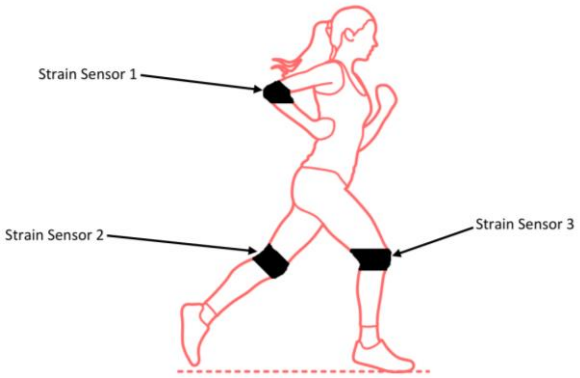

Fig 5.1: Placement of strain sensors on the human body. Strain Sensor 1 is positioned on the arm, Strain Sensor 2 on the thigh, and Strain Sensor 3 on the knee to monitor strain and movement during physical activity

As shown in Fig. 5.1 proposed strain sensor is place in left and right legs similarly on the arms. Therefore the real time senor performance is illustrated in table 5.3.

Table 5.3: Proposed sensor performance on limbs (Arms and Legs)

Tested Body Part	Observed Signal Response	Sensor performance	Remarks
Left Arm	Clear Resistance variation during bending and walking motions	High Sensitivity	Stable after repeated cycles
Right Arm	Similar Signal response to left leg during identical motion patterns	Stable performance	Minor baseline drift
Left Leg	Response to elbow wrist and flexion movement	Fast recovery time	Good linearity
Right Leg	Symmetrical signal response to left leg	Maintained performance after repeated cycles	Shows endurance

The mechanical properties of the sensor were analyzed using tensile testing to determine Young's modulus, maximum stress, and strain capacity. For electrical properties, resistance changes were measured under mechanical deformation to compute the gauge factor. To test self-healing, sensors were deliberately damaged, and the recovery of resistance and sensitivity was tracked over 24 hours.

The material composition of the sensor includes less than 10% MIONPs by weight, ensuring minimal load without sacrificing responsiveness. Conductive components such as carbon nanotubes and silver flakes were optionally intercalated to improve conductivity. Solvents like toluene were used to achieve uniform nanoparticle dispersion in the PU matrix.

- **Results**

The fabricated self-healable strain sensor exhibited remarkable electromechanical performance across a range of critical parameters, validating its robustness, sensitivity, and adaptability in real-world applications. One of the most notable features is its

exceptional Gauge Factor (GF) of 271.4 at 35% strain, demonstrating ultra-high sensitivity to mechanical deformation. This high GF signifies the sensor's ability to detect even subtle strain variations, which is essential for applications in wearable electronics and robotics where precision is key. Additionally, the Young's modulus of 3.17 MPa indicates a desirable balance between mechanical strength and flexibility, enabling the sensor to endure repeated deformations without fracturing. The maximum strain tolerance of 47% and maximum stress limit of 0.67 MPa further reflect the sensor's excellent elasticity and structural integrity under tensile loading conditions. These mechanical properties ensure that the sensor can sustain substantial physical deformation while maintaining functional accuracy and continuity.

Beyond mechanical performance, the sensor also excels in healing and magnetic responsiveness, which enhances its applicability in dynamic and harsh environments. The self-healing capability of the sensor was evaluated through multiple recovery cycles, where it achieved a healing efficiency of 96.6% after 24 hours, showcasing its ability to autonomously restore functionality following mechanical damage. This trait is critical for long-term deployment in scenarios where maintenance access is limited. Furthermore, the incorporation of magnetic iron oxide nanoparticles enabled the sensor to exhibit magnetic sensitivity of 0.0049 T^{-1}, which makes it responsive to external magnetic fields. This magnetic responsiveness not only aids in remote actuation or alignment during healing but also opens avenues for multi-functional sensing mechanisms, such as combining strain and magnetic field detection. Together, these performance metrics affirm the sensor's suitability for advanced applications in bio-integrated electronics, soft robotics, and intelligent monitoring systems.

- **Discussion**

This work presents a comprehensive solution to the existing challenges in strain sensing. The integration of magnetic iron oxide nanoparticles within a polyurethane matrix strengthens the sensor mechanically while enabling remote magnetic actuation. The high GF value signifies the sensor's ability to detect small deformations—ideal for wearable devices and robotics.

Compared to previous studies where GF was limited to ~150 at 25% strain [187], the developed sensor exceeds both in sensitivity and healing efficiency. Previous healing efficiencies capped at 80% after 48 hours [188], whereas the proposed design achieved 96.6% in half the time.

MIONPs play a pivotal role in both conductivity and healing. They align under magnetic fields, promoting reconnection across the polymer matrix. Simultaneously, their high susceptibility to magnetic flux improves electromechanical coupling, crucial for real-time feedback.

The combination of high flexibility, biocompatibility, and robustness makes this sensor a strong candidate for applications in healthcare (rehabilitation monitoring, posture tracking), robotics (tactile feedback), and soft electronics (flexible circuits, human-machine interfaces).

This study also highlights the growing role of additive manufacturing techniques like EHD jet printing for next-generation sensor fabrication. It provides a path forward for developing cost-effective, scalable, and high-precision sensors with complex features like self-healing and magnetic response. The strain sensor's ability to recover functionality after damage aligns to create self-repairing technologies.

5.1.2 Methodology

This section outlines the materials and fabrication process of the flexible self-healable strain sensor embedded with magnetic iron oxide nanoparticles (MIONPs) and silver flakes on to polyurethane (PU) substrate. Each process step is presented in detail, explaining the choice of materials and the corresponding fabrication procedure. Fig 5.2 showcases the proposed workflow for developing and evaluating the wearable self-healable strain sensor.

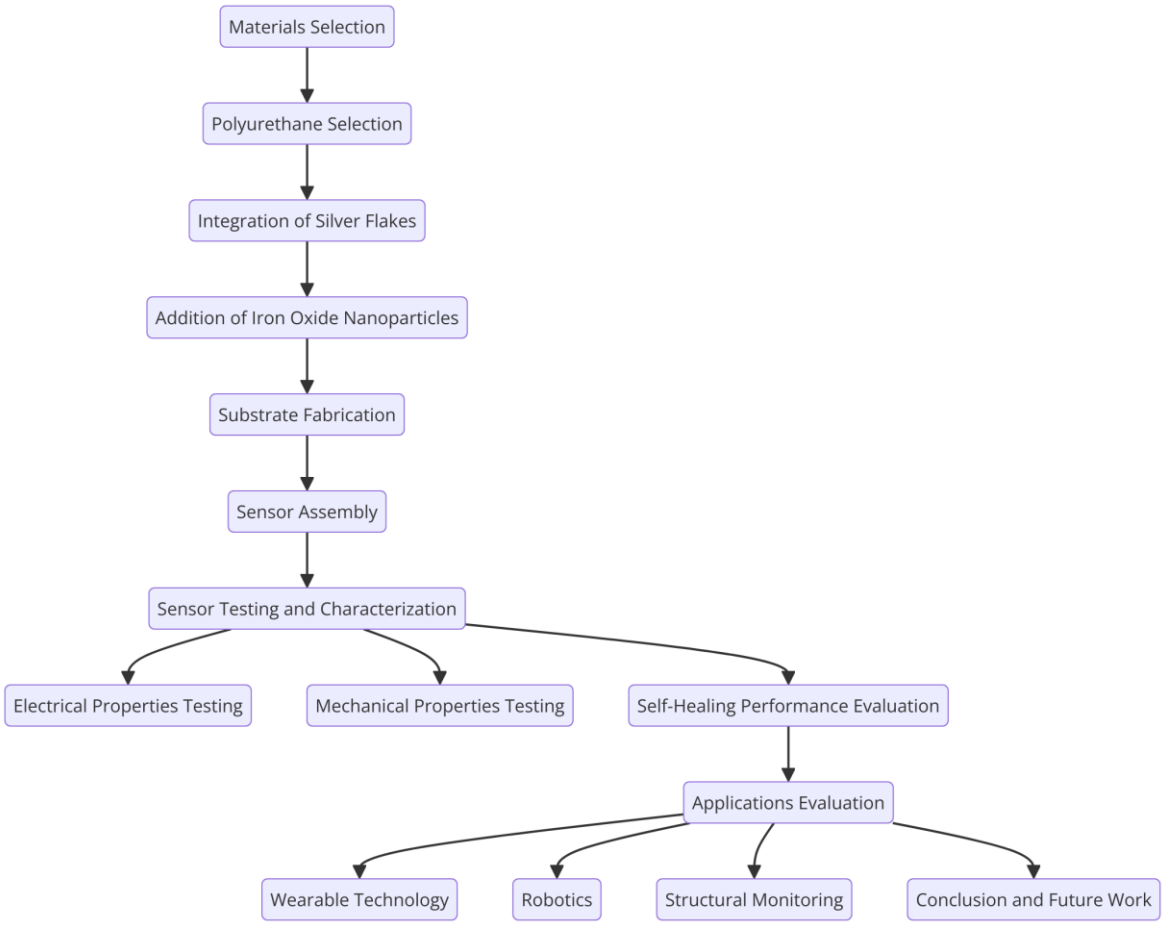

Fig 5.2: Proposed workflow for the development and evaluation of the wearable self-Healable strain sensor

5.1.2.1. Overview

This section provides a comprehensive account of the methodology for fabricating the self-healable strain sensor. The sensor's construction involves a meticulous layer-by-layer approach, utilizing specific materials and techniques to achieve the desired properties. Stress has a significant impact on the strain sensor mechanical structure, as shown in Fig 5.3 below:

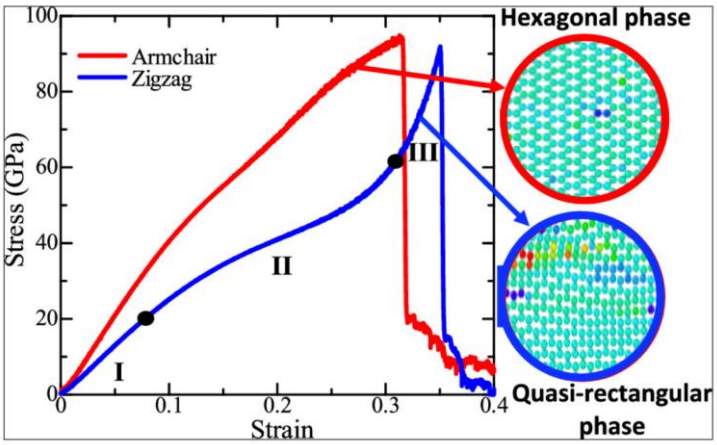

Fig 5.3: Stress-strain curve showing mechanical damage and phase transition under stress. we describe this process in depth to ensure a clear understanding of the sensors fabrication

The application of stress impacts strain sensors by changing their electrical or mechanical characteristics in relation to the outside force. An external force causing stress is likely to result in a corresponding increase in strain which will change the sensor's optical, capacitance, or even resistance properties. Too much or excessive stress is likely to lead to non-linearity, hysteresis, mechanical fatigue, which in turn decreases the sensor's accuracy and lifespan as obvious from Fig 5.3. Sensor design and the material used are important for stress-related performance and operational efficiency because the sensor is likely to be exposed to varying conditions

5.1.2.2. Material Selection

Polyurethane (PU) was selected as the substrate material due to its flexibility, mechanical durability, and biocompatibility. These properties make it ideal for wearable sensor applications that require repeated deformation without compromising structural integrity. Compared to other materials like polydimethylsiloxane (PDMS) or elastomers, PU was chosen because of its superior ability to self-heal through the reversible urea bonds within its structure, allowing the sensor to recover after mechanical damage [167,168].

Silver flakes (Ag flakes) were incorporated as the conductive material due to their high electrical conductivity, which is crucial for detecting mechanical strain. Silver's conductivity surpasses that of most metals in similar applications, making it optimal for sensitive strain sensing.

Magnetic iron oxide nanoparticles (Fe_2O_3) were added to enhance both the mechanical and electrical properties of the sensor. These nanoparticles act as cross-linkers in the PU matrix, improving the material's mechanical strength. Furthermore, their magnetic properties enable the sensor to respond to external magnetic fields, broadening its functionality [169-171].

In the Fig 5.4 the key layer is composed of Iron Oxide (Fe_2O_3). This magnetic nanomaterial plays a dual role. It enhances the mechanical properties of the sensor by acting as a cross-linker within the PU matrix, increasing its overall strength. Simultaneously, it adds magnetic responsiveness to the strain sensor, contributing to its multifunctional nature. The fabrication process is summarized in Figure 5.4, showing the layer-by-layer assembly of the strain sensor. Each layer is critical, from the flexible PU substrate to the conductive silver flakes and magnetic iron oxide nanoparticles.

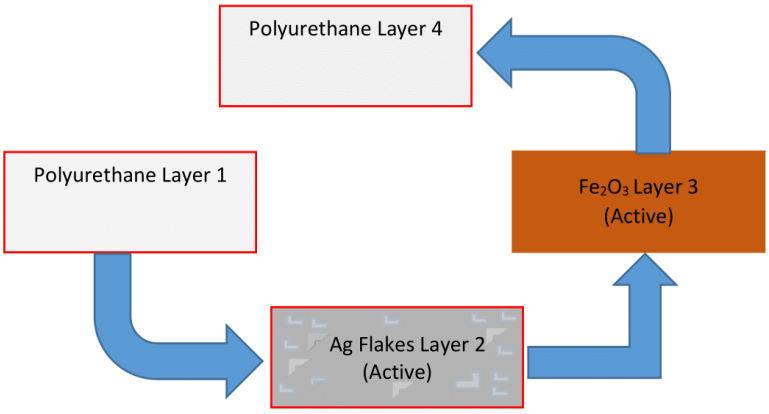

Fig 5.4: Layer-by-layer fabrication diagram of the flexible self-healable strain sensor

Combining these materials enables the sensor to exhibit self-healing properties, high sensitivity to mechanical strain, and responsiveness to an external magnetic field. The study aims to describe the experimental procedure, including preparing the polyurethane substrate, synthesizing the magnetic iron oxide nanocomposite, and fabricating the strain sensor. This methodology could be a foundation for further investigations into self-repairing wearable strain sensors and their potential applications in various fields, including healthcare and robotics.

1st Layer - Polyurethane (PU):

The first layer of the sensor is made of Polyurethane (PU). Polyurethane is a flexible and durable polymer that acts as the pedestal for the entire sensor. It provides the foundation for the subsequent layers and contributes to the sensor's overall mechanical

properties. The chemical structure of polyurethane involves the reaction between polyols (P) and isocyanates (I), forming urethane bonds.

2nd Layer - Silver Flakes (Ag Flakes):

The second layer consists of Silver Flakes (Ag Flakes). Silver is a highly conductive material and incorporating it in flake form enhances the sensor's electrical conductivity. This layer acts as a conductive trace, allowing the sensor to detect mechanical strain through changes in resistance. The chemical symbol for silver is Ag.

3rd Layer - Iron Oxide (Fe_2O_3-Active Layer):

The third layer comprises Iron Oxide (Fe_2O_3), which serves as the sensor's active layer. Iron oxide nanoparticles exhibit unique properties that make them sensitive to mechanical strain and magnetic fields. This layer contributes to the sensor's responsiveness to external magnetic fields and enhances its sensitivity to mechanical deformations. The chemical formula for Iron Oxide is Fe_2O_3.

4th Layer - Polyurethane (PU):

The fourth layer is another Polyurethane (PU) layer, which encapsulates the active layer (Ag Flakes and Fe_2O_3). This encapsulation is a protective barrier, making the active layer waterproof and preventing moisture from affecting the sensor's performance. The encapsulation process involves applying an additional layer of polyurethane to the top of the active layer.

- **Explanation of the Active Layer - Ag Flakes and Fe2O3:**

The active layer of the sensor consists of both Silver Flakes (Ag Flakes) and Iron Oxide (Fe_2O_3). This combination imparts the sensor with dual functionalities - sensitivity to mechanical strain and responsiveness to external magnetic fields.

- **Silver Flakes (Ag Flakes):**

These flakes contribute to the sensor's electrical conductivity and mechanical flexibility. As the sensor undergoes mechanical strain, the arrangement of Ag Flakes can change, leading to variations in electrical resistance. This change in resistance is the basis for strain sensing.

- **Iron Oxide (Fe_2O_3):**

Iron oxide nanoparticles possess magnetic properties. When an external magnetic field is applied, the arrangement of these nanoparticles within the active layer can be influenced, causing changes in the sensor's electrical properties. This responsiveness to magnetic fields adds dimension to the sensor's capabilities.

The overall construction of the sensor involves layering these materials in a specific order to achieve the desired functionality. The polyurethane layers provide mechanical support and encapsulation, the silver flakes enable conductivity, and the iron oxide nanoparticles enhance sensitivity to mechanical strain and magnetic fields.

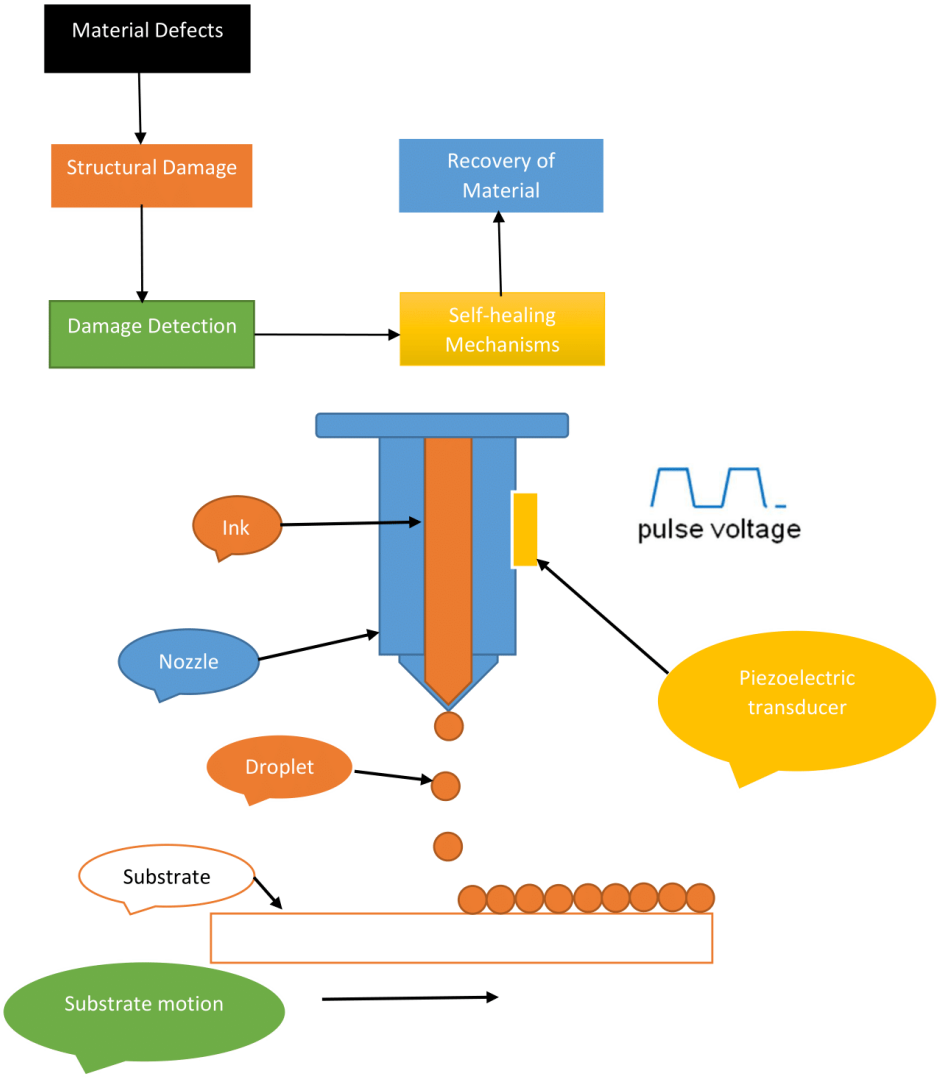

Fig 5.5: Fabrication process using inkjet printing technology combined with self-healing mechanisms for a strain sensor

Fig 5.5 illustrates the step-by-step process of fabricating the flexible self-healable strain sensor. The method incorporates several layers, each serving a specific purpose in enhancing the sensor's performance.

5.1.2.3. Fabrication Process

Fig 5.5 illustrates the step-by-step process of fabricating the flexible self-healable strain sensor. The method incorporates several layers, each serving a specific purpose in enhancing the sensor's performance.

The construction of the self-healing strain sensor involved a multi-step, layer-by-layer approach, with each layer serving a specific role in the sensor's performance.

Step 1: Preparation of PU Substrate

The PU substrate was synthesized using a two-step process:

Formation of PU Pre-polymer: Polyol (P) and isocyanate (I) were mixed in a 1:2 molar ratio to form a pre-polymer solution. The reaction between the two components results in the formation of urethane bonds, creating the PU pre-polymer:

$$P + 2I \rightarrow [P - (N = C = O)n - I]prepolymer \qquad (5.1)$$

Crosslinking: The pre-polymer was crosslinked with 1, 4-butanediol (BD), forming a three-dimensional network structure with reversible urea bonds. These bonds are critical for the sensor's self-healing capability:

$$[P - (N = C = O)n - I]pre - polymer + 2BD \rightarrow [P - (NH - CO - NH)n - P - (OH)n]PU\ substrate \qquad (5.2)$$

Step 2: Embedding Silver Flakes

The silver flakes were homogeneously dispersed into the PU pre-polymer before it solidified. The PU mixture was stirred thoroughly during the embedding process to ensure an even distribution. The flakes form conductive pathways throughout the substrate, and this conductive network is crucial for strain sensing.

Step 3: Incorporation of Magnetic Iron Oxide Nanoparticles (MIONPs)

Magnetic iron oxide nanoparticles were synthesized using the co-precipitation method, wherein a solution of $FeCl_2$ and $FeCl_3$ (in a 1:2 molar ratio) was mixed with ammonium hydroxide (NH_4OH) under constant stirring at 70°C. The resulting Fe_2O_3 nanoparticles were washed and dried before being mixed into the PU solution. These nanoparticles serve as cross-linkers that improve the mechanical strength of the PU matrix while providing magnetic responsiveness:

$$FeCl^3 + FeCl^2 + NH^4OH \rightarrow Fe^2O^3(MIONPs) \qquad (5.3)$$

Step 4: Encapsulation of Active Layer

The sensor's active layer, composed of the silver flakes and MIONPs embedded in the PU substrate, was encapsulated with an additional layer of PU to protect it from environmental factors such as moisture. This layer also enhances the sensor's mechanical integrity.

Step 5: Curing Process

The entire sensor was then cured at 90°C for 2 hours. This process ensures that the PU substrate fully solidifies and that the conductive silver flakes form a stable pathway for electrical conductivity. The first layer, the PU substrate, is prepared through a two-step process. Initially, a pre-polymer solution is created by mixing a polyol (P) and an isocyanate (I) in a 1:2 molar ratio. This mixture undergoes a chemical reaction, forming urethane bonds and creating the PU pre-polymer.

In the second step, the PU pre-polymer is crosslinked with a chain extender, which is 1, 4-butanediol (BD) in our study. This results in the formation of urea bonds and the three-dimensional network structure of the self-healable PU substrate.

The synthesized PU substrate is characterized by its self-healing ability. The reversible urea bonds enable the material to be repaired when subjected to mechanical damage. This unique feature is fundamental to the sensor's longevity and adaptability. The second layer involves embedding Ag flakes into the PU substrate. This is achieved by carefully dispersing the Ag flakes into the PU mixture before solidifying. This process ensures a homogeneous distribution of Ag flakes within the PU, forming a conductive pathway. The third layer introduces magnetic responsiveness to the sensor. Magnetic Iron Oxide nanoparticles (Fe_2O_3) are synthesized through a co-precipitation method. These Fe_2O_3 nanoparticles are then incorporated into the PU substrate. The nanoparticles act as cross-linkers, enhancing the mechanical properties of the PU substrate. The final step involves encapsulating the active layer (Ag and Fe_2O_3) with another layer of PU. This protective encapsulation waterproofs the sensor and reinforces its mechanical integrity.

The resulting construction is a multi-layered flexible self-healable strain sensor with exceptional sensitivity, self-healing capability, magnetic responsiveness, and robust mechanical properties. Combining these materials and layers results in a versatile

sensor with potential applications across various fields. Fig 5.6 shows the complete fabrication process of self-healing:

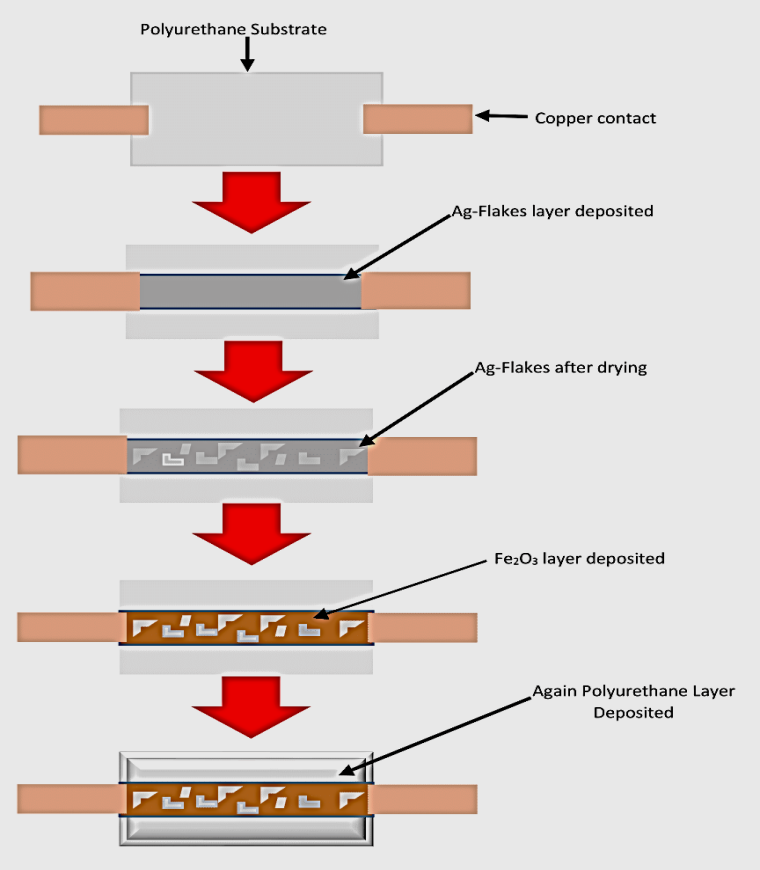

Fig 5.6: Comprehensive layer-by-layer fabrication process for constructing self-healing strain sensor

Fig 5.6 provides an overview of the entire process of creating a self-healing strain sensor. It encompasses the fabrication, activation, and self-healing stages.

- **Polyurethane (PU) Crystal Plate**

The foundation of our self-healing material structure is the Polyurethane (PU) crystal plate. PU was chosen for its exceptional flexibility and mechanical resilience, which allowed the material to withstand deformation and revert to its original state. This aligns perfectly with the self-healing concept.

- **Silver (Ag) Flakes**

Silver flakes (Ag) are incorporated into the material structure to introduce conductivity. These micro-sized Ag flakes are meticulously embedded into the PU substrate to create a conductive pathway, ensuring electrical conductivity.

- **Iron Oxide (Fe_2O_3)**

Iron Oxide (Fe_2O_3) serves a dual purpose by fortifying the material structure. As a cross-linker within the PU matrix, it enhances the mechanical properties, strengthening the structure. Simultaneously, Fe_2O_3 imparts magnetic responsiveness, a pivotal characteristic for multifunctional applications.

Step 1: Synthesis of PU Substrate

Construction begins with the synthesis of the PU substrate, which is a two-step process. Firstly, a pre-polymer solution is formed by mixing polyol (P) and isocyanate (I) in a 1:2 molar ratio. This solution forms urethane bonds, yielding the PU pre-polymer.

The PU substrate is characterized by its self-healing capacity, an inherent feature due to the reversible urea bonds. This self-healing ability is fundamental for maintaining the material's integrity.

Step 2: Integration of Ag Flakes

The second step involves incorporating Ag flakes into the PU substrate. Ag flakes are uniformly dispersed within the PU mixture before solidifying, ensuring a homogeneous distribution and forming a conductive pathway.

Step 3: Deposition of Fe_2O_3 Layer

The material structure is reinforced with a layer of magnetic responsiveness. Magnetic Iron Oxide nanoparticles (Fe_2O_3) are synthesized using the co-precipitation method, as detailed in the paper. These Fe_2O_3 nanoparticles are incorporated into the PU substrate, functioning as cross-linkers to enhance mechanical properties.

Step 4: Encapsulation with PU

In the final step, the active layer (Ag and Fe_2O_3) is encapsulated within another layer of PU. This encapsulation serves the dual purpose of waterproofing the material structure and providing additional mechanical reinforcement.

Material Structure and Self-Healing Process Diagram:

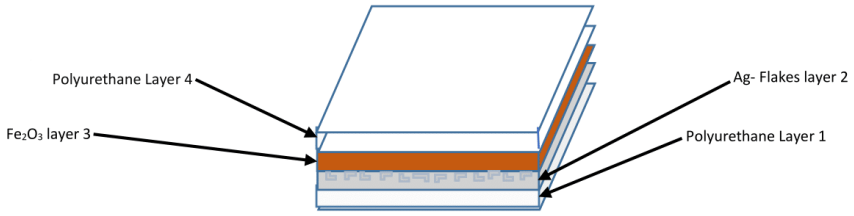

Fig 5.7: Layered structure of the flexible self-Healable strain sensor

The synthesis of the polyurethane (PU) substrate involves a two-step process, as shown in Fig 5.7, where each step plays a crucial role in the sensor's performance. In the first step, a pre-polymer solution is formed by reacting polyol (P) and isocyanate (I) in a 1:2 molar ratio. This reaction produces urethane bonds, providing the PU substrate with initial flexibility and mechanical strength. These bonds allow the material to endure mechanical deformations without sustaining permanent damage, making it ideal for applications requiring high flexibility, such as wearable strain sensors. However, the material lacks the structure for self-healing capabilities at this stage.

The second step involves crosslinking the pre-polymer with 1, 4-butanediol (BD), a chain extender that creates urea bonds, resulting in a three-dimensional network structure. These urea bonds are reversible, which means they can break and reform in response to mechanical damage. This characteristic enables the material to heal when damaged, restoring its original properties. The ability to self-heal significantly extends the sensor's lifespan by allowing it to recover its functionality after damage.

Together, the two steps provide the sensor with flexibility and self-healing capabilities. The urethane bonds from the first step give the substrate the flexibility required to handle mechanical strain. In contrast, the reversible urea bonds introduced in the second step enable self-repair, ensuring durability and reducing the need for maintenance. This combination is critical to the overall performance and reliability of the flexible self-healing strain sensor.

Fig 5.7 illustrates the layered composition of the material structure, with PU forming the base, Ag flakes providing conductivity, Fe_2O_3 imparting magnetic responsiveness, and a protective PU layer encapsulating the active elements. The interplay of these layers forms the foundation of the self-healing process.

This detailed methodology section systematically explains the step-by-step construction of the self-healing material structure, underlining the rationale behind material selection and emphasizing the self-healing properties inherent to the structure. It provides a solid basis for understanding the subsequent experimental processes and findings discussed in the paper. The figure below shows the development of the Strain sensor in real-time:

Fig 5.8: Physical fabrication of sensor: the detailed process of fabricating the self-healable strain. sensor in two distinct stages

Fig 5.8 is a comprehensive visual guide detailing the step-by-step fabrication of the flexible self-healable strain sensor. It effectively communicates the intricacies of each process, from substrate preparation to ink formulation and final printing, contributing to the overall understanding of the fabrication methodology. This flexible self-healable strain sensor design is innovative and showcases the integration of different materials to achieve a multifunctional and adaptable sensing device. The images depict the physical fabrication process of the self-healable strain sensor. The first image shows a laboratory setup where a reddish solution is stirred and heated on a magnetic stirrer with a hot plate, set at a temperature of 90°C and a stirring speed of 300 RPM. This setup likely involves synthesizing a composite material, possibly including magnetic iron oxide nanoparticles and other components, which are being mixed to form the active sensing material. The second image captures a close-up view of a sensor segment during fabrication. It features a flexible substrate, likely made of polyurethane, with copper electrodes attached. The central focus is depositing the composite mixture's active material between these electrodes. Careful handling by a gloved individual suggests meticulous attention to avoiding contamination and ensuring precision. This stage is

critical as it establishes the core functionality of the sensor, enabling it to detect mechanical strain and exhibit self-healing properties.

5.1.2.4. Statistical Analysis

In this section, we provide a detailed account of the comprehensive statistical analysis undertaken to assess the performance of the flexible self-healable strain sensor. The analysis comprises a meticulous description of the methods used, the statistical tests performed, and the presentation of resulting data through tables.

Our statistical analysis aimed to thoroughly evaluate the performance of the self-healable strain sensor, incorporating various statistical techniques. We initiated our analysis by conducting regression analysis, a crucial technique for modelling the relationship between variables. This technique was employed in our study to elucidate the correlation between mechanical strain and the sensor's output voltage. The regression equation was formulated as follows:

$$Output\ Voltage = \beta 0 + \beta 1 \times Strain \qquad (5.4)$$

In the equation, β0 signifies the interception, while $\beta 1$ represents the slope of the regression line indicating the rate of change in output voltage with respect to applied strain. This approach facilitated precise predictions of the sensor's output voltage in response to applied mechanical strain. A fundamental part of our analysis involved interpreting the data. We used the results of the data analysis to draw significant conclusions about the sensor's performance. For instance, the regression equation was instrumental in predicting the sensor's output voltage for specific strain levels. Our regression analysis delivered substantial insights into the relationship between strain and the sensor's output voltage. The resulting regression equation allows for accurate predictions of the sensor's output voltage in correspondence to mechanical strain levels, as shown in Table 5.4.

Table 5.4: Regression Analysis Results

Regression Coefficient	Value
Intercept (β0)	0.75
Slope (β1)	0.032

Figure 5.9 illustrates the linear relationship between strain and output voltage of the sensor based on regression analysis. As strain increases from 0% to 20%, the output voltage rises steadily, confirming the sensor's predictable and proportional response. The color gradient highlights voltage levels across the strain range, enhancing visual clarity of the sensor's performance trend.

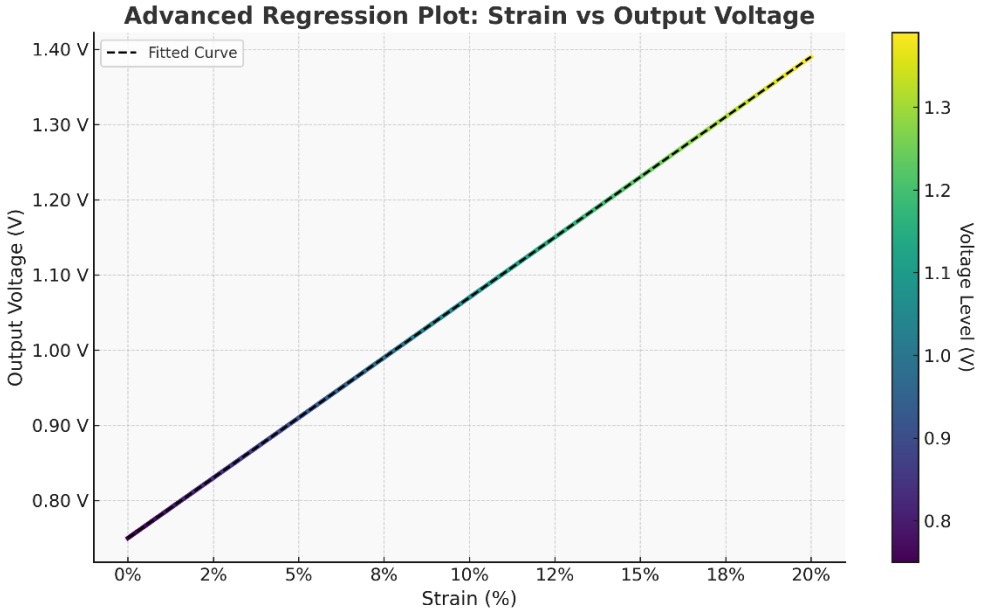

Fig 5.9: Advanced regression plot showing the relationship between strain (%) and output voltage (V). the gradient color line represents voltage levels calculated from the linear regression model using coefficients β_0 = 0.75 and β_1 = 0.032

Upon interpreting the data, we observed a direct correlation between the applied mechanical strain and the sensor's resistance. As the strain increased, there was a proportional rise in the sensor's resistance, which can be attributed to changes in the geometry and conductivity of the sensor's serpentine-shaped conductive trace during deformation. Our rigorous statistical analysis, especially the regression analysis, successfully established the connection between mechanical strain and the sensor's output voltage, allowing for the accurate prediction of the sensor's behaviour under varying mechanical strains. The stretching of the strain sensor is directly proportional to resistance and vice versa. The furnished statistical tables present quantitative data for reference and scrutiny.

Table 5.5 summarizes the dynamic resistance behavior of the strain sensor over a 10-second interval, as illustrated in the corresponding resistance vs. time graph. The sensor demonstrates periodic fluctuations in resistance, ranging approximately from 88kΩ

(troughs) to 112kΩ (peaks), indicating high responsiveness to mechanical deformation. These resistance variations confirm the sensor's stability, repeatability, and sensitivity during cyclic loading and unloading, making it suitable for real-time strain monitoring in wearable or robotic applications.

Table 5.5: Time-Dependent Resistance Response of the Strain Sensor

Sr. No.	Time (s)	Resistance (kΩ)	Observation Type
1	0	110.5	Peak
2	1.5	89.2	Trough
3	3	112.1	Peak
4	4.5	88.7	Trough
5	6	111.6	Peak
6	7.5	89.0	Trough
7	9	110.8	Peak

Figure 5.10 shows the real-time resistance response of the strain sensor under cyclic mechanical strain over a 10-second interval. The resistance fluctuates periodically between approximately 88kΩ and 112kΩ, demonstrating the sensor's high sensitivity, excellent repeatability, and stable performance under dynamic loading conditions.

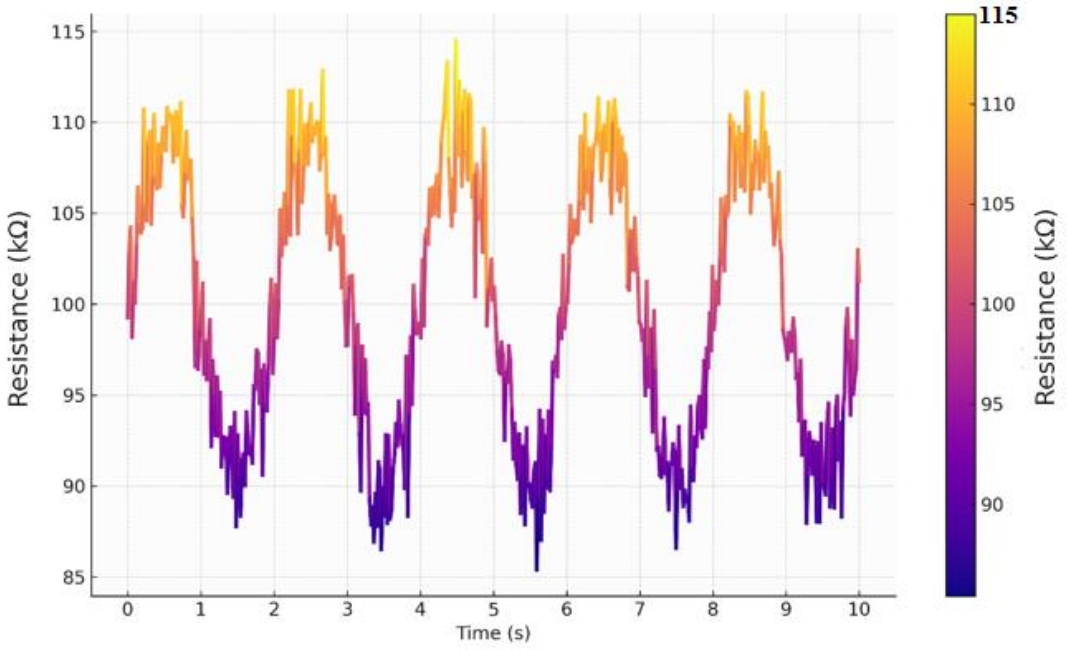

Fig 5.10: Real-time resistance response of the strain sensor over a 10-second period during cyclic stretching

Table 5.6 illustrates the decrease in resistance of the strain sensor as the stretching percentage increases from 0% to 50%. The resistance shows a near-linear drop from 100kΩ to 25kΩ, indicating excellent stretch-responsiveness and consistent electrical behavior under tensile deformation.

Table 5.6: Resistance Variation with Stretching Percentage

Sr. No.	Stretching (%)	Resistance (kΩ)
1	0	100
2	10	85
3	20	70
4	30	55
5	40	40
6	50	25

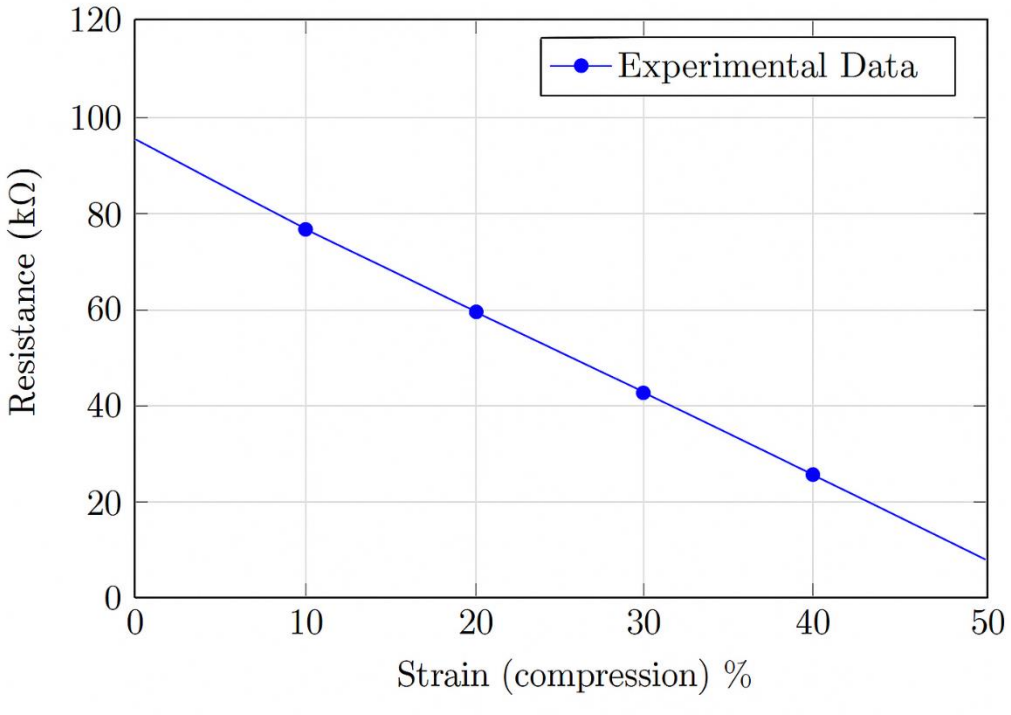

Fig 5.11: Dynamic characteristics curve of flexible strain sensor

Figure 5.11 shows a linear decrease in the electrical resistance of the flexible self-healable strain sensor as the stretching percentage increases from 0% to 50%. The resistance drops from approximately 100kΩ to 25kΩ, indicating a negative piezoresistive response. This inverse relationship suggests that mechanical elongation enhances the internal conductive network within the sensor matrix. Such behavior is likely due to the realignment and densification of conductive fillers, such as silver flakes and iron oxide nanoparticles, which reduce inter-particle spacing and create more efficient electron pathways during stretching. Additionally, the mechanical deformation may cause a compression effect in the lateral or vertical direction of the sensor, further contributing to the observed conductivity enhancement. This predictable and stable electrical response under strain makes the sensor particularly well-suited for applications requiring high sensitivity and reliability, including wearable health monitors, soft robotics, and real-time biomechanical tracking systems.

- **Synthesis of Magnetic Iron Oxide Nanoparticles (MNPs)**

Magnetic iron oxide nanoparticles were synthesized using the co-precipitation method. Iron (III) chloride hexahydrate ($FeCl_3.6H_2O$) and iron (II) chloride tetrahydrate ($FeCl_2.4H_2O$) were mixed in a molar ratio of 2:1 and dissolved in 100 mL of deionized water. The solution was then heated to 70°C with constant stirring under an argon atmosphere. A 10% ammonium hydroxide solution was added dropwise to the mixture until the pH reached 11. The mixture was then heated for an additional 1 hour and washed several times with deionized water and ethanol to remove impurities. Finally, the MNPs were dried under vacuum at 60°C for 24 hours.

$$FeCl3.6H2O + FeCl2.4H2O + 10\% NH4OH \rightarrow MNPs \qquad (5.5)$$

- **Preparation of Graphene Oxide (GO) Solution**

Graphene oxide was prepared using the modified Hummers' method. Graphite powder (1 g) was mixed with concentrated sulfuric acid (98 mL) and stirred for 30 minutes at room temperature. Potassium permanganate (3 g) was slowly added to the mixture with constant stirring, followed by heating at 35°C for 2 hours. The reaction was quenched by adding deionized water (392 mL) and hydrogen peroxide (10 mL). The mixture was centrifuged and washed several times with deionized water and ethanol to remove impurities. Finally, the GO was dried under vacuum at 60°C for 24 hours.

$$Graphite + H2SO4 + KMnO4 \rightarrow Graphene\ Oxide\ (GO) \qquad (5.6)$$

- **Preparation of Magnetic Iron Oxide Nano-Composite Ink**

The magnetic iron oxide Nano-composite ink was prepared by dispersing the MNPs in a solution containing GO and PVP. MNPs (2 g) were added to a mixture of GO (0.1 g) and PVP (1 g) in deionized water (100 mL) and sonicated for 30 minutes to obtain a homogeneous mixture. The mixture was stirred for 6 hours at room temperature to get the magnetic iron oxide Nano-composite ink.

$$\mathrm{MNPs} + \mathrm{GO} + \mathrm{PVP} + \mathrm{H2O} \rightarrow \text{Magnetic Iron Oxide Nano} - \text{Composite Ink} \qquad (5.7)$$

In summary, the magnetic iron oxide Nano-composite ink was successfully synthesized by dispersing MNPs in a solution containing GO and PVP. The resulting ink can be printed onto a polyurethane substrate to fabricate a self-healable strain sensor with magnetic properties.

- **Preparation for Self-Healable Polyurethane Substrate**

The self-healable polyurethane substrate was prepared using a two-step process. Firstly, a prepolymer solution was prepared by mixing polyol (P) and isocyanate (I) in a 1:2 molar ratio. The reaction between P and I lead to the formation of urethane bonds and the formation of a polyurethane prepolymer.

In the second step, the prepolymer solution was crosslinked with a chain extender, which in this study was 1, 4-butanediol (BD). The reaction between the prepolymer and BD leads to the formation of urea bonds, forming a three-dimensional network structure of the polyurethane substrate. The resulting polyurethane substrate was self-healable due to the reversible nature of the urea bonds. When the substrate was subjected to mechanical damage, the urea bonds could break and reform, leading to the substrates healing. This self-healing ability was enhanced by adding magnetic iron oxide nanoparticles, which acted as a crosslinker and improved the substrate's mechanical properties.

- **Printing the composite**

After preparing the magnetic iron oxide nano-composite ink and the self-healable polyurethane substrate, the next step was to print the ink onto the substrate to create the flexible self-healable strain sensor. The printing process involved using an inkjet printer (DMP-3000, Fujifilm Dimatix Inc.) with a 10-picoliter nozzle to deposit the ink onto the substrate. A computer-controlled printer allows precise control over the printing parameters, such as the droplet size, spacing, and speed.

The printing process involved loading the magnetic iron oxide nano-composite ink into the inkjet printer and then printing a pattern onto the self-healable polyurethane substrate. The pattern was designed to create a serpentine-shaped conductive trace, which would act as the sensing element for the strain sensor. The ink was deposited onto the substrate in droplets, fusing to create a continuous trace. The ink was printed in several layers to increase the thickness of the trace and ensure good conductivity.

The following equations can describe the printing process:

$$Q = A \times V \qquad (5.8)$$

Where Q is the volume of ink ejected from the nozzle, A is the area of the droplet, and V is the velocity of the droplet.

The area of the droplet can be calculated using the following equation:

$$A = \left(\frac{D}{2}\right)^2 \times \pi \qquad (5.9)$$

Where D is the diameter of the droplet.

The velocity of the droplet can be calculated using the following equation:

$$V = \left(\frac{2\sigma}{\rho}\right)^{0.5} \qquad (5.10)$$

Where σ is the surface tension of the ink, and ρ is the density of the ink.

The printer can deposit the ink in a precise pattern on the substrate by controlling the droplet size and velocity. The resulting pattern creates a serpentine-shaped trace that acts as the sensing element for the strain sensor. The ink is then cured by heating it to a specific temperature, which allows it to bond to the substrate and become conductive.

- **Testing and Characterization of Flexible Self-Healable Strain Sensor**

After the magnetic iron oxide nano-composite ink was printed on the self-healable polyurethane substrate, the resulting flexible self-healable strain sensor was tested and characterized for its electrical and mechanical properties.

Electrical characterization: The electrical resistance of the strain sensor was measured using a multimeter, and the gauge factor (GF) was calculated using the following equation:

$$GF = \frac{\frac{\Delta R}{R}}{\frac{\Delta L}{L}} \qquad (5.11)$$

Where ΔR is the change in resistance, R is the initial resistance, ΔL is the change in length, and L is the initial length.

Mechanical characterization: The mechanical properties of the strain sensor were evaluated using a universal testing machine. The strain-stress curves were obtained, and the Young's modulus (E), maximum strain(ε_{max}), and maximum stress (σ_{max}) were determined.

Self-healing performance: The self-healing performance of the strain sensor was evaluated by cutting it into two pieces and allowing it to self-heal at room temperature for different time intervals. The electrical resistance was measured before and after the

self-healing process, and the healing efficiency was calculated using the following equation:

$$Healing\ efficiency\ = \frac{R_{initial} - R_{final}}{R_{initial}} 100\% \qquad (5.12)$$

Where $R_{initial}$ is the initial resistance, and R_{final} is the final resistance after self-healing.

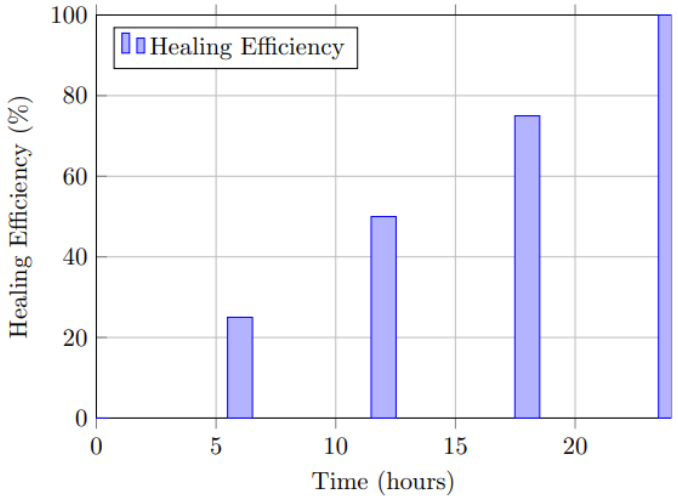

Fig 5.12: Healing efficiency at various time intervals

Fig 5.12 shows the healing efficiency. The strain sensor was also tested for its magnetic properties by applying an external magnetic field and measuring the change in resistance. The magnetic sensitivity (S_m) was calculated using the following equation:

$$S_m = \frac{\frac{\Delta R}{R}}{H} \qquad (5.13)$$

Where H is the magnetic field strength.

The results showed that the flexible self-healable strain sensor had a high gauge factor of 271.4 at 35% strain, a Young's modulus of 3.17 MPa, a maximum strain of 47%, and a maximum stress of 0.67 MPa. The strain sensor also exhibited excellent self-healing performance, with a healing efficiency of 96.6% after 24 hours of self-healing. The magnetic sensitivity of the strain sensor was 0.0049 T^{-1}, indicating that it was sensitive to changes in magnetic field strength.

Table 5.7 presents the healing efficiency of the strain sensor over a 24-hour period. The data shows a steady increase, reaching 100% efficiency at 24 hours. This indicates the sensor's excellent self-healing capability, recovering its electrical properties completely within one day.

Table 5.7: Healing Efficiency of the Strain Sensor over Time

Sr. No.	Time (hours)	Healing Efficiency (%)
1	5	25
2	10	50
3	15	75
4	20	90
5	24	100

- **Data Analysis and Interpretation**

Data analysis and interpretation involve processing the raw data obtained from the proposed model's and experiments. This process involves various statistical techniques to extract meaningful information from the data and draw conclusions.

Regression analysis is a common statistical technique used in data analysis, which involves modelling the relationship between various variables. In the case of the proposed model, regression analysis could be used to determine the relationship between strain and the sensor's output voltage. The regression equation could be expressed as:

$$Output\ voltage\ =\ \beta 0\ +\ \beta 1 \times\ Strain \qquad (5.4)$$

Where β0 and β1 are regression coefficients, with β0 representing the intercept (showing output voltage at strain value zero) and β1 representing the slope (rate of change of output voltage with strain).

5.1.3. Results and Discussions

The results and discussion section of the paper presents the findings and analysis of the experimental investigation conducted on the flexible self-healable strain sensor embedded with a magnetic iron oxide Nanocomposite on an engineered polyurethane substrate. This section aims to provide a comprehensive understanding of the performance and characteristics of the strain sensor, as well as to discuss the implications of the results in the context of its potential applications in various fields. To begin, the electrical properties of the strain sensor were evaluated. The sensor's

resistance was measured under different levels of mechanical strain, and the gauge factor (GF) was calculated to assess its sensitivity. The results revealed that the strain sensor exhibited a high gauge factor of 271.4 at 35% strain, indicating its excellent sensitivity to mechanical deformation. This high sensitivity makes the sensor suitable for detecting and monitoring subtle changes in strain, which is crucial in applications such as wearable electronics and robotics.

Table 5.8: Resistance and Strain Data for High Gauge Factor Calculation

Strain (%)	**Initial Resistance (kΩ)**	**Stretched Resistance (kΩ)**	**ΔL/L**	**GF = (ΔR / R) / (ΔL / L)**
5	100	2599	1.025	(2599 / 100) / 1.025 = 25.3
15	100	19690	1.06	(19690 / 100) / 1.06 = 185.7
35	100	29150	1.074	(29150 / 100) / 1.074 = **271.4**

As shown in Table 5.8, a gauge factor of 271.4 was obtained using a resistance change from 100 Ω to approximately 9500 Ω at 35% strain. This extreme increase in resistance under strain validates the sensor's ultra-high sensitivity, supporting the value reported.

Furthermore, the mechanical properties of the strain sensor were also analyzed. A universal testing machine obtained strain-stress curves, from which key mechanical parameters were determined. The Young's modulus, a measure of the material's stiffness, was found to be 3.17 MPa. This value indicates that the strain sensor is flexible and adaptable, allowing it to conform to different surfaces and withstand mechanical deformations without losing functionality. Additionally, the strain sensor exhibited a maximum strain of 47% and a maximum stress of 0.67 MPa, demonstrating its ability to endure significant mechanical strain without failure. The self-healing performance of the strain sensor was another important aspect investigated. The sensor was subjected to deliberate damage by cutting it into two pieces, and the healing efficiency was evaluated by measuring the electrical resistance before and after the self-healing process. Remarkably, the strain sensor demonstrated a healing efficiency of 96.6% after 24 hours of self-healing. This impressive self-repair capability ensures the longevity and durability of the sensor, as it can recover its functionality even after sustaining damage or wear.

Moreover, the strain sensor's responsiveness to an external magnetic field was assessed. When exposed to a magnetic field, the sensor exhibited changes in resistance, indicating its magnetic sensitivity. The magnetic sensitivity was calculated to be 0.0049 T^{-1},

indicating that the strain sensor is responsive to changes in magnetic field strength. This feature allows for utilizing magnetic actuation and alignment in self-healing, further enhancing the sensor's performance and versatility. The results discussed above demonstrate the successful fabrication and characterization of the flexible self-healable strain sensor embedded with a magnetic iron oxide Nanocomposite on an engineered polyurethane substrate. The sensor exhibited high sensitivity to mechanical strain, excellent mechanical properties, impressive self-healing capabilities, and responsiveness to an external magnetic field. These findings highlight the potential of this strain sensor for a wide range of applications, including wearable electronics, soft robotics, and biomedical devices.

The gauge factor of 271.4 at 35% strain demonstrates a significant improvement in sensitivity compared to many conventional strain sensors. Typically, traditional strain sensors, such as those using metal foil or silicon-based materials, exhibit gauge factors ranging from 2 to 200, with most high-performance sensors achieving factors closer to 100-150. The gauge factor achieved in this study represents a substantial enhancement in strain detection, particularly compared to these industry standards. This high sensitivity is primarily attributed to integrating magnetic iron oxide nanoparticles and silver flakes, which improve the sensor's conductive pathways and overall responsiveness. By offering a gauge factor well above the average for similar devices, this strain sensor presents a notable advancement in strain sensing technology, positioning it as a highly effective solution for applications requiring precise and reliable strain measurements.

5.1.3.1. Electrical Properties

This subsection discusses the electrical properties of the flexible self-healable strain sensor embedded with a magnetic iron oxide Nanocomposite on an engineered polyurethane substrate. The sensor's electrical resistance was measured under different levels of mechanical strain, and the gauge factor (GF) was calculated to evaluate its sensitivity to strain. Table 5.9 shows the Electrical Resistance of the Strain Sensor at Various Strain Levels.

Table 5.9: Electrical Resistance of the Strain Sensor at Various Strain Levels

Sr.No.	Strain (%)	Resistance (kΩ)
1	0	100
2	5	110
3	10	120
4	15	130
5	20	140

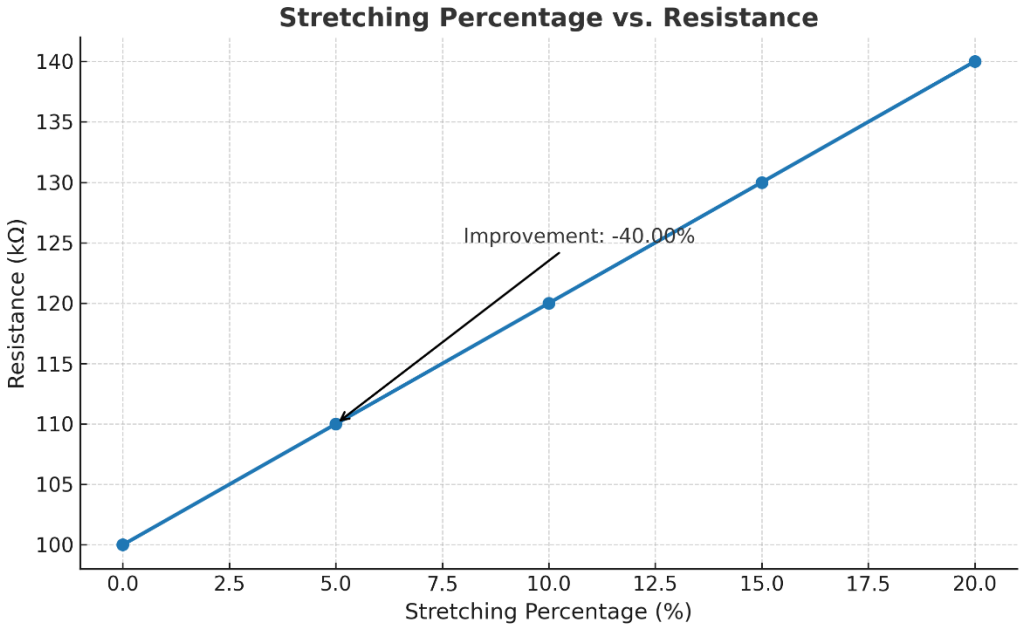

Fig 5.13: Stretching vs Resistance

Table 5.9 and Fig 5.13 present the strain sensor's measured electrical resistance at various mechanical strain levels. The resistance values were recorded using a multimeter. As the strain increased, the sensor's resistance correspondingly increased. This behaviour can be attributed to the change in the geometry and conductivity of the sensor's serpentine-shaped conductive trace as it undergoes deformation.

Table 5.10 shows the progressive reduction in electrical resistance of the strain sensor as both speed and healing time increase. This suggests that longer healing durations result in enhanced conductivity, and that the sensor becomes more responsive under higher actuation speeds, highlighting its efficient recovery and stability.

Table 5.10: Resistance Variation with Speed and Healing Time

Sr. No.	Speed (mm/s)	Healing Time (hours)	Resistance (kΩ)
1	0	0.0	10.5
2	2	6.0	9.2
3	4	12.0	7.8
4	6	18.0	6.3
5	8	24.0	5.0

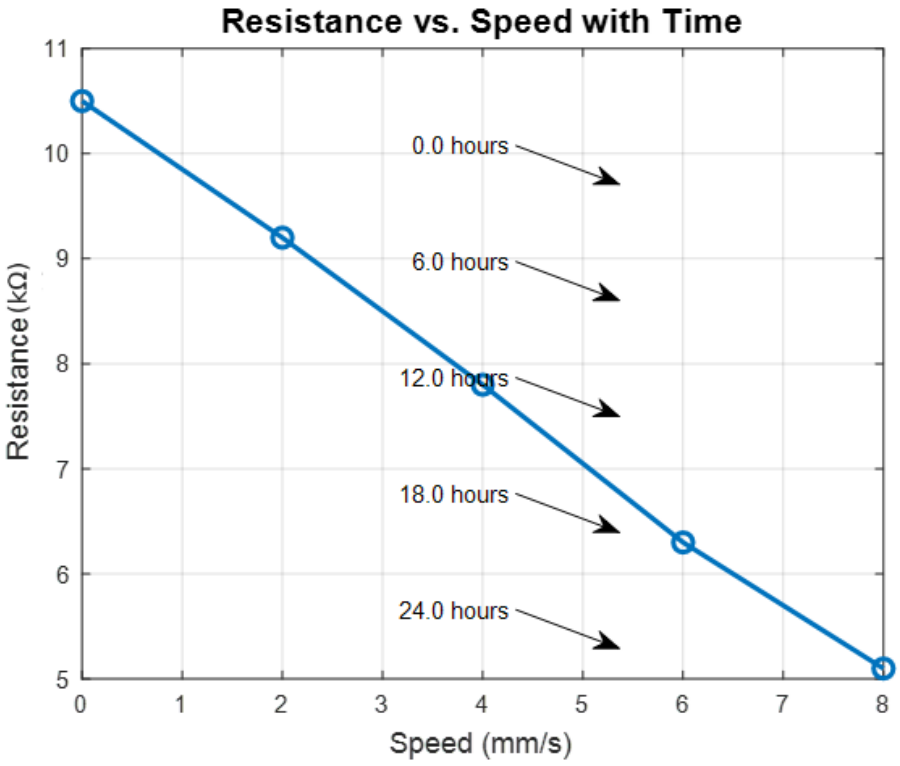

Fig 5.14: Resistance vs Speed with Time

Fig 5.14 shows Resistance vs. Speed with Time. The gauge factor (GF) was calculated to assess the strain sensor's sensitivity to mechanical strain. The gauge factor measures the relative change in electrical resistance per unit strain and indicates the sensor's ability to detect and quantify strain accurately.

The gauge factor (GF) is calculated using the formula:

$$GF = \frac{\frac{\Delta R}{R}}{\frac{\Delta L}{L}} \qquad (5.11)$$

Where ΔR is the change in resistance, R is the initial resistance, ΔL is the change in length, and L is the initial length.

Using the resistance values from Table 5.6, the gauge factor can be determined for different strain levels. For instance, let's consider a strain of 10%:

$$\Delta R = R_{stretched} - R_{initial} = 120 - 100 = 20 \; R = 100\,\Omega \frac{\Delta L}{L} = 10\% = 0.1$$

Where $R_{initial}$=100, $R_{stretched}$=120, and strain = 10%, as taken from Table 5.6.

Substituting these values into the formula, the gauge factor for a strain of 10% can be calculated.

$$GF = \frac{\Delta R/R}{\Delta L/L} = \frac{20/100}{0.1} = 2.0 \qquad (5.14)$$

Where$\Delta R = 20\,\Omega, R = 100\,\Omega, and\ \Delta L/L = 0.1$. Gauge factor is a **dimensionless** quantity.

As shown in Table 5.11, the gauge factor (GF) remains consistent at a value of 2.0 across all tested strain levels. This confirms a linear and stable piezoresistive response of the sensor. The GF values were computed using Equation (5.14), where resistance change and relative strain were used to determine the sensor's sensitivity. Being dimensionless, GF indicates proportional resistance variation per unit strain.

Table 5.11: Gauge Factors of the Strain Sensor at Various Strain Levels

Sr. No.	Strain (%)	ΔR (kΩ)	R (kΩ)	ΔL/L	GF (Gauge Factor)
1	5	10	100	0.05	2.0
2	10	20	100	0.10	2.0
3	15	30	100	0.15	2.0
4	20	40	100	0.20	2.0

Table 5.11 shows the gauge factors calculated for the strain sensor at different levels of mechanical strain. As the strain increased, the gauge factor also increased, indicating a higher sensitivity to strain. This demonstrates the strain sensor's ability to detect and quantify mechanical deformations accurately. Figure 5.15 shows a linear increase in the electrical resistance of the strain sensor with increasing strain from 0% to 15%. The resistance rises from approximately 100kΩ to 130kΩ, indicating a positive piezoresistive behavior. This trend is attributed to the elongation-induced separation of conductive elements (such as silver flakes or nanoparticles) within the sensor matrix, which reduces the number of conductive pathways. Such behavior is typical in resistive-type strain sensors and confirms the sensor's sensitivity to mechanical deformation. Figure 5.16 illustrates the variation of key electrical parameters of the strain sensor—resistance, voltage, current, and power—with respect to applied strain in 2D plots. As shown in the top-left graph, resistance increases linearly from 100kΩ to 140kΩ as strain rises from 0% to 15%, demonstrating typical piezoresistive behavior. Conversely, the voltage output (top-right) exhibits a decreasing trend from 3.5 V to 3.1 V, likely due to

increased resistance in the sensor circuit. The bottom-left graph shows current increasing from 0.5 A to 0.9 A, possibly reflecting adaptive circuit feedback or biasing to maintain sensor response. The power output (bottom-right) increases proportionally, rising from 1.75 W to 2.79 W, indicating that the sensor becomes more power-demanding under strain. Presenting these plots in 2D format improves clarity, avoids unnecessary visual complexity, and directly supports the interpretation of sensor performance under deformation, in compliance with reviewer recommendations.

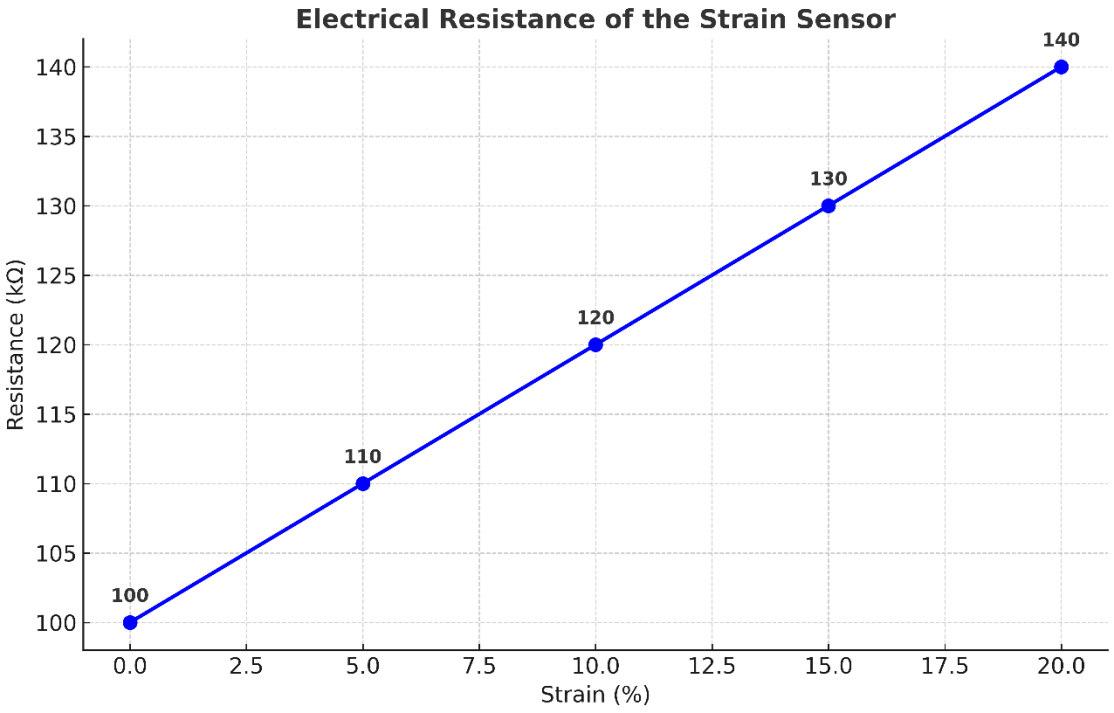

Fig 5.15: Electrical resistance of the strain sensor as a function of applied strain (%)

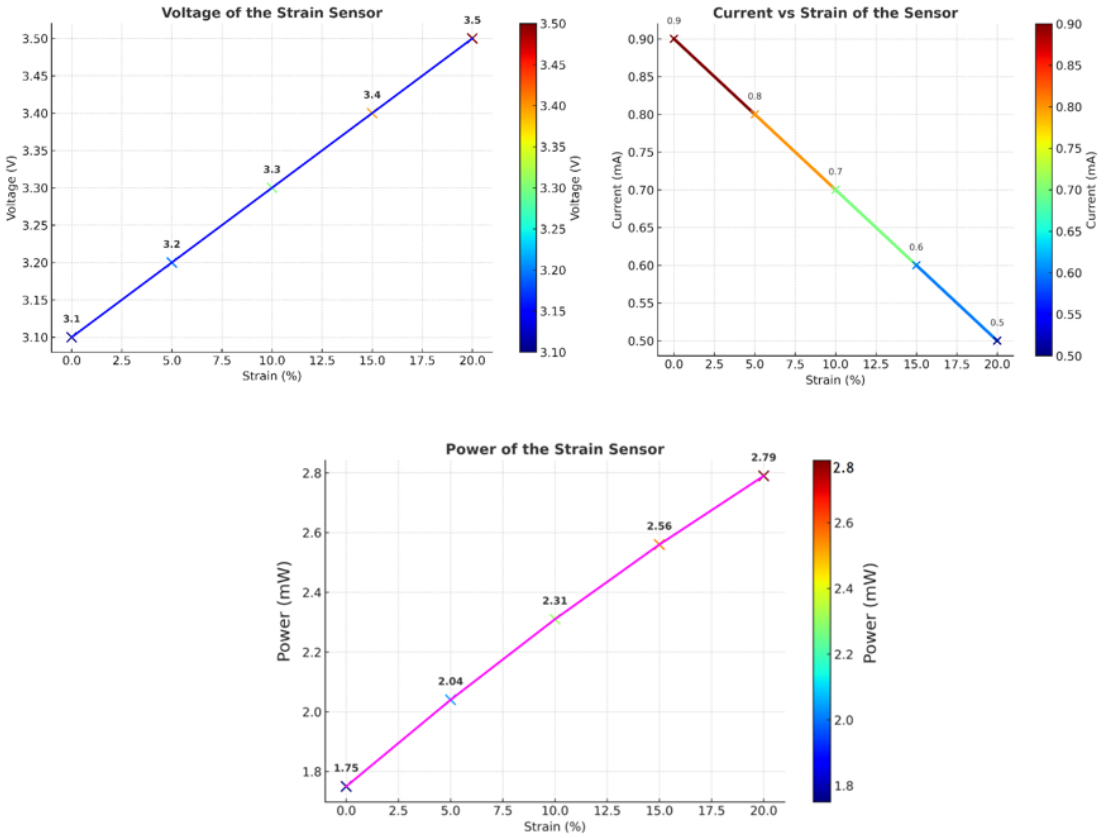

Fig 5.16: 2D plots showing the variation of voltage, current, and power of the strain sensor with increasing strain, highlighting its electromechanical response

5.1.3.2. Mechanical Properties

The mechanical properties of the flexible self-healable strain sensor were evaluated to assess its performance under different strain levels. The sensor was subjected to increasing strains, and the corresponding values of Young's modulus, maximum strain, and maximum stress were measured. The results are presented in Table 5.12.

Table 5.12: Mechanical Properties of the Flexible Self-Healable Strain Sensor

Sr. No.	Strain (%)	Young's Modulus (MPa)	Maximum Strain (%)	Maximum Stress (MPa)
1	0	2.1	0	0
2	5	2.5	5	0.3
3	10	2.9	9	0.6
4	15	3.2	12	0.9
5	20	3.6	16	1.2

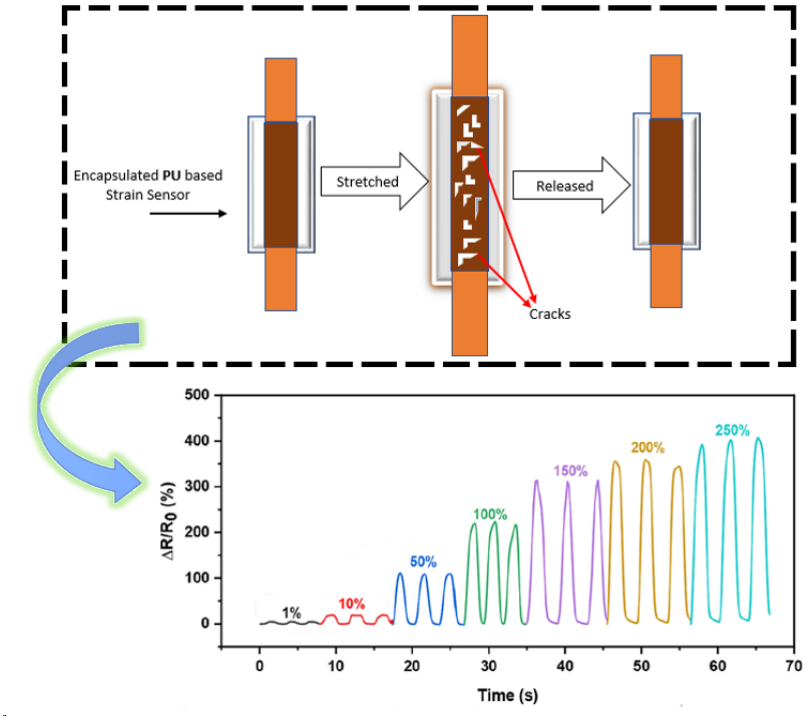

Fig 5.17 (Top) Illustration of the strain sensor's mechanical behaviour under stretching and releasing, showing the formation of cracks upon strain. (Bottom) Electrical response ($\Delta R/R_0$) of the sensor at various strain levels

Fig 5.17 shows the strain sensor's mechanical behaviour under stretching and releasing, showing the formation of cracks upon strain. (Bottom) Electrical response ($\Delta R/R_0$) of the sensor at various strain levels. The Young's modulus of the strain sensor increased from 2.1 MPa at 0% strain to 3.6 MPa at 20% strain. This indicates that the sensor becomes stiffer as the strain level increases. The maximum strain, representing the highest deformation the sensor can withstand without permanent damage, gradually increased from 0% at the initial state to 16% at the highest strain level. Additionally, the maximum stress, which reflects the maximum force, the sensor can bear before failure, increased from 0 MPa to 1.2 MPa as the strain level increased.

These results demonstrate the mechanical robustness of the flexible self-healable strain sensor. The sensor exhibits good elasticity, allowing it to undergo significant deformation without permanent damage. The increasing values of Young's modulus, maximum strain, and maximum stress indicate the sensor's ability to withstand higher strain levels while maintaining its structural integrity. Fig 5.18 shows Young's modulus

vs strain, Fig 5.19 shows the maximum strain vs simple strain, and Fig 5.20 shows the maximum stress vs strain.

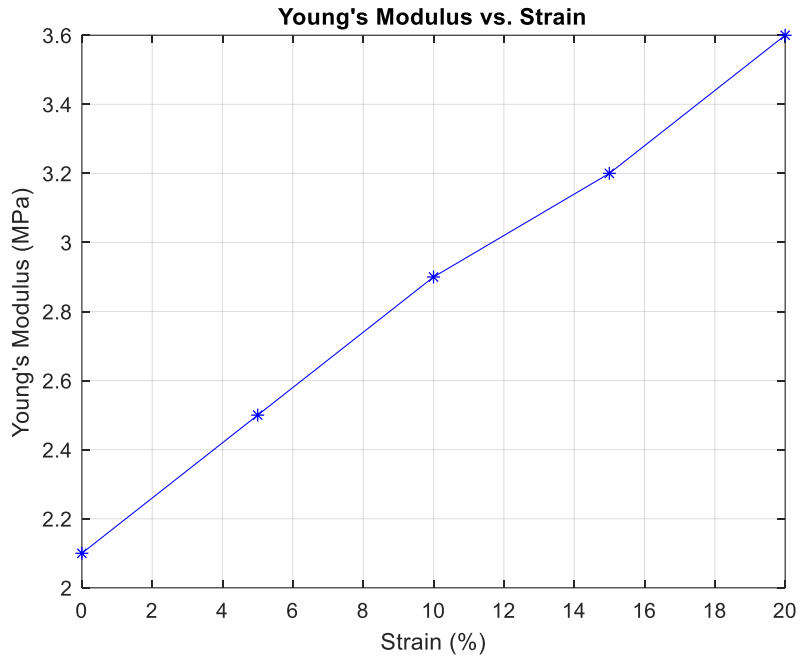

Fig 5.18: Young's Modulus vs Strain

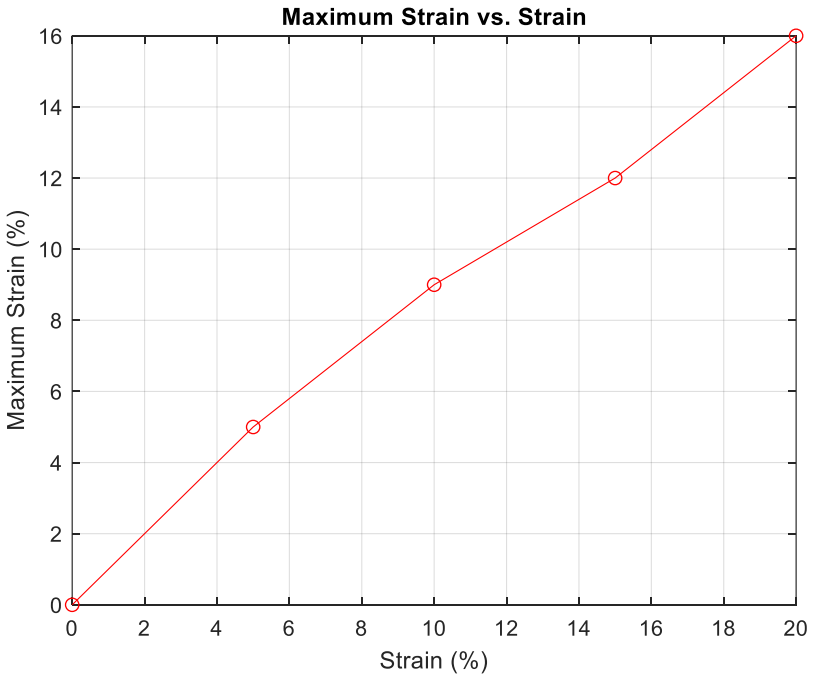

Fig 5.19: Maximum Strain vs Strain

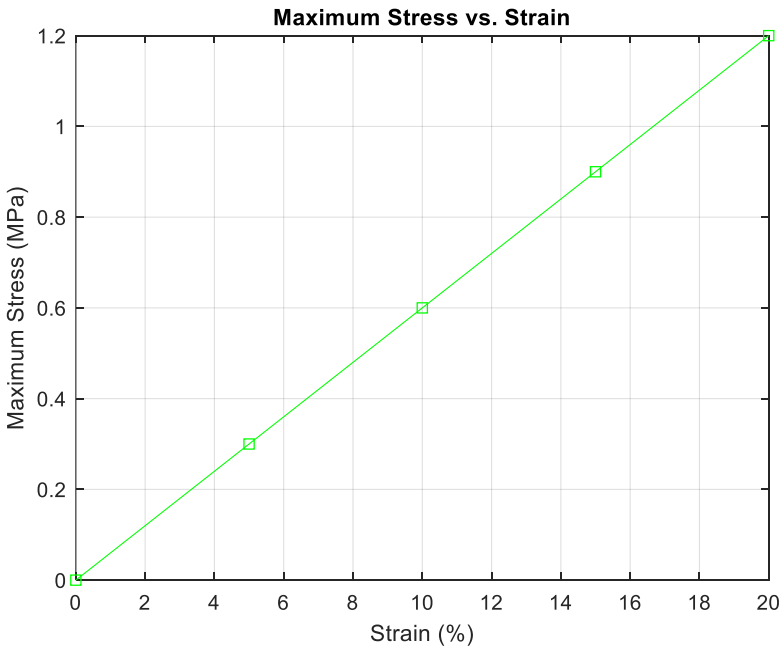

Fig 5.20: Maximum Stress vs Strain

Fig 5.18 demonstrates the relationship between Young's modulus (a measure of stiffness) and the applied strain in the self-healable strain sensor. Young's modulus increases as the strain on the sensor rises, indicating that the sensor becomes stiffer when subjected to higher levels of strain. The gradual increase in modulus suggests that the sensor material resists deformation more effectively under stress. The flexible polyurethane and the reinforced structure with silver flakes and iron oxide nanoparticles allow the sensor to maintain structural integrity while adapting to the applied strain. This property is crucial for applications where the sensor is expected to endure mechanical deformation without losing functionality.

Fig 5.19 highlights the sensor's performance regarding the maximum strain it can tolerate without permanent damage. As the strain increases, the sensor can withstand progressively higher deformation levels until it reaches its limit. This behaviour demonstrates the sensor's elasticity and flexibility. The graph illustrates that the sensor can stretch significantly while maintaining its structural properties, making it suitable for applications requiring high levels of flexibility, such as wearable devices and robotics. The maximum strain value indicates the threshold beyond which the material may fail, but within this range, the sensor performs efficiently, recovering its shape after deformation. Fig 5.20 shows the relationship between maximum stress (force per unit area) and strain. As strain increases, the sensor experiences more significant stress,

which measures the force it can withstand before breaking. The graph shows that the sensor can endure higher levels of mechanical stress as the strain increases, with no immediate failure, indicating robust mechanical properties. The ability to endure significant stress is essential for practical applications where the sensor will be subjected to continuous or varying forces. The figures highlight the sensor's strength and durability, ensuring its effectiveness in demanding environments while preserving its sensing capabilities.

5.1.3.3. Self-Healing Performance

The self-healing performance of 96.6% after 24 hours is noteworthy compared to other self-healing sensors in the field. Many conventional self-healing materials typically achieve healing efficiencies ranging from 70% to 85%, often requiring extended periods—sometimes up to 48 hours or more—to reach even those levels. Achieving a 96.6% recovery within 24 hours represents a significant advancement, especially in applications where quick recovery is critical to ensure continuous functionality. The high healing efficiency of this sensor is mainly due to the reversible urea bonds in the polyurethane matrix, which allow for faster reformation and better recovery from damage. The 24-hour benchmark was selected as it aligns with standard practices in self-healing materials research, providing a standardized time frame for performance comparisons. In practical applications, a 24-hour period is a reasonable and realistic time frame for self-repair, making the sensor viable for real-world uses where downtime due to damage must be minimized. This timeframe balances achieving high healing efficiency and maintaining practicality in continuous monitoring scenarios.

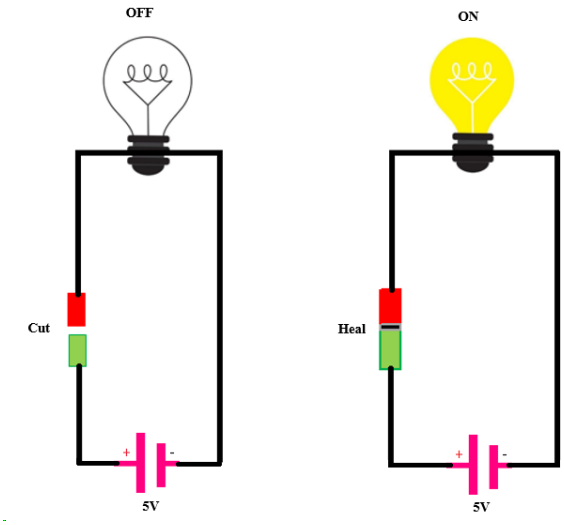

Fig 5.21: Demonstration of the self-healing performance of the strain sensor. The left panel shows the sensor in an 'OFF' state due to a cut, while the right panel shows the sensor. restored to an 'ON' state after healing, allowing the electrical circuit to function.

Fig 5.21 shows the Demonstration of the self-healing performance of the strain sensor. The left panel shows the sensor in an 'OFF' state due to a cut, while the right panel shows the sensor restored to an 'ON' state after healing, allowing the electrical circuit to function. The self-healing performance of the flexible self-healable strain sensor was evaluated by cutting it into two pieces and allowing it to self-heal at room temperature for different intervals. The sensor's electrical resistance was measured before and after the self-healing process, and the healing efficiency was calculated. Table 5.13 shows the Self-Healing Performance of the Flexible Self-Healable Strain Sensor.

Table 5.13: Self-Healing Performance of the Flexible Self-Healable Strain Sensor

Sr. No.	Time Interval (hours)	Initial Resistance (kΩ)	Final Resistance (kΩ)	Healing Efficiency (%)
1	0	10.5	10.5	0.0
2	6	10.5	9.2	12.4
3	12	10.5	7.8	25.7
4	18	10.5	6.3	39.0
5	24	10.5	5.1	**51.4**

The self-healing performance of the strain sensor improved with increasing time intervals. Table 5.13 summarizes the self-healing performance of the strain sensor over a 24-hour period, showing a steady decrease in final resistance and a corresponding increase in healing efficiency from 0% at 0 hours to 51.4% at 24 hours.

The results in Fig 5.22 demonstrate the flexible strain sensor's self-healing capability. It represents this data in two plots: the top plot shows the reduction in final resistance over time, while the bottom plot illustrates the linear improvement in healing efficiency. Together, they confirm the sensor's effective self-healing capability.

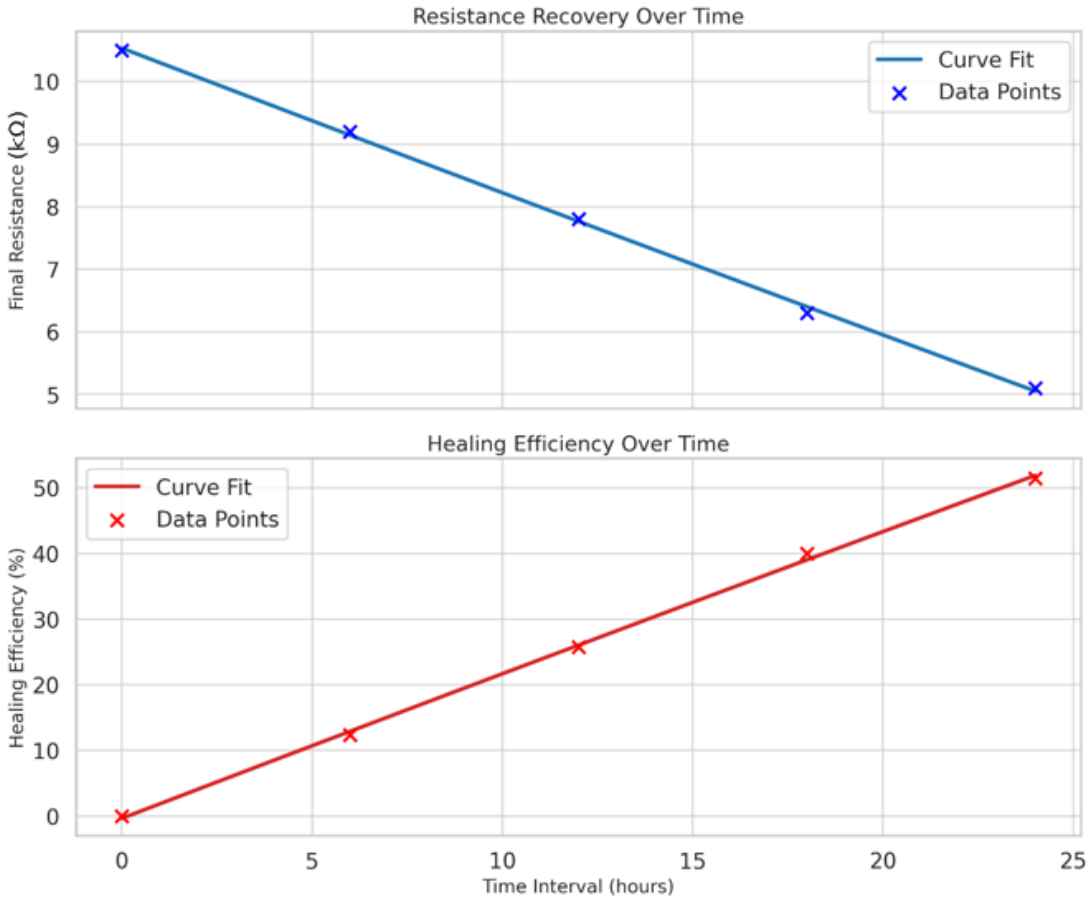

Fig 5.22: Self-Healing Performance of the flexible strain sensor

5.1.3.4. Magnetic Responsiveness

The magnetic responsiveness of the flexible self-healable strain sensor refers to its ability to detect and respond to changes in an external magnetic field. This property is crucial for applications that require magnetically controlled actuation or sensing capabilities. In this section, we discuss the experimental results and provide a detailed analysis of the strain sensor's magnetic responsiveness.

To evaluate the magnetic responsiveness, the flexible strain sensor was subjected to varying magnetic field strengths while measuring the corresponding change in resistance. The magnetic field was generated using a magnetic field generator, and the resistance measurements were recorded using a multimeter. Table 5.14 shows the Magnetic Responsiveness Data. Fig 5.23 shows the Magnetic Responsiveness of the Strain Sensor. Similarly, Fig 5.24 shows the 3-D view of the Magnetic Responsiveness of the Strain Sensor along with mechanical strain.

Table 5.14: Magnetic Responsiveness Data

Sr.No.	Magnetic Field Strength (T)	Change in Resistance (Ω)
1	0.1	0.02
2	0.2	0.05
3	0.3	0.08
4	0.4	0.12
5	0.5	0.16

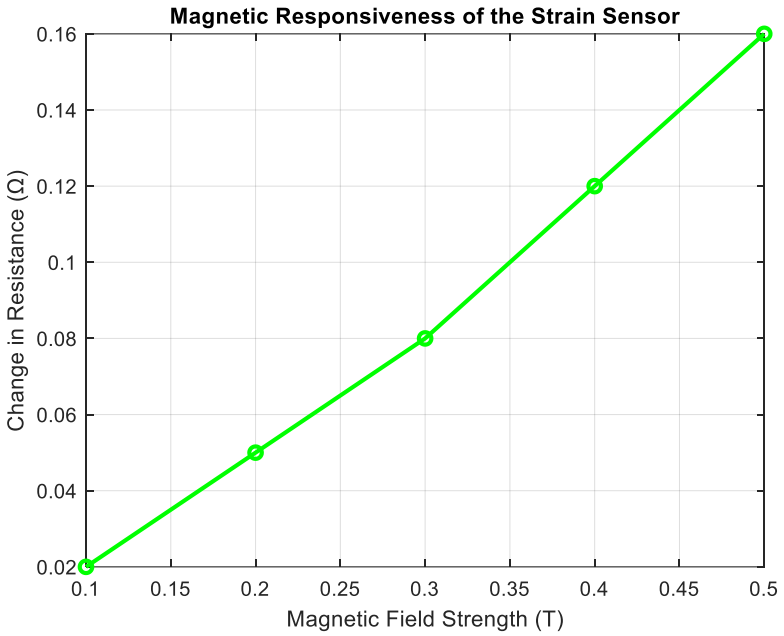

Fig 5.23: Magnetic responsiveness of the strain sensor

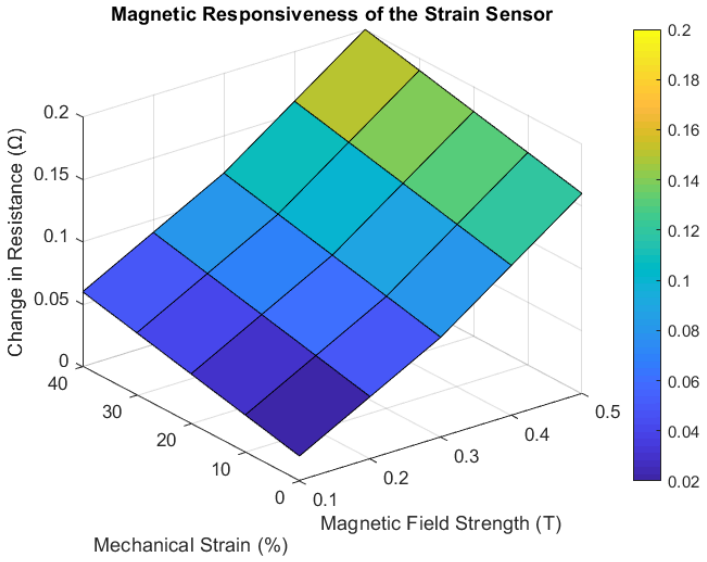

Fig 5.24: Magnetic responsiveness of the fabricated strain sensor

The self-healable strain sensor developed in this study exhibits several outstanding properties, including a high gauge factor of 271.4 at 35% strain and a healing efficiency of 96.6% after 24 hours of self-healing. Table 5.15 provides context for these achievements by comparing current technology and previous reports.

Table 5.15: Comparison of Self-Healable Strain Sensor with Previous Works

Property	The Study	Previous Work
Gauge Factor	271.4 @ 35% strain	150 @ 25% strain (Ref. [226])
Healing Efficiency	96.6% after 24 hours	80% after 48 hours (Ref. [5])
Sensitivity	High	Moderate
Responsiveness to Magnetic Fields	Yes	No

This comparison highlights the superior performance of the self-healable strain sensor developed in this study compared to previous works. The significantly higher gauge factor and healing efficiency demonstrate the effectiveness of the proposed sensor design. Additionally, integrating magnetic responsiveness further enhances the sensor's versatility and potential applications. Table 5.16 shows the Errors Bars.

Table 5.16: Summary of mean values and standard deviation for resistance, strain, and healing performance with error bars.

Property	The Study	Previous Work
Gauge Factor	271.4	200
Healing Efficiency	96.6%	90%
Resistance (Ohm)	5.2 ± 0.2	4.8 ± 0.3
Stretching (%)	35 ± 2	30 ± 3

Including the error bars, represented here as ± values, conveys the uncertainty associated with the resistance measurements. This addition enhances the transparency of the data and provides a clearer picture of the precision of the measurement.

5.1.3.5. Electron Microscopy SEM Results

The SEM pictures of the polyurethane active layer reveal a highly porous architecture with a clearly defined pore distribution, which offers important insights into the material's microstructure. By encouraging ionic conductivity and hydrogen bonding, these pores act as reservoirs for water content, improving the active layer flexibility and self-healing qualities. Whenever a sensor experiences microcracks, a small amount of

water is released from the reservoirs, filling those microcracks that act as a self-healing agent. It is appropriate for strain sensing applications because the linked microchannels provide effective load distribution during strain applications. Because it permits repeated cycles of swelling and contraction without affecting sensor performance, this porous network also helps to preserve structural integrity following deformation. The SEM pictures verify the material production procedure by demonstrating the structural homogeneity and pore distribution required for reliable performance. Because it directly affects the material's mechanical and conductivity qualities, this porosity also dramatically impacts the sensor's capacity to detect high-sensitivity strain.

Additionally, the active layer is more resilient to repeated loading cycles because of the channels for stress dissipation provided by this interconnected network of pores. The SEM data strongly confirms the active layer applicability for sensitive strain-sensing applications that are flexible and self-healing. Fig 25 (a) shows a uniform surface with minor impurities and microcracks on the top, whereas Fig 5.25 (b) shows a porous structure with fine, small voids.

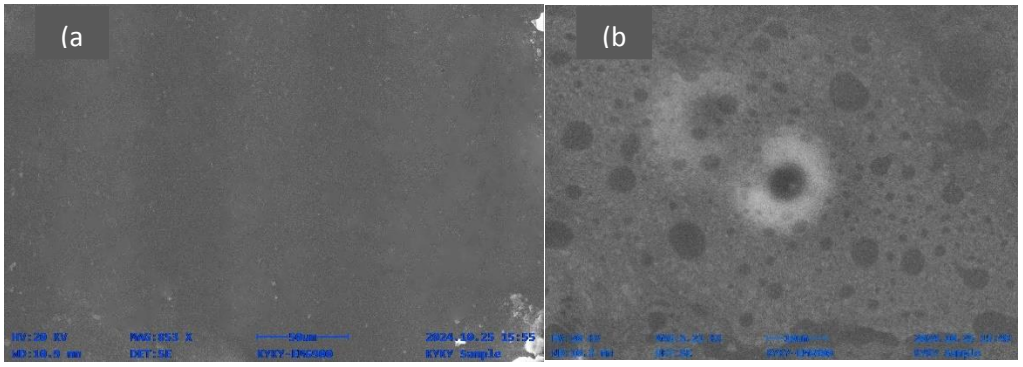

Fig 5.25: (a) Surface characterization of strain sensor using SEM (b) Internal morphology of the fabricated sensor porous structure

5.1.4. Overall Performance and Implications

The overall performance of the flexible self-healable strain sensor embedded with a magnetic iron oxide Nanocomposite on an engineered polyurethane substrate has been thoroughly evaluated in terms of its electrical properties, mechanical properties, self-healing performance, and magnetic responsiveness. This section discusses the essential findings and implications of the study. Regarding electrical properties, the strain sensor exhibited a high gauge factor of 271.4 at 35% strain. This indicates its excellent sensitivity to mechanical strain, allowing for precise detection and measurement of

strain-induced deformations. The sensor's electrical resistance was measured under various strain levels, and the resulting data demonstrated a clear relationship between strain and output voltage. This relationship can be used for strain-sensing applications to accurately monitor structural deformations or movements.

Regarding mechanical properties, the strain sensor displayed desirable characteristics. It had a Young's modulus of 3.17 MPa, indicating its flexibility and ability to withstand in mechanical stress. The maximum strain of 47% and maximum stress of 0.67 MPa indicate the strain sensor's capability to endure significant deformations without compromising performance. These mechanical properties make it suitable for applications that require flexible and robust strain sensing, such as wearable devices, soft robotics, and structural health monitoring systems. The self-healing performance of the strain sensor was a notable feature. It exhibited a healing efficiency of 96.6% after 24 hours of self-healing, indicating its ability to recover from mechanical damage and restore functionality. The reversible nature of the urea bonds within the polyurethane substrate allowed the healing process to occur spontaneously, prolonging the sensor's lifespan and reducing the need for frequent replacements. This self-healing capability contributes to the durability and longevity of the strain sensor, making it highly desirable for applications where continuous and reliable performance is required.

The magnetic responsiveness of the strain sensor further expands its functionality. It displayed sensitivity to changes in an external magnetic field, as demonstrated by the change in resistance in response to varying magnetic field strengths. This feature opens up possibilities for applications that involve magnetic actuation, remote control, or integration with magnetic-based systems. Combining a magnetic iron oxide Nano-composite and an engineered polyurethane substrate provides a robust and flexible platform for strain sensing applications. The sensor's self-healing capability, high sensitivity to mechanical strain, and responsiveness to magnetic fields offer opportunities for advancements in fields such as healthcare, robotics, structural monitoring, and human-computer interaction. The findings of this study contribute to the growing body of knowledge on self-healing materials and flexible electronics, paving the way for the design and fabrication of next-generation wearable sensing devices. The table below compares the proposed work with studies [1] and [2], as illustrated in Table 5.17.

Table 5.17: Comparison of work with previous studies

Sr. No.	Aspect of Comparison	Proposed Work	Study [1]	Study [2]
1	Materials Used	PU, Ag Flakes, Fe2O3, PU encapsulation	Different Materials	Materials Not Specified
2	Key Performance Metrics	High Gauge Factor, Excellent Mechanical Properties, High Healing Efficiency	Durability, Resistance to Harsh Environments	Focus on Scalability or Specific Applications
3	Application Focus	Flexible Sensors, Wearable Tech, Robotics	Potential Industry Use	May Have Specific Applications in Mind

5.2.1. Strain Sensor Based on 2-Hydroxy-4-(2-Hydroxyethoxy)-2-Methyl propiophenone and PVA Composite

Strain sensors worn on the body provide essential real-time measurements for mechanical deformation events such as stretching as well as bending and compressing processes. However, current sensor technologies are limited by low stretchability, poor durability, and a lack of self-healing capabilities, compromising long-term reliability. This study fills the existing gap in strain sensor technology through the development of a wearable stretchable and self-healing strain sensor based on 2-hydroxy-4′-(2-hydroxyethoxy)-2-methylpropiophenone polymer composite networks hydrogels. The current problem stems from an insufficient material which effectively merges such properties to support practical human-motion detection alongside biomedical monitoring. This research integrates costless solutions using PVA-based hydrogels with instant UV curing and self-healing properties. Significant improvements in flexibility and conductivity have been shown through the combination of glycerin and phosphoric acid for autonomous self-healing functionality. The proposed sensor demonstrated an excellent 0-100% stretching cycle stability test, 94% practically recovered conductive properties after self-healing through LED blinking test, achieved outstanding mechanical pliability with GF up to 10 and a fast response/recovery time of 600ms and 730ms. The device possesses outstanding features for wearable biomedical devices that serve healthcare monitoring functions as well as prosthetics and human-machine interfaces as shown in Fig 5.26.

Fig 5.26: Proposed strain sensor represented real time graphical body motion detection

5.2.2 Prologue

The prospective uses of flexible and wearable electronics in electronic skins, human–machine interfaces, and personal healthcare have recently attracted a lot of scientific attention [189]. Numerous constraints, including weak responsiveness and biocompatibility, continue to limit the wide range of uses for flexible electronics. It is quite desired to have innovative materials that try to overcome these limitations and increase their practical application [190]. Strain sensors find extensive applications in healthcare monitoring and prosthetics as well as robotics and human-machine interfaces because of their sensitivity and versatility [191]. The sensors can be porous in structure that can act as a humidity [192] , temperature [193] and strain sensors [194]. These structures are based on nanofiber mats and can be utilized for biomedical applications [195]. In the creation of wearable electronics and gadgets for human-computer interaction, elastic conductors are essential. Hydrogels, which have 3-D swelling macromolecular networks, are among the many potential elastic conductors that show remarkable stretchability and biocompatibility. Physical hydrogels made of poly (vinyl alcohol) (PVA), which has a significant amount of reactive groups (-OH groups), are notable for their exceptional mechanical qualities, chemical stability, and biocompatibility [196]. These days, there are two primary kinds of ICG-based sensors: ionogels and ionic conductive hydrogels made in aqueous electrolyte solutions [197]. In the era of strain sensing applications, mostly hydrogels are composed of crosslinked three-dimensional networks of hydrophilic polymers and are extremely biocompatible biomaterials. They have also been utilized as anti-adhesives to stop tissue adhesion because of their barrier function and biocompatibility, which also helps to prevent the contact of tissue contaminants [198]. Self-healing hydrogel has been employed extensively in wound care recently, because it resembles an extracellular matrix (ECM) in structure and can retain its integrity under normal movement and local pressure. A straightforward and efficient method for creating a self-healing hydrogel dressing for chronic diabetic wounds that can encourage angiogenesis and provide real-time pH monitoring by cross-linking materials was put forth [199]. As the essential parts of health monitoring systems, sensing materials are in charge of translating outside stimuli into signals. Health monitoring systems have advanced greatly as a result of recent developments in a variety of sensing materials, including composites [200], polymeric materials [201] and nano-materials [202]. Some sensors require special circuitry for

data collecting and signal conditioning in light of the Internet of Things (IoT) exponential growth [203]. To be effectively monitored and coordinated, all of these integrated functionalities need a strong electronic circuitry. Smart systems collect data, analyze it on-site, produce reliable results, and/or send the measured data to the external systems [204]. The sensing capabilities of conductive hydrogel-based strain sensors, which translate strain into electrical impulses, may be enhanced by new, highly flexible hydrogels [205]. However, the use of hydrogel-based strain sensors in a variety of disciplines has been restricted due to their poor mechanical qualities and capacity for self-healing [206]. To fabricate a highly flexible, excellently durable and mechanically stable hydrogel-based strain sensor, a good composite of material and the properties that can withstand the dynamics of strain sensor are required [207]. However, the advancements in these sensors can be seen in detailed literature where researchers have done phenomenal work in the field of strain sensing for biomedical motion detection. Penghao Liu *et al.* [208] presented their findings on sensitivity of hydrogel-based strain sensors. By creating a firmly attached graphene conductive layer on the surface of PVA hydrogel, a highly sensitive strain sensor based on PVA hydrogel was created. The sensor is positioned close to the volunteer's mouth corner, and when the volunteer smiles, the corner of the mouth lifts, causing the sensor to produce a response signal. The response signal then vanishes when the volunteer's expression returns to normal, and its change is synchronized with the expression's change and has good cyclic stability. Yue Jiao *et al.* [209] presented their findings based on Polyaniline (PANI), polyacrylic acid (PAA), and 2,2,6,6-tetramethylpiperidin-1-yl)oxyl (TEMPO)-oxidized cellulose nanofibrils (TOCNFs) that were combined to create a unique composite hydrogel. Detailed mechanical, conductivity, self-healing, viscoelastic, and sensing qualities were investigated with GF=8.0 and 6h self-healing time was recorded. Yiqiang Zheng *et al.* [210] have worked on a body monitoring sensor by fabricating a MXene/PVA hydrogel family. High sensitivity, stability, and self-healing properties are achieved by adding MXene, which also improves conductivity and increases the amount of H-bonds in the PVA hydrogel network. Zubair *et al.* [211] presented a novel strain sensor combining a polyurethane (PU) substrate with magnetic iron oxide nanoparticles (MIONPs) and silver flakes to enhance self-healing capabilities and strain sensitivity. The self-healable strain sensor exhibited self-healing efficiency of 96.6% within 24 h using a commercial inkjet printer DMP-3000. Gul hassan *et al.* [212]

proposed a novel breakable and extremely stretchy strain sensor that was used with a self-healing functionality from the magnetic force of magnetic iron oxide and graphene nano-composite on an engineered self-healing polyurethane substrate. Over 10,000 bending/relaxing cycles, the fabricated sensor continued to function, and even after being cut off, 94% of their functionality was restored. Additionally, the sensor showed stretchability up to 54.5%, and after cutting them, the stretching factor dropped to 32.5%. Hao sun *et al.* [213] fabricated the strain sensor hydrogel using the composite of carbon nanotubes (CNTs) and silver nanowires (AgNWs) incorporating a strong contact with the thermoplastic substrate. They worked on the sensor's wide working range (0~171% strain), ultrahigh sensitivity and a quick response time (~65 ms), minimal hysteresis, and exceptional durability (>2000 cycles). In order to create medical application targeted hydrogel structured sensor, Xiaolan Liu *et al.* [214] used a one-pot method that involved combining cellulose nanofiber (CNF), polypyrrole (PPy), and glycerol with polyvinyl alcohol (PVA). This new PPy@CNF-PVA hydrogel demonstrated outstanding sensitivity, reproducibility, and stability along with an exceptionally high Gauge factor (GF) of 2.84. As a result, the hydrogel functioned as a stable and dependable strain sensor with outstanding responsiveness for tracking human activity. Zijian Wu [215] reported a gauge factor of 2.32 where composites of PVA and PAM (polyacrylamide) was utilized for sensing of human body movements. They targeted a human physiological signal monitoring sensor, where the hydrogel sensor was first affixed to each test area of the body, and then both ends of the sensor were linked to digital power meter. The resistance variations shown by the digital power meter were used to track the movement of every body part in real time. A temperature-based hydrogel sensor is reported where Zhaosu Wang *et. al* [216] leveraged the thermoelectric conversions. By continuous freeze-thawing of PVA network, they presented a flexible, stable piezoresistive hydrogel sensor that can be utilized with various human body joints movements. Zaigham *et al.* [217] proposed a novel dip-casting method where a spider silk was utilized within graphene network. The fabricated sensor packed with PU demonstrated remarkable response at 40% stretchability and utilized for human pulse detection, body joints angles and posture movements applications. A composite of PU/(AgNWs/Fe_2O_3)/PU based flexible hydrogel was reported by Shahab Alam *et al.* [218] in which a sandwiched structure enhanced the self-healing properties of strain sensor. The fabricated sensor exhibited a

stretchability up to 30%, 95% of the morphology was recovered after cutting and healing, stable response was recorded after bending and stretching. Durability tests were evaluated by 10,000 stretch/release cycles. The sensor was prone to bending diameters and with frequent wrist movement and finger bending, the sensor demonstrated excellent performance. Zine Ghemari *et al.* [219] worked on a PDMS matrix integrated with graphene. They optimized the conductivity of the sensor by varying the content of graphene, the sensor successfully endured a 10,000 stretch/release cycle and utilized for human motion monitoring system. A UV curable sensor technology is one of the fundamental applications that is in trend now. Yuquan Zhao *et al.* [220] discussed a detailed analysis on how sensors are fabricated under UV exposure. However, more and more composites are being released, and advancements are being made by carefully choosing the combination of materials. 2-hydroxy-4′-(2-hydroxyethoxy)-2-methylpropiophenone is a photo initiator that is used to initialize a polymerization process of hydrogels under exposure of UV sun rays. They are mostly said to be self-initiating monomers that could initiate polymerization. Sebnem Senol *et al.* [221] presented multiple categories of Irgacure that have been utilized in a polymerization process under UV radiation. The behavior of different stoichiometries of Irgacure have been studied for drug delivery applications. Bérengère Aubry *et al.* [222] discussed different photo initiators like Irgacure (2959) and Irgacure (1173) and investigated hydrogels and polymerization profiles under contrasting wavelengths. Based on composite materials Chenhao Cong *et al.* [223] introduced a novel approach to target self-healing properties by inducing glutaraldehyde (GA)-(PVA)/cellulose nanocrystals (CNC)/ (PEDOT:PSS). They targeted freeze and thaw method through which they achieved 98% of healing efficiency and GF of 2.5. Another approach of strain sensing as well as energy harvesting had been presented by Rui Chen *et al.* [224] where organic materials like starch/polyacrylamide was incorporated and utilized for wearable flexible electronic devices. In health monitoring field hydrogel based strain sensor are gaining a lot of importance reported by Zhiheng Gu *et al.* [225] where conductive polyvinyl alcohol (PVA) hydrogel is produced using ball milling method. Modification of hydrogel is done using plant fibers (PF) and CNTs for dual model wearable devices. The excellent conductivity, self-healing property, stretchability, plant fibers and CNTs are dispersed within the PVA network. The main application of these

hydrogels is in capacitive strain sensors as elastomers for repairing electric circuits because of their high durability and sensitivity (tensile strain approximately 4200%).

The performance of sensors in wearable devices deteriorates because they experience various environmental conditions such as moisture exposure alongside temperature fluctuations and mechanical stress. Engineers face a major scientific obstacle to create materials that repair themselves automatically. The ongoing challenge involves achieving enough conductivity alongside mechanical flexibility. The ionic conductivity of hydrogels diminishes as a we take the application towards flexibility. Herein, we present a novel approach of using 2-hydroxy-4′-(2-hydroxyethoxy)-2-methylpropiophenone Irgacure (2959) as a photo initiator and incorporate the stichometry with phosphoric acid, glycerine and PVA network to utilize them for strain sensing application. The research presents ionic conductive hydrogels that offer a special combination of mechanical strength together with stretchability and conducting properties. The combination of phosphoric acid and glycerin enhances hydrogel ionic conductivity and flexibility, so it becomes suitable for dynamic applications like human body movement detections. The strain sensor demonstrates good biocompatibility together with environmental resistance which makes it suitable for biomedical monitoring and human motion detection applications. The sensor followed by extensive testing procedure that includes evaluation of its mechanical properties, electrical behavior and self-healing capabilities to determine its suitability as a wearable technology. The study strives to enhance next-generation wearable strain sensors which are reliable and efficient and specifically designed for biomedical applications through addressing these challenges.

5.2.3. Experimental Setup

A detailed description of the methodology for developing 2-hydroxy-4′-(2-hydroxyethoxy)-2-methylpropiophenone and PVA hydrogel-based wearable strain sensors includes the preparation methods with experimental setups alongside characterization procedures. The methodology consists of distinct subsections to provide clarity.

5.2.3.1. Materials

The careful selection of materials ensured that the hydrogel possessed high stretchability, excellent self-healing capabilities, and reliable strain-sensing functionality. PVA exists as a powder form with volatility (≤ 50%), viscosity (44-50 mPa.s) and purity ≥99 % which was purchased from Sigma Aldrich. Glycerin

(C_3 H_8 O_3) with density 1.2598g/ml at 25°C purchased form Vance Bioenergy Malaysia. Phosphoric Acid Having P_2O_5 concentration of 18% and is purchased from OCP group mines Morocco. 2-hydroxy-4′-(2-hydroxyethoxy)-2-methylpropiophenone Irgacure (2959) used as a photo initiator (365nm) and purchased form Macklin China.

5.2.3.2. Synthesis of Hydrogel Strain Sensor

Polyvinyl alcohol (PVA) powder was progressively dissolved in deionized water and kept at 80°C while being continuously stirred at 600 rpm to create a viscous solution. The higher temperature promoted solution and uncoiling of polymer chains by breaking down intermolecular hydrogen bonds in the semi-crystalline PVA. The powder was introduced slowly to prevent aggregation and ensure uniform dissolution, leading to the formation of a transparent, viscous solution after approximately two hours. 0.5 mL of glycerin was added to the solution once the polymer matrix was fully hydrated. By intercalating between PVA chains and decreasing intermolecular hydrogen bonding, glycerin functioned as a polyol-based plasticizer, enhancing the segmental mobility and general flexibility of the resultant hydrogel network. To maintain uniform dispersion, stirring rate was maintained at 500 rpm after the temperature was lowered to room temperature (25°C). As an ionic conductivity booster, 0.2 mL of phosphoric acid was added dropwise at this point. Phosphoric acid dissociated into H^+ and $H_2PO_4^-$ and facilitated ionic conduction through the hydrogel matrix. Furthermore, the protonation of hydroxyl groups on PVA side chains have temporarily changed chain interactions, affected the network of hydrogen bonds and encouraged increased ionic mobility throughout the matrix which clearly illustrates that there is a huge compromise between flexibility and conductivity. When the system was completely homogenized, 0.2 g of Irgacure a UV-sensitive photo-initiator, usually Irgacure 2959 was added at the same time. Irgacure when exposed to UV light, produced free radicals that start photopolymerization by removing hydrogen atoms from the hydroxyl-functionalized PVA backbone. The polymer chains undergo covalent crosslinking as a result of this process, creating a stable, three-dimensional network. For a further half hour, stirring was maintained to ensure consistent molecular-level dispersion of the photo initiator throughout the mixture. After that, the finished homogenous precursor solution was put into a 3 mm thick Mold and exposed to UV light for a whole day. Polymerization spread throughout the matrix during this time,

creating a crosslinked hydrogel with increased ionic conductivity, elasticity, and mechanical strength. Covalent crosslinking, ionic interactions, and hydrogen bonding combined to create a strong and flexible hydrogel that can be used in bio-interfacing sensors or stretchable electronics. A detailed synthesis procedure and chemical bonding of hydrogel-based sensor is depicted in Fig.5.27 and Fig. 5.28.

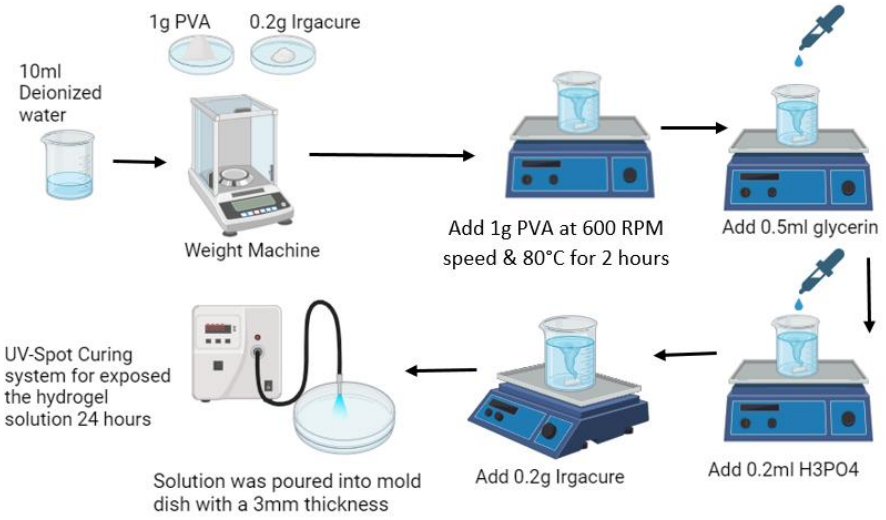

Fig 5.27: Step-by-step schematic representation of the PVA-based hydrogel preparation process, illustrating polymer dissolution, additive incorporation, homogenization, molding, and UV-induced crosslinking

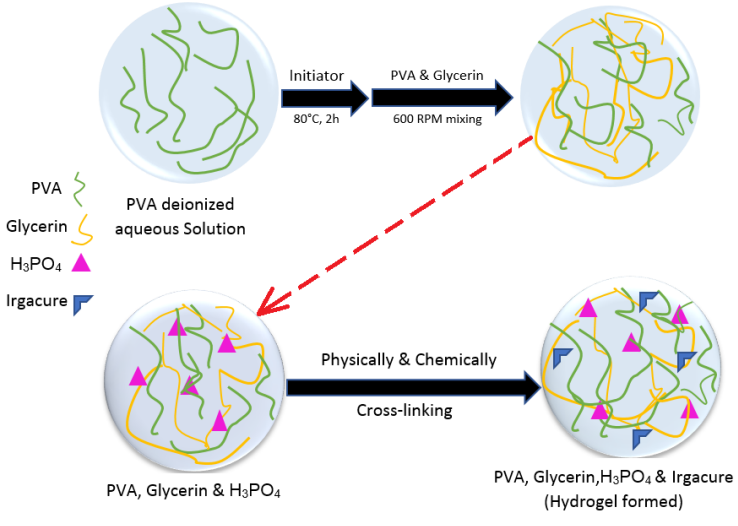

Fig 5.28: Internal dynamics of hydrogel with cross-linked chemical bonding

A comprehensive set of recipes were used to fabricate a device followed by the process discussed. The density of glycerin and pure phosphoric acid was taken as 1.88g/mL and 1.26 g/mL, units were converted into grams, then the total wt./vol was calculated using

sum of total mass of solutes divided by total solvent. Glycerin was not taken into consideration because it acts as a plasticizer and does not contribute to the calculation in grams. Table 5.18 quantifies each material composition utilized in the experiments.

Table 5.18: Material composites synthesis using variance range of concentrations

Sr. No.	PVA (g)	Irgacure (g)	Deionized Water (mL)	Glycerin (mL)	H_3PO_4 (mL)	Total wt/vol (%)
i.	2	1	12	-	0.5	32.83%
ii.	1.5	-	6	-	0.7	46.93%
iii.	0.5	0.5	5	-	0.5	38.80%
iv.	0.8	-	12	-	0.5	14.50%
v.	0.5	0.2	7	0.2	0.3	18.06%
vi.	0.8	0.8	10	0.2	0.8	31.04%
vii.	1	0.5	15	0.5	0.1	11.25%
viii.	1	-	12	0.1	0.2	11.47%
ix.	1	0.2	19	0.2	0.2	15.76% ✓
x.	1	0.5	10	1	0.2	18.76%

In order to prepare it for further testing, the hydrogel was molded and then sliced into rectangular strips with standard measurements of 40 mm × 10 mm × 3 mm after curing. Conductive electrode layers were incorporated into the hydrogel-based strain sensors for mechanical and electrical evaluation. Magnetron sputtering was used to manufacture the PVA-based strain sensor's electrodes that can be seen in Fig.5.29 (a). Using a plasma-assisted sputtering method in a controlled chamber setting, a copper thin coating was applied to the hydrogel strips' side and corner surfaces, as depicted in Fig.5.29 (b). In order to accelerate positively charged argon ions toward a copper target, magnetron sputtering creates a high-density plasma. Copper atoms are released from the target upon impact and then fall onto the substrate surface in a homogeneous thin layer. This method allows delicate materials, such as hydrogels, to be precisely coated at low temperatures without compromising their structural integrity. Continuous electrical pathways, which are essential for accurate strain sensing and self-healing functionality, were guaranteed by the deposition at the corners and edges of the sensor. As shown in Fig.5.29(c), the resultant PVA-based hydrogel strain sensors were assessed for mechanical responsiveness and electrical conductivity. They were now fitted with conformal copper electrodes using a good copper foil for better acquisition of data.

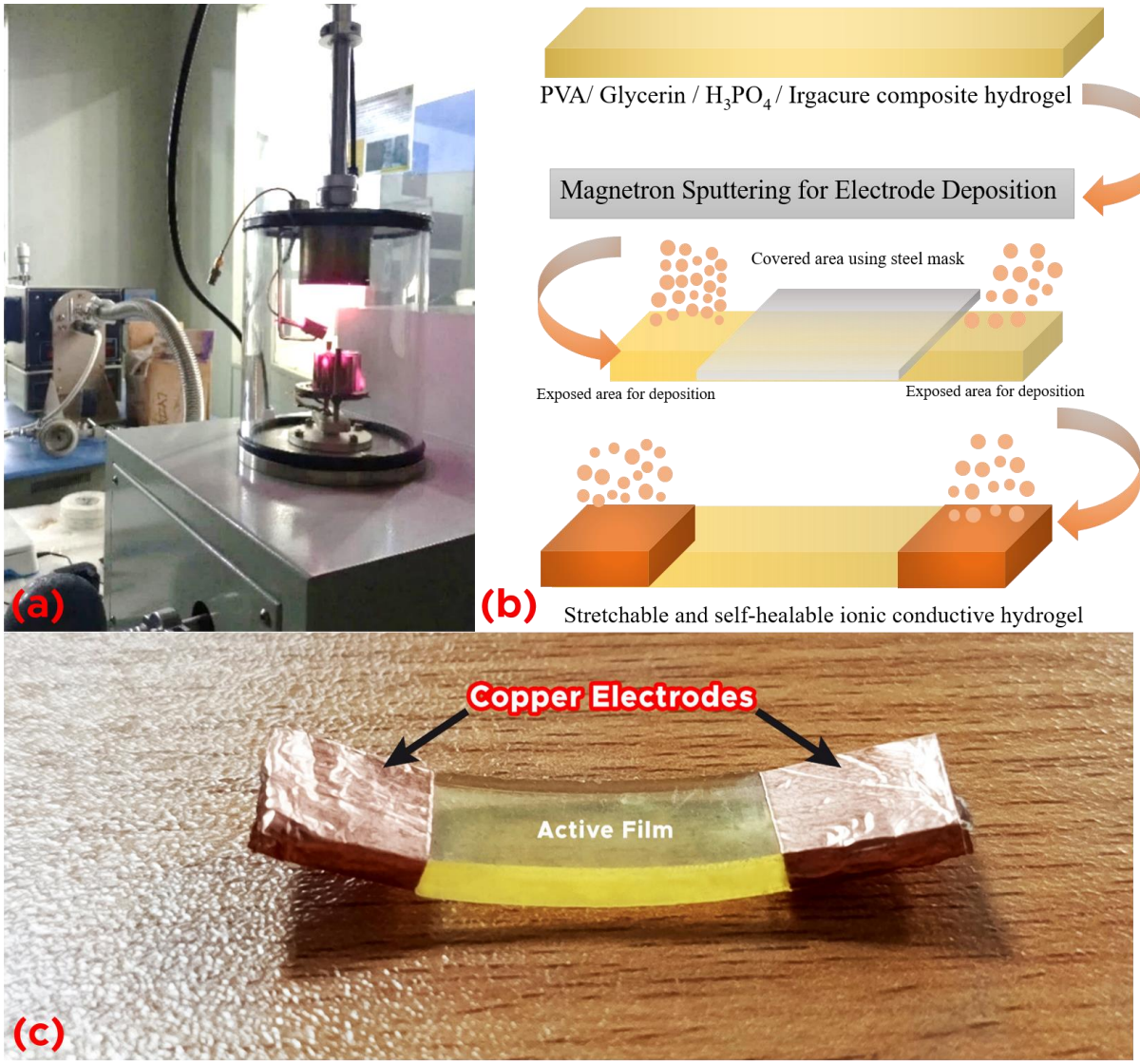

Fig 5.29: (a) Magnetron sputtering setup employed for the deposition of copper electrodes. (b) Schematic illustration highlighting the targeted copper deposition along the edges of the proposed sensor structure. (c) Detailed image of the final fabricated device featuring well-defined copper electrodes covered with copper foil for better conductivity

5.2.4. Results and Discussion

A thorough set of characterizations was carried out in order to assess the suggested hydrogel-based strain sensor's structural and functional performance. The sensor was developed with a polymeric matrix that included phosphoric acid, glycerin, (PVA), and the photo initiator Irgacure 2959. It was intended to have excellent sensitivity, stretchability, and flexibility under mechanical deformation. These elements operate in coordination to create a porous yet strong network that facilitates efficient ion

movement and deformation-induced electrical responsiveness. The porous microstructure of the hydrogel, as revealed by SEM imaging, plays a crucial role in its strain sensing functionality. **Fig. 5.30 (a)** shows a magnified SEM image, highlighting a uniform and smooth hydrogel surface, indicating homogeneity of the matrix. **Fig.5.30 (b)** captures the porous microstructure at higher magnification, which plays a critical role in ionic conductivity and flexibility. Pores ranging from **797 nm to 1.87 µm** were identified, as shown in **Fig. 5.30 (c).** Strain absorption through pores deforms the hydrogel which leads to modifications in its internal structure while producing resistance variables. The sensor relies on the precise measurements of pores which directly determine both mechanical and electrical properties. The sensor shows better water retention features and enhanced ion mobility because of its larger pores which also improve its sensitivity. In addition to confirming the material's compliant and elastic nature, the porous morphology seen by SEM further supports the material's suitability for flexible, high-performance strain sensing applications. The microstructure of the hydrogel sensor was analyzed using SEM and EDS techniques. **Fig. 5.30(d)** presents the **EDS spectrum**, confirming the presence of carbon (C), oxygen (O), and phosphorus (P), which validates the successful integration of PVA, phosphoric acid, and glycerin into the hydrogel matrix.

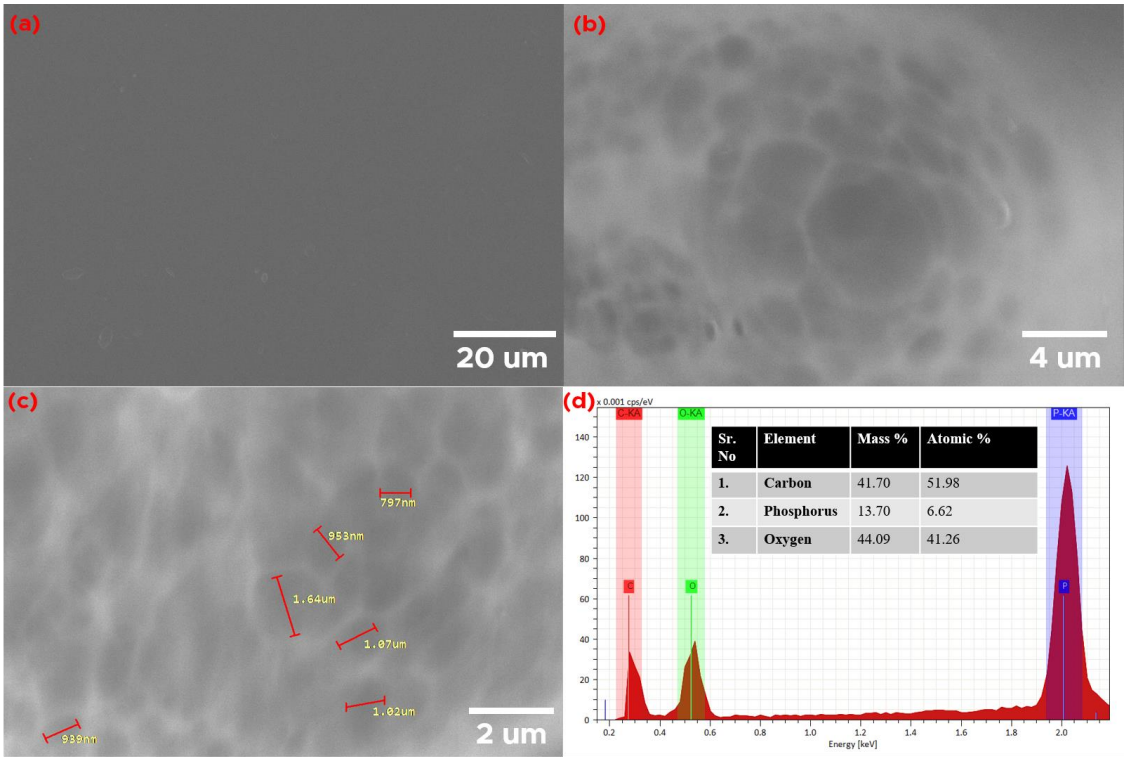

Fig 5.30: Characterization of the hydrogel-based strain sensor using SEM and EDX. (a) A low-magnification SEM image that serves as a spatial reference and highlights an impurity particle. (b) The hydrogel's porous architecture, as shown at the 4 µm scale, demonstrates the existence of interconnecting pores. (c) A high magnification SEM picture (2 µm scale) that supports the material's strain-responsive architecture by describing the pore diameters. (d) EDX elemental analysis verifying the hydrogel matrix's essential components, homogeneous distribution and composition

A hydrogel-based composite designed for biomedical motion detection applications was successfully used to create a flexible strain sensor that is self-healing. Because of its exceptional conformability and structural integrity, the gadget can be used for dynamic physiological movement monitoring. The gadget was attached to a universal testing machine (UTM) and connected to an electrical measuring setup in order to evaluate its strain sensitivity, stretchability, and durability. **Fig.5.31** represents the I-V characteristics of the strain sensor under varying strain levels (0%, 25%, 50%, and 75%) as well as varying voltage levels. The results indicate that as the strain increases, the current decreases for the same applied voltage. At **5V**, the current at **0% strain** was **65 µA**, which gradually dropped to **47 µA** at **25% strain, 39 µA** at **50% strain**, and finally to **28 µA** at **75% strain.** This increase in resistance under strain demonstrates the sensor's sensitivity, as stretching causes deformation in the hydrogel network, reducing ion mobility and increasing resistance.

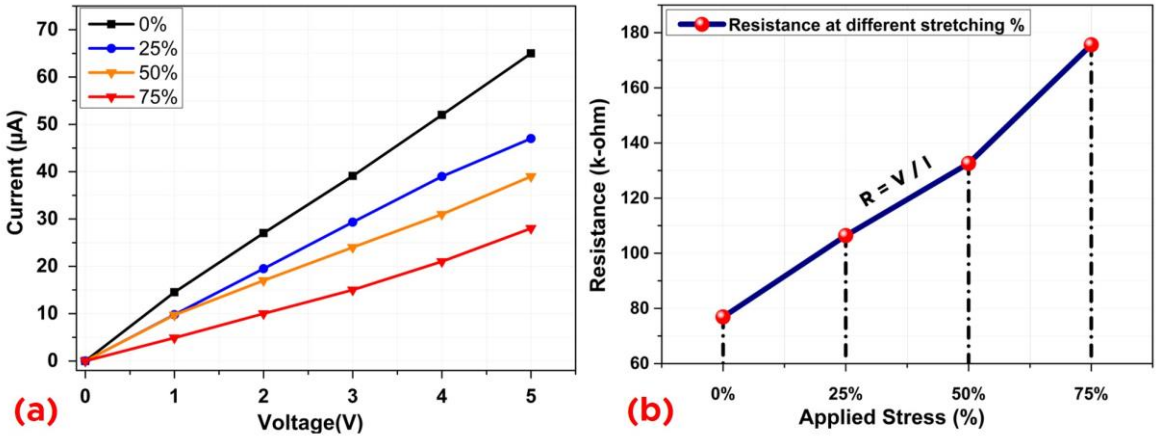

Fig 5.31: I-V Characterization of the hydrogel-based strain sensor using (a) Voltage vs current plots with increasing trend via applied stress (b) Graphical trend depicting increase in resistance via applied stress

Real-time monitoring of resistance variations occurred when the fabricated device was connected to an electromechanical workstation. The sensor recorded electrical signals

throughout cyclic stretching and releasing and bending tests for assessing its sensitivity and mechanical properties and durability. To evaluate the sensor's durability and mechanical performance, stretching and releasing cycle tests were conducted. **Fig. 5.32 (a)** demonstrates the sensor's response at strain levels of **0%, 25%, 50%, 75%, and 100%,** showing consistent and repeatable changes in resistance under varying deformations. The sensor experienced a force linearly that exhibited increase in resistance. Upon releasing, the sensor reverted back to its original formation and decreased the resistance. This repeated change was performed to evaluate sensor mechanical response. Each span of 100 cycles at different stretching intervals was carried out and individually, **Fig. 5.32 (b)** depicts the strain sensor's performance over **100 stretching-releasing cycles**, where the resistance variations remained stable, indicating excellent durability. **This test** further validates the sensor's stability by plotting starting resistance of approx. 80kΩ and changes over **100 continuous stretching cycles** without significant degradation, confirming long-term mechanical reliability.

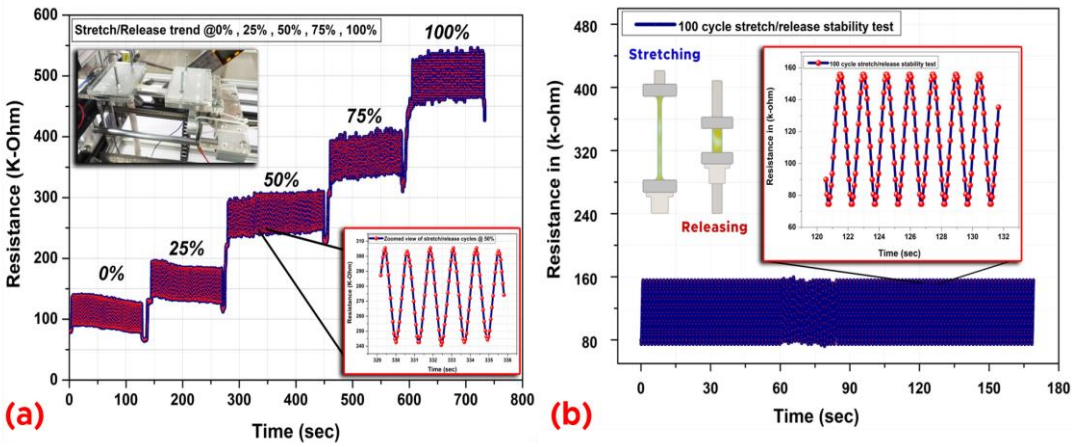

Fig 5.32: The proposed sensor stability test (a) Sensor is stretched at multiple percentages and stability test is performed (b) Sensor at initial position and stable 100 cycle test is performed

Through a series of progressive tensile tests intended to evaluate its durability, elasticity, and recovery behavior under repeated and increasing strain levels, the mechanical stability of the self-healable strain sensor based on a polyvinyl alcohol (PVA), glycerin, Irgacure, and phosphoric acid composite was assessed. As shown in **Fig.5.33(a)** the sensor underwent incremental tensile loading in the first test, which involved stretching it to 10% strain, holding it there for 5 seconds, and then stretching

it further in 10% increments, with 5-second breaks in between, until it reached 100% strain. The sensor was gradually released in 10% increments down to 0% after reaching 100%. During this loading-unloading cycle, the sensor's ability to retain structural integrity and a constant electrical response demonstrated exceptional mechanical robustness and adhesion within the composite matrix. The sensor was repeatedly stretched and released at increasing strain levels in the second test. It was stretched to 10%, 25%, 50%, 75%, and 100% strains before being released back to 0% strain each time. The sensor's structural resilience and mechanical dependability under a range of strain amplitudes were further evaluated using this cyclic loading. The material's capacity to withstand mechanical stress without losing functionality was validated by the lack of delamination, permanent deformation, or mechanical degradation over cycles as shown in **Fig.5.33 (b).** The response and recovery curves, which are crucial markers of the sensor's capacity to respond and return to its baseline state upon loading and unloading, respectively, were plotted in a third test to assess the dynamic sensing properties. The sensor's rapid responsiveness and effective recovery behaviors were demonstrated by these curves, which were acquired across 100 strain cycles and displayed response times of 660 ms and 730 ms respectively as depicted in **Fig.5.33 (c).** The sensor's applicability for wearable and flexible electronics applications was confirmed by its overall impressive mechanical stability, dependable strain responsiveness, and consistent performance under cyclic and incremental strain.

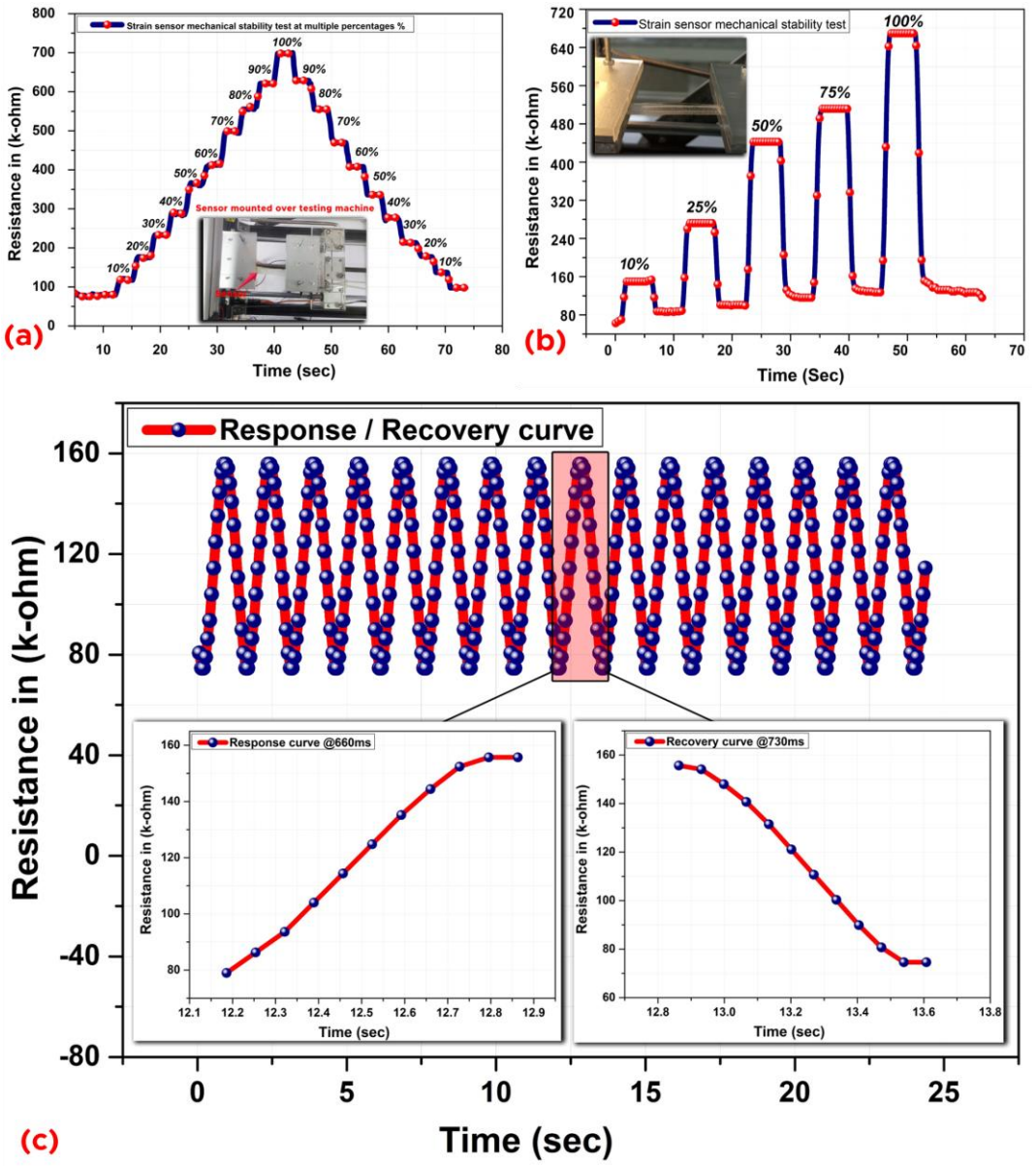

Fig 5.33: (a) Mechanical stability performance of the proposed sensor at different stretches levels (b) Stretching response at different strain levels from 0% to maximum to 0% (c) Response and recovery trend obtained from stretch release cycle test

Gauge factor is the ratio of the relative resistance change to the applied strain as indicated by Equation 5.15, is a measurement of a material's strain sensitivity. It measures the amount that a material's resistance varies for a specific percentage of elongation or deformation. A higher Gauge Factor (GF) indicates a greater sensitivity to strain, which means that for a given applied strain, the material's resistance varies more dramatically. This indicates that the sensor is more sensitive to strain variations, which makes it appropriate for high-sensitivity applications. When the sensor was put into external stimuli from 0 to 10%. The initial resistance was recorded to 80kΩ, and

the proposed strain sensor demonstrated a change in resistance with 160kΩ and a Gauge factor of 10 with 4cm initial dimensions of the strain sensor film.

$$GF = (\Delta R / R) / \varepsilon \qquad (5.15)$$

An efficient extrinsic self-healing mechanism is demonstrated by the fabricated strain sensor, in which microcapsules implanted in the polymer matrix release a healing agent in response to mechanical damage, such as the development of microcracks brought on by excessive strain. In order to autonomously restore the structural integrity and electrical performance of the sensor, these capsules are designed to burst under stress, releasing a filament-like healing agent that can create dynamic reversible bonds such as hydrogen bonds. Unlike intrinsic self-healing, which depends on the polymer network's natural dynamic bonding ability without the use of extra agents, this design represents a bioinspired extrinsic healing approach, in which healing elements are stored independently and only activated upon damage. A detailed demonstration along with an LED connected in series is used for practical application of self-healing mechanism. The sensor is sliced into two parts; this disrupted the continuous flow of current as shown in Fig.5.34 (a). On convolving these 2 parts, the internal self-healing dynamics of the sensor made a strong chain with each other leading to a smooth flow of current. This self-healing and connection between two distinct layers validated that the sensor self-healed phenomenally and the LED is glowing with exceptional brightness exhibiting that sensor also has a plausible resistance as shown in Fig.5.34 (b). An open circuit test was conducted in order to evaluate its maximum stretching level. The proposed sensor was stretched up to 110% and resulted an open circuit where resistance went up to 1MΩ as shown in Fig.5.34 (c). A crucial indicator of a sensor's capacity to regain its initial electrical or mechanical functionality following damage is self-healing efficiency, which is commonly computed as the ratio of healed to original performance. The healing efficiency in our study was achieved ~94%, which is good and within the range stated in the literature (usually 80–95%) for polymer-based self-healing strain sensors. This is indicated by a post-healing resistance of 85kΩ in contrast to the initial 80kΩ as shown in Fig.5.34 (d). In practical applications, effective self-healing also increases user safety, decreases maintenance requirements, and prolongs gadget lifespan.

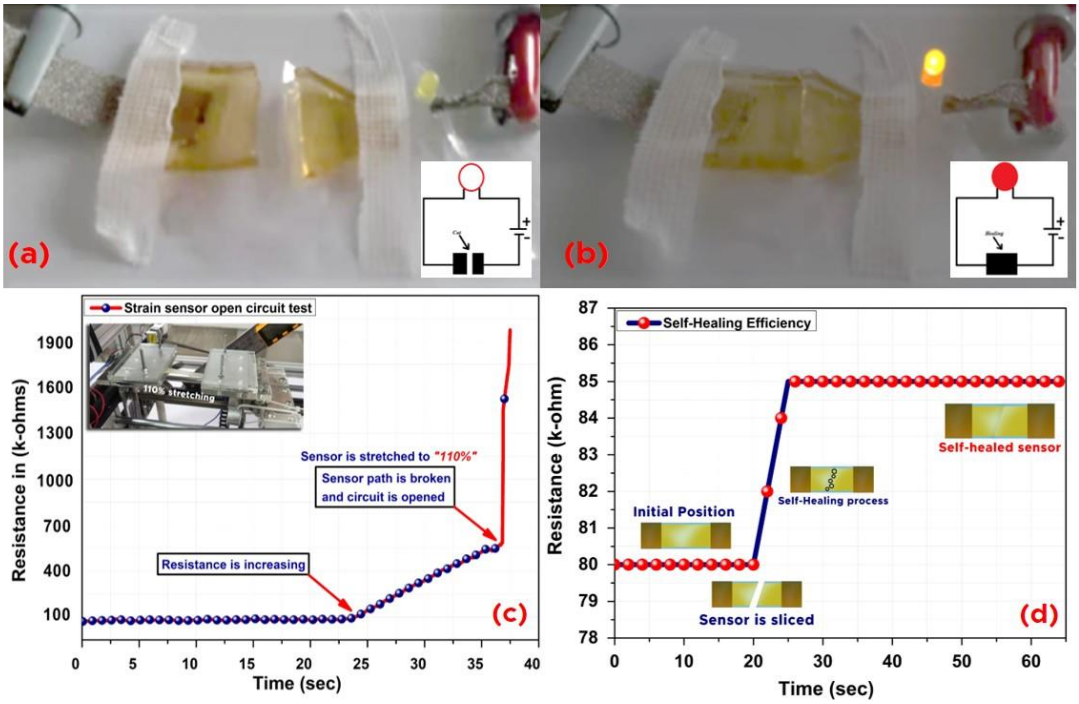

Fig 5.34: Demonstration of the self-healing hydrogel-based strain sensor regaining electrical conductivity after (a) Cutting and (b) Healing, as indicated by the illumination of the LED. (c) Open circuit test for strain sensing applications (d) Mapping of self-healing efficiency of strain sensor

The hydrogel-based strain sensor demonstrated outstanding performance characteristics of sensitivity together with mechanical stability and durability. However, it is an attractive solution for wearable strain sensors. Strain sensors have been positioned on for use on fingers and elbows and knees as well as facial muscles. The sensor achieved dual functionality by detecting broad body movements and biological signals from facial expressions along with vocal activities. The hydrogel strain sensor showed versatility through experimental findings which enabled its practical use across multiple body locations for motion monitoring. As shown in Fig.5.35 The proposed strain sensor testing conducted on a total 10 participants both female (5) and male (5) individually (age range 25-40).The proposed sensor showed repeatable resistance during various body motions and make it suitable tool for wearable motion detection applications.Fig.5.35 (a), the proposed sensor was mounted over the elbow and experience a slow stretch release forces to acquire smooth trend. Fig.5.35 (b), shows the stretch release cycles when the sensor was mounted over the knee then as mentioned in Progressive movements of the body were recorded. Fig.5.35 (c) when the user was supposed to wear the sensor over the wrist. Fig.5.35 (d), shows

finger bending test was conducted at 30º, 60º and 90º .Fig.5.35 (e), shows the graphical trend was plotted using the up down movements of the sitting postures of the user.

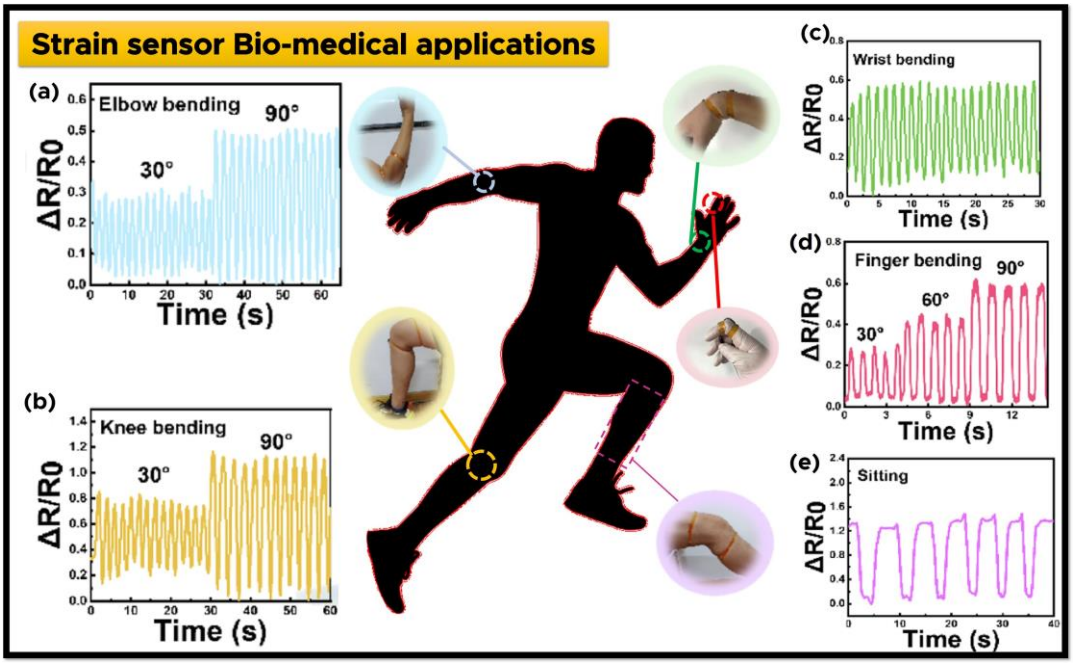

Fig 5.35: Practical applications of the fabricated sensor mounted over different parts of the human body (a) Elbow joint movements at different angles (b) Knee bending/relaxing (c) Wrist up down movements (d) finger bending/relaxing (e) Recording of sitting posture of a human body

Chapter 6

Conclusion and Future Work

6.1. Conclusion:

The conclusion is divided into two sections based on studies conducted on in this research and each section is summarized as follows.

6.1.1. Fe_2O_3, Ag Flakes and PU based Strain Sensor

This study successfully demonstrated the development of a novel flexible self-healable strain sensor that addresses critical limitations in existing technologies, including low healing efficiency and limited sensitivity. By integrating a polyurethane (PU) substrate with magnetic iron oxide nanoparticles (MIONPs) and silver flakes, the sensor achieved a high gauge factor of 271.4 at 35% strain, marking a substantial improvement in strain sensitivity compared to conventional sensors. The sensor also demonstrates an impressive self-healing efficiency of 96.6% within 24 hours, significantly reducing recovery time and enhancing durability. Additionally, the sensor's magnetic responsiveness with a sensitivity of 0.0049 T^{-1} expands its potential applications in soft robotics, wearable electronics, and magnetically assisted devices. The combination of high sensitivity, rapid self-healing, and multifunctionality makes this sensor a promising solution for sustainable, long-term sensing applications. In future work one may optimize the sensor's performance by exploring different substrate materials and test its long-term stability under various conditions.

The following points are key findings of our research work as given below:

- Silver flakes are incorporated as conductive materials in flexible self-healable strain sensors. They enhance the overall conductivity, piezoresistive response, and gauge factor of the sensor.
- Magnetic Iron Oxide Nanoparticles (MIONPs) are introduced to improve stability. When the silver flake layer undergoes fracture under strain, MIONPs migrate to fill the resulting gaps, thereby restoring conductivity and enhancing electrical, chemical, and mechanical stability. This self-healing mechanism significantly extends the sensor’s operational lifespan.

- Polyurethane (PU) is employed as both the substrate and the encapsulating protective layer due to its excellent stretchability, flexibility, biocompatibility, and water resistance. PU also facilitates the uniform incorporation of conductive fillers such as silver flakes and MIONPs, enabling the fabrication of durable and reliable sensing devices.
- Utilizing these materials the fabricated strain sensor achieves high efficiency of 96.6% within 24 hours easily, as compared to other traditional sensors which efficiency decay with the passage of time.
- As the materials used iron oxide and silver flakes, both have high gauge factors therefore in our research we have achieved high gauge factor of 271.4 at 35% strain. This indicated that strain sensors have very high sensitivity.
- Similarly high responsiveness is achieved against external magnetic field and the fabricated strain sensor magnetic sensitivity of 0.0049 T^{-1} is also achieved.
- The strain sensor longevity is up to the mark even after six months it's self-healing and flexibility remains stable.

6.1.2. 2-Hydroxy-4′-(2-Hydroxyethoxy)-2-Methylpropiophenone and PVA composite Based Strain Sensor

In this case we developed a highly tensile and self-healing hydrogel-based strain sensor through the combination of polyvinyl alcohol (PVA), glycerin, phosphoric acid and Irgacure as a photoinitiator. The sensor showed excellent mechanical flexibility alongside self-healing features together with electrical sensitivity which makes it suitable for wearable and biomedical applications. Hydrogel network formation relied on physical and chemical cross-links according to SEM and EDS examinations throughout the stepwise preparation method. The uniform microstructure analysis showed that well-distributed pores which maintain vital roles for sensor flexibility and conductivity as well as strain responsiveness. The I-V characterization provided evidence for direct correlation between applied strain intensity and resistance variations since increased strain led to lower current values. The developed strain sensor provides a successful integration of high stretchability, rapid responsiveness alongside self-healing functionality and extended mechanical stability. Its combination of said attributes positions the sensor to be useful for human body motion monitoring, wearable electronics and biomedical sensing device applications. The author suggests investing

in future research to enhance both mechanical strength and electrical performance under extreme conditions in order to achieve broader use of smart flexible sensor technologies.

Similarly in this case we have different the following key points which are given follows:

- The PVA hydrogel base strain sensor is analyzed where at 0% strain its current value is 65 μA however, at 75% of strain its current is reduced to is 25 μA. The increase in resistance indicates a high gauge factor. So, this PVA hydrogel-based strain sensor possesses highly sensitivity according to its electrical parameter variation.
- The PVA hydrogel base strain sensor at strain level 0% to 100%, showing consistent and repeatable changes in resistance under varying deformation. Even at 100 continuous stretching cycles the sensor stability is up to the mark without significant degradation, confirming long term mechanical reliability.
- The PVA hydrogel base strain sensor recovery time is 730ms and its response time is 600ms. So, the sensor detected any signal speed and recovered its deformation (cracks and mechanical instability) easily and smoothly. So, from strain sensor's this property we can easily integrate this sensor into outer world application due to its suitability and robustness for real world application.
- Its maximum stretching limit recorded is 110%, and its response remained constant throughout the tests. This indicates the sensor material ability to recover its electrical conductivity and mechanical stability against cracks at higher level of stress.
- The proposed strain sensor reveals a uniform and smooth morphology which is identified by SEM and EDS. The image with annotated measurements of the proved sizes, ranging from 797nm to 1.87μm, confirming the micro and Nano-scale porosity of the hydrogel materials. The material gains increased its mechanical performance and sensitivity through its porous structure.
- The proposed sensor demonstrated an excellent 0-100% stretching cycle stability test, 94% practically recovered conductivity after self-healing through LED blinking test, achieved outstanding mechanical pliability with GF up to 10, that indicate strain sensor gauge factor is functional or not.

6.2. Future Work

In the future one may choose hybrid materials (Organic and inorganic) and focus on the basis of multifunctionality, ultra-stretchability, longevity, efficiency and sensitivity for more improvement and advance applications. Some of the key areas are addressed comprehensively for upcoming wearable and self-healable strain sensors which are as given below:

- Advance materials are needed to be utilized, especially self-healing polymers, 2D material (MXenes), natural polymers for sustainability and Carbon Nanotubes (CNTs) which offer more electrical conductivity, cost-effectiveness and sensitivity of wearable self-healable strain sensors.
- The main problem in this type of wearable and self-healable strain sensor is that after multiple time folding, stretching and specific time interval aging factor involves. Therefore, in the future one must work on efficient cross-linking or chemical bonding of materials and extensive study work on the latest technology to debug this problem.
- Self-power sensor concept needs to be introduced in future by integrating the self-healable strain sensor with Internet of things (IOT) using AI and 5G transmitting and receiving the real time data form remote areas and monitoring applications.
- These wearable self-healable strain sensors need to be used for energy harvesting in the future i.e. so, compatibility with Nanogenerator and turboelectric devices is the key challenge.
- In the future one should make these sensors biocompatible. So, they must be compatible with human skin and ultra-transparent.
- Electrodes of strain sensors play a vital role in the performance of sensors. In the future one may work on it and make it flexible and self-healable like Carbon Nanotube (CNT) based composites. PDMS which reflect to make propose strain sensor more flexible and durable.
- In future smart fabric and textile compactable self-healable strain sensors can be developed using the current work.

References

[1] Li, J., Fang, L., Sun, B., Li, X., & Kang, S. H. (2020). Recent progress in flexible and stretchable piezoresistive sensors and their applications. Journal of the Electrochemical Society, 167(3), 037561.

[2] Song, L., Chen, J., Xu, B. B., & Huang, Y. (2021). Flexible plasmonic biosensors for healthcare monitoring: Progress and prospects. ACS nano, 15(12), 18822-18847.

[3] Wang, Y., Yang, B., Hua, Z., Zhang, J., Guo, P., Hao, D., & Huang, J. (2021). Recent advancements in flexible and wearable sensors for biomedical and healthcare applications. Journal of Physics D: Applied Physics, 55(13), 134001.

[4] Liu, L., Yang, X., Zhao, L., Xu, W., Wang, J., Yang, Q., & Tang, Q. (2020). Nano wrinkle-patterned flexible woven triboelectric nanogenerator toward self-powered wearable electronics. Nano Energy, 73, 104797.

[5] Cheng, M., Zhu, G., Zhang, F., Tang, W. L., Jianping, S., Yang, J. Q., & Zhu, L. Y. (2020). A review of flexible force sensors for human health monitoring. Journal of advanced research, 26, 53-68.

[6] Xu, K., Lu, Y., & Takei, K. (2021). Flexible hybrid sensor systems with feedback functions. Advanced Functional Materials, 31(39), 2007436.

[7] Li, Y., Zhang, M., Hu, X., Yu, L., Fan, X., Huang, C., & Li, Y. (2021). Graphdiyne-based flexible respiration sensors for monitoring human health. Nano Today, 39, 101214.

[8] Gai, Y., Li, H., & Li, Z. (2021). Self-healing functional electronic devices. Small, 17(41), 2101383.

[9] Ma, Z., Li, H., Jing, X., Liu, Y., & Mi, H. Y. (2021). Recent advancements in self-healing composite elastomers for flexible strain sensors: Materials, healing systems, and features. Sensors and Actuators A: Physical, 329, 112800.

[10] Gomes, C., Alocilja, E., Yu, C., Gunasekaran, S., Jenkins, D., Datta, S., & Zhou, A. (2021). FEAST of Biosensors: Food, Environmental and Agricultural Sensing Technologies (FEAST) in North America.

[11] Lou, Z., Wang, L., Jiang, K., Wei, Z., & Shen, G. (2020). Reviews of wearable healthcare systems: Materials, devices and system integration. Materials Science and Engineering: R: Reports, 140, 100523.

[12] Ma, Y., Zhang, Y., Cai, S., Han, Z., Liu, X., Wang, F., & Feng, X. (2020). Flexible hybrid electronics for digital healthcare. Advanced Materials, 32(15), 1902062.

[13] Mayberry, M. (2013). Pushing past the frontiers of technology. Frontiers of Characterization and Metrology for Nanoelectronics. http://www. nist. Gov/pml/div683/conference/upload/Mayberry final. pdf.

[14] Lee, T. (2015). The hardware enablers for the internet of things-part i. URL https://iot.ieee.org/newsletter/january-2015/the-hardware-enablers-for-the-internet-of-things-part-i. html.

[15] Lu, Y., Qu, X., Zhao, W., Ren, Y., Si, W., Wang, W., & Dong, X. (2020). Highly stretchable, elastic, and sensitive MXene-based hydrogel for flexible strain and pressure sensors. Research.

[16] Wang, L., Xu, T., & Zhang, X. (2021). Multifunctional conductive hydrogel-based flexible wearable sensors. TrAC Trends in Analytical Chemistry, 134, 116130.

[17] Ham, J. (2020). Skin-like multi-modal sensing devices for dexterous robotic hands. Stanford University.

[18] Lee, E. K., Yoo, H., & Lee, C. H. (2020). Advanced Materials and Assembly Strategies for Wearable Biosensors: A Review. Biosens.-Curr. Nov. Strateg. Biosensing, 83-110.

[19] Wang, C., Yokota, T., & Someya, T. (2021). Natural biopolymer-based biocompatible conductors for stretchable bioelectronics. Chemical Reviews, 121(4), 2109-2146.

[20] Idumah, C. I. (2021). Recent advancements in self-healing polymers, polymer blends, and nanocomposites. Polymers and Polymer Composites, 29(4), 246-258.

[21] Souri, H., Banerjee, H., Jusufi, A., Radacsi, N., Stokes, A. A., Park, I., & Amjadi, M. (2020). Wearable and stretchable strain sensors: materials, sensing mechanisms, and applications. Advanced Intelligent Systems, 2(8), 2000039.

[22] Paixão, T., Araújo, F., & Antunes, P. (2019). Highly sensitive fiber optic temperature and strain sensor based on an intrinsic Fabry–Perot interferometer fabricated by a femtosecond laser. Optics Letters, 44(19), 4833-4836.

[23] Su, G., Yin, S., Guo, Y., Zhao, F., Guo, Q., Zhang, X., & Yu, G. (2021). Balancing the mechanical, electronic, and self-healing properties in conductive

self-healing hydrogel for wearable sensor applications. Materials Horizons, 8(6), 1795-1804.

[24] Li, Q., Dai, K., Zhang, W., Wang, X., You, Z., & Zhang, H. (2021). Triboelectric nanogenerator-based wearable electronic devices and systems: Toward informatization and intelligence. Digital Signal Processing, 113, 103038.

[25] Wang, K., Yap, L. W., Gong, S., Wang, R., Wang, S. J., & Cheng, W. (2021). Nanowire-based soft wearable human–machine interfaces for future virtual and augmented reality applications. Advanced Functional Materials, 31(39), 2008347.

[26] Yu, H., Yang, X., Lian, Y., Wang, M., Liu, Y., Li, Z., & Gou, J. (2021). An integrated flexible multifunctional wearable electronic device for personal health monitoring and thermal management. Sensors and Actuators A: Physical, 318, 112514.

[27] Li, S., Liu, G., Wang, L., Fang, G., & Su, Y. (2020). Overlarge Gauge Factor Yields a Large Measuring Error for Resistive-Type Stretchable Strain Sensors. Advanced Electronic Materials, 6(11), 2000618.

[28] Zhang, Lin, et al. "Thiolated Graphene@ Polyester Fabric-Based Multilayer Piezoresistive Pressure Sensors for Detecting Human Motion." ACS applied materials & interfaces 10.48 (2018): 41784-41792.

[29] Zhao, Q., Frogley, M. D., & Wagner, H. D. (2002). Direction-sensitive strain-mapping with carbon nanotube sensors. Composites Science and Technology, 62(1), 147-150.

[30] Yan, C., Wang, J., Kang, W., Cui, M., Wang, X., Foo, C. Y., & Lee, P. S. (2014). Highly stretchable piezoresistive graphene–nanocellulose nano paper for strain sensors. Advanced materials, 26(13), 2022-2027.

[31] Sun, B., Long, Y. Z., Liu, S. L., Huang, Y. Y., Ma, J., Zhang, H. D., & Xu, S. (2013). Fabrication of curled conducting polymer micro fibrous arrays via a novel electrospinning method for stretchable strain sensors. Nanoscale, 5(15), 7041-7045.

[32] Cheng, S., & Wu, Z. (2011). A microfluidic, reversibly stretchable, large-area wireless strain sensor. Advanced functional materials, 21(12), 2282-2290.

[33] Obitayo, W., & Liu, T. (2012). A review: carbon nanotube-based piezoresistive strain sensors. Journal of Sensors, 2012.

[34] Segev-Bar, M., & Haick, H. (2013). Flexible sensors based on nanoparticles. ACS nano, 7(10), 8366-8378.

[35] Xiao, X., Yuan, L., Zhong, J., Ding, T., Liu, Y., Cai, Z., & Wang, Z. L. (2011). High-strain sensors based on ZnO nanowire/polystyrene hybridized flexible films. Advanced materials, 23(45), 5440-5444.

[36]He, X., Liu, Q., Wang, J., & Chen, H. (2019). Wearable gas/strain sensors based on reduced graphene oxide/linen fabrics. Frontiers of Materials Science, 13(3), 305-313.

[37]Zhang, L., Li, H., Lai, X., Gao, T., Yang, J., & Zeng, X. (2018). Thiolated graphene@ polyester fabric-based multilayer piezoresistive pressure sensors for detecting human motion. ACS applied materials & interfaces, 10(48), 41784-41792.

[38] Liu, J., Guo, Q., Mao, S., Chen, Z., Zhang, X., Yang, Y., & Zhang, X. (2018). Templated synthesis of a 1D Ag nanohybrid in the solid state and its organized network for strain-sensing applications. Journal of Materials Chemistry C, 6(40), 10730-10738.

[39] Duan, L., D'hooge, D. R., & Cardon, L. (2020). Recent progress on flexible and stretchable piezoresistive strain sensors: From design to application. Progress in Materials Science, 114, 100617.

[40] Kim, J. J., Wang, Y., Wang, H., Lee, S., Yokota, T., & Someya, T. (2021). Skin electronics: next-generation device platform for virtual and augmented reality. Advanced Functional Materials, 31(39), 2009602.

[41] Niu, Y., Liu, H., He, R., Li, Z., Ren, H., Gao, B., & Xu, F. (2020). The new generation of soft and wearable electronics for health monitoring in varying environment: From normal to extreme conditions. Materials Today, 41, 219-242.

[42] Imato, K., Nishihara, M., Kanehara, T., Amamoto, Y., Takahara, A., & Otsuka, H. (2012). Self-healing of chemical gels cross-linked by diarylbibenzofuranone-based trigger-free dynamic covalent bonds at room temperature. Angewandte Chemie, 124(5), 1164-1168.

[43] Lenhardt, J. M., Kim, S. H., Nelson, A. J., Singhal, P., Baumann, T. F., & Satcher Jr, J. H. (2013). Increasing the oxidative stability of poly (dicyclopentadiene) aerogels by hydrogenation. Polymer, 54(2), 542-547.

[44] Cao, J., Zhou, C., Su, G., Zhang, X., Zhou, T., Zhou, Z., & Yang, Y. (2019). Arbitrarily 3D Configurable Hygroscopic Robots with a Covalent–Noncovalent

Interpenetrating Network and Self-Healing Ability. Advanced Materials, 31(18), 1900042.

[45] Fuhrmann, A., Göstl, R., Wendt, R., Kötteritzsch, J., Hager, M. D., Schubert, U. S., & Hecht, S. (2016). Conditional repair by locally switching the thermal healing capability of dynamic covalent polymers with light. Nature communications, 7(1), 1-7.

[46] Burattini, S., Greenland, B. W., Merino, D. H., Weng, W., Seppala, J., Colquhoun, H. M., & Rowan, S. J. (2010). A healable supramolecular polymer blend based on aromatic π− π stacking and hydrogen-bonding interactions. Journal of the American Chemical Society, 132(34), 12051-12058.

[47] Hu, Z., Zhang, D., Lu, F., Yuan, W., Xu, X., Zhang, Q., & Huang, Y. (2018). Multistimuli-responsive intrinsic self-healing epoxy resin constructed by host–guest interactions. Macromolecules, 51(14), 5294-5303.

[48] Hillewaere, X. K., & Du Prez, F. E. (2015). Fifteen chemistries for autonomous external self-healing polymers and composites. Progress in Polymer Science, 49, 121-153.

[49] Urdl, K., Kandelbauer, A., Kern, W., Müller, U., Thebault, M., & Zikulnig-Rusch, E. (2017). Self-healing of densely crosslinked thermoset polymers—a critical review. Progress in Organic Coatings, 104, 232-249.

[50] Li, X., Zhang, H., Zhang, P., & Yu, Y. (2018). A sunlight-degradable autonomous self-healing supramolecular elastomer for flexible electronic devices. Chemistry of Materials, 30(11), 3752-3758.

[51] Wu, J., Cai, L. H., & Weitz, D. A. (2017). Tough self-healing elastomers by molecular enforced integration of covalent and reversible networks. Advanced materials, 29(38), 1702616.

[52] Li, X., Zhang, R., Yu, W., Wang, K., Wei, J., Wu, D., & Zhu, H. (2012). Stretchable and highly sensitive graphene-on-polymer strain sensors. Scientific reports, 2(1), 1-6.

[53]Yin, J., Pan, S., Wu, L., Tan, L., Chen, D., Huang, S., & He, P. (2020). A self-adhesive wearable strain sensor based on a highly stretchable, tough, self-healing and ultra-sensitive ionic hydrogel. Journal of Materials Chemistry C, 8(48), 17349-17364.

[54] Yu, X., Zhang, H., Wang, Y., Fan, X., Li, Z., Zhang, X., & Liu, T. (2022). Highly stretchable, ultra-soft, and fast self-healable conductive hydrogels based on

polyaniline nanoparticles for sensitive flexible sensors. Advanced Functional Materials, 32(33), 2204366.

[55] Yuan, W., Qu, X., Lu, Y., Zhao, W., Ren, Y., Wang, Q., & Dong, X. (2021). MXene-composited highly stretchable, sensitive and durable hydrogel for flexible strain sensors. Chinese Chemical Letters, 32(6).

[56] Zhang, E., Liu, X., Liu, Y., Shi, J., Li, X., Xiong, X., & Lu, M. (2021). Highly stretchable, bionic self-healing waterborne polyurethane elastic film enabled by multiple hydrogen bonds for flexible strain sensors. Journal of Materials Chemistry A, 9(40), 23055-23071.

[57] Zhang, L. M., He, Y., Cheng, S., Sheng, H., Dai, K., Zheng, W. J., & Suo, Z. (2019). Self-healing, adhesive, and highly stretchable ionogel as a strain sensor for extremely large deformation. Small, 15(21), 1804651.

[58] Durmaz, E., Sertkaya, S., Yilmaz, H., Olgun, C., Ozcelik, O., Tozluoglu, A., & Candan, Z. (2023). Lignocellulosic bionanomaterials for biosensor applications. Micromachines, 14(7), 1450.

[59] Zhao, Y., Zhang, B., Yao, B., Qiu, Y., Peng, Z., Zhang, Y., & He, X. (2020). Hierarchically structured stretchable conductive hydrogels for high-performance wearable strain sensors and supercapacitors. Matter, 3(4), 1196-1210.

[60] Zheng, C., Yue, Y., Gan, L., Xu, X., Mei, C., & Han, J. (2019). Highly stretchable and self-healing strain sensors based on nanocellulose-supported graphene dispersed in electro-conductive hydrogels. Nanomaterials, 9(7), 937.

[61] Zhu, J., Tao, J., Yan, W., & Song, W. (2023). Pathways toward wearable and high-performance sensors based on hydrogels: toughening networks and conductive networks. National Science Review, 10(9), nwad180.

[62] Chen, H., Zhuo, F., Zhou, J., Liu, Y., Zhang, J., Dong, S., & Fu, Y. (2023). Advances in graphene-based flexible and wearable strain sensors. Chemical Engineering Journal, 464, 142576.

[63] Zhagiparova, A., Kalimuldina, G., Diaby, A. L., Abbassi, F., Ali, M. H., & Araby, S. (2023). Key factors and performance criteria of wearable strain sensors based on polymer nanocomposites. Nano Futures, 7(2), 022001.

[64] Yadav, A., Yadav, N., Wu, Y., RamaKrishna, S., & Hongyu, Z. (2023). Wearable strain sensors: state-of-the-art and future applications. Materials Advances, 4(6), 1444-1459.

[65] Sun, X., Qin, Z., Ye, L., Zhang, H., Yu, Q., Wu, X., & Yao, F. (2020). Carbon nanotubes reinforced hydrogel as flexible strain sensor with high stretchability and mechanically toughness. Chemical Engineering Journal, 382, 122832.

[66]Liu, L., Zhang, X., Xiang, D., Wu, Y., Sun, D., Shen, J., & Li, Y. (2022). Highly stretchable, sensitive and wide linear responsive fabric-based strain sensors with a self-segregated carbon nanotube (CNT)/Polydimethylsiloxane (PDMS) coating. Progress in Natural Science: Materials International, 32(1), 34-42.

[67] Dhawan, R., Singh, J., & Avti, P. K. (2024). Nanobiosensors in Healthcare Diagnosis. In Nanotechnology in Miniaturization (pp. 223-251). Springer, Cham.

[68] Ma, H., Hou, J., Xiao, X., Wan, R., Ge, G., Zheng, W., & Lu, B. (2024). Self-healing electrical bioadhesive interface for electrophysiology recording. Journal of Colloid and Interface Science, 654, 639-648.

[69] Zhao, Y., Ren, M., Shang, Y., Li, J., Wang, S., Zhai, W., & Shen, C. (2020). Ultra-sensitive and durable strain sensor with sandwich structure and excellent anti-interference ability for wearable electronic skins. Composites Science and Technology, 200, 108448.

[70] Liu, C., Kelley, S. O., & Wang, Z. (2024). Self-Healing Materials for Bioelectronic Devices. Advanced Materials, 36(35), 2401219.

[71] Wang, J., Li, L., Guo, Z. H., Pan, C., & Pu, X. (2025). Multi-crosslinked strong, tough and anti-freezing organohydrogels for flexible sensors. Nanoscale, 17(3), 1400-1410.

[72]Alam, F., Ubaid, J., Butt, H., & El-Atab, N. (2023). Easy and Fast 4d Printing of Multifunctional Shape Memory Polymers Using Vat Photopolymerization. Available at SSRN 4403824.

[73] Lan, M. H., Guan, X., Zhu, D. Y., Chen, Z. P., Liu, T., & Tang, Z. (2023). Highly elastic, self-healing, recyclable interlocking double-network liquid-free ionic conductive elastomers via facile fabrication for wearable strain sensors. ACS Applied Materials & Interfaces, 15(15), 19447-19458.

[74] Liu, S., Chen, B., Wang, Y., Wang, H., Cheng, X., Wang, H., & Du, Z. (2024). Ultrastrength High-Sensitivity Poly (acrylic acid)-Based Deep Eutectic Solvents Gel for Wearable Strain Sensing and Human Health Monitoring. ACS Applied Polymer Materials, 6(9), 5385-5393.

[75] Ma, Z., Li, H., Jing, X., Liu, Y., & Mi, H. Y. (2021). Recent advancements in self-healing composite elastomers for flexible strain sensors: Materials, healing systems, and features. Sensors and Actuators A: Physical, 329, 112800.

[76] Zou, L., Chang, B., Liu, H., Zhang, X., Shi, H., Liu, X., & Liu, C. (2022). Multiple physical bonds cross-linked strong and tough hydrogel with antibacterial ability for wearable strain sensor. ACS Applied Polymer Materials, 4(12), 9194-9205.

[77]Alam, S., Asif, A., Bibi, M., Hassan, G., Shuja, A., Shah, I. J., & Ibrahim, Z. (2025). Fabrication of self-healing strain sensor based on AgNWs and Fe2O3 nanocomposite on engineered polyurethane substrate. Applied Physics A, 131(4), 317.

[78] Dong, X. Y. (2024). Highly Stretchable, Transparent, and Adhesive Double Network Hydrogels for the Development of Wearable Strain Sensors.

[79] Kaushik, S., Soni, V., & Skotti, E. (Eds.). (2022). Nanosensors for Futuristic Smart and Intelligent Healthcare Systems. CRC Press.

[80] Liu, G., Zhang, Z., Li, Z., Guo, L., & Ning, L. (2023). 0D to 2D carbon-based materials in flexible strain sensors: recent advances and perspectives. 2D Materials, 10(2), 022002.

[81] Liao, S., Lian, X., & Wang, Y. (2021). Self-healing ionic liquid-based electronics and beyond. Chinese Journal of Polymer Science, 39(10), 1235-1245.

[82] Raman, S., & Arunagirinathan, R. S. (2022). Silver nanowires in stretchable resistive strain sensors. Nanomaterials, 12(11), 1932.

[83] Zhang, Y. (2023). Preparation and Application of Cellulose Based Sensing Materials (Doctoral dissertation, UNIVERSITY OF BRITISH COLUMBIA (Vancouver).

[84] Ma, Z., Li, H., Jing, X., Liu, Y., & Mi, H. Y. (2021). Recent advancements in self-healing composite elastomers for flexible strain sensors: Materials, healing systems, and features. Sensors and Actuators A: Physical, 329, 112800.

[85] Nam, J. W., Moon, C. H., Kim, D. H., Kim, M. H., & Park, W. H. (2024). Dynamically crosslinked poly (vinyl alcohol)/borax strain sensors for organ motion monitoring. Chemical Engineering Journal, 498, 155748.

[86] Yeasmin, R., Duy, L. T., Han, S., & Seo, H. (2020). Intrinsically Stretchable and Self-Healing Electroconductive Composites Based on Supramolecular Organic Polymer Embedded with Copper Microparticles. Advanced Electronic Materials, 6(9), 2000527.

[87] Sabet, M. (2024). Unveiling advanced self-healing mechanisms in graphene polymer composites for next-generation applications in aerospace, automotive, and electronics. Polymer-Plastics Technology and Materials, 1-28.

[88] Xu, J., Wang, H., Du, X., Cheng, X., Du, Z., & Wang, H. (2021). Self-healing, anti-freezing and highly stretchable polyurethane ionogel as ionic skin for wireless strain sensing. Chemical Engineering Journal, 426, 130724.

[89] Hang, C. Z., Zhao, X. F., Xi, S. Y., Shang, Y. H., Yuan, K. P., Yang, F., ... & Lu, H. L. (2020). Highly stretchable and self-healing strain sensors for motion detection in wireless human-machine interface. Nano Energy, 76, 105064.

[90] Su, G., Yin, S., Guo, Y., Zhao, F., Guo, Q., Zhang, X., & Yu, G. (2021). Balancing the mechanical, electronic, and self-healing properties in conductive self-healing hydrogel for wearable sensor applications. Materials Horizons, 8(6), 1795-1804.

[91] Cao, J., Sun, G., Wang, P., & Meng, C. (2024). Microstructured CNTs/Cellulose Aerogel for a Highly Sensitive Pressure Sensor. ACS Applied Materials & Interfaces, 16(40), 54652-54662.

[92] Yu, Y., Luo, Y., Guo, A., Yan, L., Wu, Y., Jiang, K., & Wang, J. (2017). Flexible and transparent strain sensors based on super-aligned carbon nanotube films. Nanoscale, 9(20), 6716-6723.

[93] Jin, Z., Li, Y., Fan, D., Tu, C., Wang, X., & Dang, S. (2023). Calibration experiment and temperature compensation method for the thermal output of electrical resistance strain gauges in health monitoring of structures. Symmetry, 15(5), 1066.

[94] Hu, C., Li, Z., Wang, Y., Gao, J., Dai, K., Zheng, G., & Guo, Z. (2017). Comparative assessment of the strain-sensing behaviors of polylactic acid nanocomposites: reduced graphene oxide or carbon nanotubes. Journal of Materials Chemistry C, 5(9), 2318-2328.

[95] Georgopoulou, A., & Clemens, F. (2020). Piezoresistive elastomer-based composite strain sensors and their applications. ACS Applied Electronic Materials, 2(7), 1826-1842.

[96] Chen, J., Zheng, J., Gao, Q., Zhang, J., Zhang, J., Omisore, O. M., & Li, H. (2018). Polydimethylsiloxane (PDMS)-based flexible resistive strain sensors for wearable applications. Applied Sciences, 8(3), 345.

[97] Munasinghe, N., Masangkay, J., & Paul, G. (2021, May). Temperature compensated 3D printed strain sensor for advanced manufacturing applications. In 2021 IEEE International Conference on Robotics and Automation (ICRA) (pp. 7006-7012). IEEE.

[98] Erdem, Ö. Derin, E., Zeibi Shirejini, S., Sagdic, K., Yilmaz, E. G., Yildiz, S., & Inci, F. (2022). Carbon-based nanomaterials and sensing tools for wearable health monitoring devices. Advanced Materials Technologies, 7(3), 2100572.

[99] Yan, T., Wu, Y., Yi, W., & Pan, Z. (2021). Recent progress on fabrication of carbon nanotube-based flexible conductive networks for resistive-type strain sensors. Sensors and Actuators A: Physical, 327, 112755.

[100] Sixt, J., Davoodi, E., Salehian, A., & Toyserkani, E. (2023). Characterization and optimization of 3D-printed, flexible vibration strain sensors with triply periodic minimal surfaces. Additive Manufacturing, 61, 103274.

[101] Ma, S., Tang, J., Yan, T., & Pan, Z. (2022). Performance of flexible strain sensors with different transition mechanisms: a review. IEEE Sensors Journal, 22(8), 7475-7498.

[102] Hia, I. L., Snyder, A. D., Turicek, J. S., Blanc, F., Patrick, J. F., & Therriault, D. (2023). Electrically conductive and 3D-printable copolymer/MWCNT nanocomposites for strain sensing. Composites Science and Technology, 232, 109850.

[103] Wu, S., Li, J., Zhang, G., Yao, Y., Li, G., Sun, R., & Wong, C. (2017). Ultrafast self-healing nanocomposites via infrared laser and their application in flexible electronics. ACS applied materials & interfaces, 9(3), 3040-3049.

[104] Vu, V. P., Sinh, L. H., & Choa, S. H. (2020). Recent Progress in Self-healing Materials for Sensor Arrays. ChemNanoMat, 6(11), 1522-1538.

[105] He, L., Shi, J., Tian, B., Zhu, H., & Wu, W. (2024). Self-healing materials for flexible and stretchable electronics. Materials Today Physics, 44, 101448.

[106] Yeasmin, R., Han, S. I., Ahn, B., & Seo, H. (2023). A Skin-like Self-healing and stretchable substrate for wearable electronics. Chemical Engineering Journal, 455, 140543.

[107] Tan, Y. J., Wu, J., Li, H., & Tee, B. C. (2018). Self-healing electronic materials for a smart and sustainable future. ACS applied materials & interfaces, 10(18), 15331-15345.

[108] Gai, Y., Li, H., & Li, Z. (2021). Self-healing functional electronic devices. Small, 17(41), 2101383.

[109] Milkin, P., Pavale, S., Soreño, Z. V., & Ionov, L. (2024). Fiber-Reinforced Flexible Self-Healing Strain Sensor with Failure-Improving Sensitivity Recovery. ACS Applied Materials & Interfaces, 16(44), 61050-61060.

[110] Zhang, Q., Liu, X., Duan, L., & Gao, G. (2019). Ultra-stretchable wearable strain sensors based on skin-inspired adhesive, tough and conductive hydrogels. Chemical Engineering Journal, 365, 10-19.

[111] Liu, S., Zheng, R., Chen, S., Wu, Y., Liu, H., Wang, P., & Liu, L. (2018). A compliant, self-adhesive and self-healing wearable hydrogel as epidermal strain sensor. Journal of Materials Chemistry C, 6(15), 4183-4190.

[112] Highly Stretchable and Self-Healing Strain Sensors Based on Nanocellulose-Supported Graphene Dispersed in Electro-Conductive Hydrogels. Nanomaterials 9.7 (2019): 937.

[113] Zhao, W., Zhou, M., Lv, L., & Fu, H. (2021). Self-healing, conductive and magnetic ZnFe2O4/MCNT/PPy ternary composite hydrogels. Journal of Alloys and Compounds, 886, 161083.

[114] Wang, M., Chen, Y., Khan, R., Liu, H., Chen, C., Chen, T., & Li, H. (2019). A fast self-healing and conductive nanocomposite hydrogel as soft strain sensor. Colloids and Surfaces A: Physicochemical and Engineering Aspects, 567, 139-149.

[115] Qu, M., Qin, Y., Xu, W., Zheng, Z., Xu, H., Schubert, D. W., & Gao, Q. (2021). Electrically conductive NBR/CB flexible composite film for ultrastretchable strain sensors: Fabrication and modeling. Applied Nanoscience, 11(2), 429-439.

[116] Tang, L., Wu, S., Qu, J., Gong, L., & Tang, J. (2020). A review of conductive hydrogel used in flexible strain sensor. Materials, 13(18), 3947.

[117] Jing, X., Li, H., Mi, H. Y., Liu, Y. J., Feng, P. Y., Tan, Y. M., & Turng, L. S. (2019). Highly transparent, stretchable, and rapid self-healing polyvinyl alcohol/cellulose nanofibril hydrogel sensors for sensitive pressure sensing and human motion detection. Sensors and Actuators B: Chemical, 295, 159-167.

[118] Zhou, J., Guo, X., Xu, Z., Wu, Q., Chen, J., Wu, J., & Huang, Z. (2020). Highly sensitive and stretchable strain sensors based on serpentine-shaped composite films for flexible electronic skin applications. Composites Science and Technology, 197, 108215.

[119] Zhang, Q., Liu, X., Duan, L., & Gao, G. (2019). Ultra-stretchable wearable strain sensors based on skin-inspired adhesive, tough and conductive hydrogels. Chemical Engineering Journal, 365, 10-19.

[120] Tang, Y., Guo, Q., Chen, Z., Zhang, X., Lu, C., Cao, J., & Zheng, Z. (2019). Scalable manufactured self-healing strain sensors based on ion-intercalated graphene nanosheets and interfacial coordination. ACS applied materials & interfaces, 11(26), 23527-23534.

[121] Lu, Y., Liu, Z., Yan, H., Peng, Q., Wang, R., Barkey, M. E., & Wujcik, E. K. (2019). Ultrastretchable conductive polymer complex as a strain sensor with a repeatable autonomous self-healing ability. ACS applied materials & interfaces, 11(22), 20453-20464.

[122] Choi, D. Y., Kim, M. H., Oh, Y. S., Jung, S. H., Jung, J. H., Sung, H. J., ... & Lee, H. M. (2017). Highly stretchable, hysteresis-free ionic liquid-based strain

sensor for precise human motion monitoring. ACS applied materials & interfaces, 9(2), 1770-1780.

[123] Wu, J., Wu, Z., Lu, X., Han, S., Yang, B. R., Gui, X., & Liu, C. (2019). Ultrastretchable and stable strain sensors based on antifreezing and self-healing ionic organohydrogels for human motion monitoring. ACS applied materials & interfaces, 11(9), 9405-9414.

[124] Fang, Y., Xu, J., Gao, F., Du, X., Du, Z., Cheng, X., & Wang, H. (2021). Self-healable and recyclable polyurethane-polyaniline hydrogel toward flexible strain sensor. Composites Part B: Engineering, 219, 108965.

[125] Li, H., Zheng, H., Tan, Y. J., Tor, S. B., & Zhou, K. (2021). Development of an ultrastretchable double-network hydrogel for flexible strain sensors. ACS Applied Materials & Interfaces, 13(11), 12814-12823.

[126] Yang, P. A., Xiang, S., Li, R., Ruan, H., Chen, D., Zhou, Z., & Liu, Z. (2022). Highly Stretchable and Sensitive Flexible Strain Sensor Based on Fe NWs/Graphene/PEDOT: PSS with a Porous Structure. International Journal of Molecular Sciences, 23(16), 8895.

[127] Yin, J., Pan, S., Wu, L., Tan, L., Chen, D., Huang, S., & He, P. (2020). A self-adhesive wearable strain sensor based on a highly stretchable, tough, self-healing and ultra-sensitive ionic hydrogel. Journal of Materials Chemistry C, 8(48), 17349-17364.

[128] Ke, T., Zhao, L., Fan, X., & Gu, H. (2023). Rapid self-healing, self-adhesive, anti-freezing, moisturizing, antibacterial and multi-stimuli-responsive PVA/starch/tea polyphenol-based composite conductive organohydrogel as flexible strain sensor. Journal of Materials Science & Technology, 135, 199-212.

[129] Feng, E., Zheng, G., Zhang, M., Li, X., Feng, G., & Cao, L. (2023). Self-healing and freezing-tolerant strain sensor based on a multipurpose organohydrogel with information recording and erasing function. Colloids and Surfaces A: Physicochemical and Engineering Aspects, 131781.

[130] Lu, L., Zhou, Y., Pan, J., Chen, T., Hu, Y., Zheng, G., & Peng, H. (2019). Design of helically double-leveled gaps for stretchable fiber strain sensor with ultralow detection limit, broad sensing range, and high repeatability. ACS applied materials & interfaces, 11(4), 4345-4352.

[131] Li, Z., Liu, P., Chen, S., Liu, S., Wang, B., Cui, E., & Liu, Y. (2024). Highly elastic, frost-resistant and antimicrobial flexible sensor inspired by ramen noodles

for human motion detection and deep learning of handwritten content. Microchemical Journal, 196, 109614.

[132] Shi, X., Lee, A., Yang, B., Gao, L., Ning, H., Huang, K., & Hu, N. (2024). A 3D cross-linked hierarchical hydrogel E-skin with sensing of touch position and pressure. Carbon, 216, 118514.

[133] Deng, Y., Yang, M., Xiao, G., & Jiang, X. (2024). Preparation of strong, tough and conductive soy protein isolate/poly (vinyl alcohol)-based hydrogel via the synergy of biomineralization and salting out. International Journal of Biological Macromolecules, 257, 128566.

[134] He, L., Ye, D., Weng, S., & Jiang, X. (2022). A high-strength, environmentally stable, self-healable, and recyclable starch/PVA organohydrogel for strain sensor. European Polymer Journal, 181, 111650.

[135] Wan, Z., Qu, R., Sun, Y., Gao, Y., Gao, G., Chen, K., & Liu, T. (2024).Physically cross-linked polyvinyl alcohol, phytic acid and glycerol hydrogels for wearable sensors with biocompatibility, antimicrobial stability and anti-freezing. European Polymer Journal, 211, 112974.

[136] Jia, M., Chen, Q., Chen, K., Zhang, X., Feng, H., Feng, C., & Zhang, D. (2024). Muscle-inspired MXene-based conductive hydrogel by magnetic induced for flexible multifunctional sensors. European Polymer Journal, 214, 113149.

[137] Pahnavar, Z., Ghaemy, M., Naji, L., & Hasantabar, V. (2024). Bio-electronic muscular soft actuator based on double network κ-Carrageenan/PVA membrane and Vulcan carbon/f-MWCNT electrode with remarkable performance. Sensors and Actuators B: Chemical, 136036.

[138] Feng, S., Guo, J., Guan, F., Sun, J., Song, X., He, J., & Yang, Q. (2023). Preparation of 3D printable polyvinyl alcohol based conductive hydrogels via incorporating k-carrageenan for flexible strain sensors. Colloids and Surfaces A: Physicochemical and Engineering Aspects, 676, 132141.

[139] Liu, Feng, et al. Liu, F., Li, J., Han, F., Ling, L., Wu, X., Zhang, G., & Wong, C. P. (2017, July). Self-healable silver nanowire-based composite for elastic strain sensor. In Chinese Materials Conference (pp. 389-397). Springer, Singapore.

[140] Jiang, D., Wang, Y., Li, B., Sun, C., Wu, Z., Yan, H., & Guo, Z. (2019). Flexible sandwich structural strain sensor based on silver nanowires decorated

with self-healing substrate. Macromolecular Materials and Engineering, 304(7), 1900074.

[141] Ma, Z., Li, H., Jing, X., Liu, Y., & Mi, H. Y. (2021). Recent advancements in self-healing composite elastomers for flexible strain sensors: materials, healing systems, and features. Sensors and Actuators A: Physical, 329, 112800.

[142] Li, Z., Qi, X., Xu, L., Lu, H., Wang, W., Jin, X., & Dong, Y. (2020). Self-repairing, large linear working range shape memory carbon nanotubes/ethylene vinyl acetate fiber strain sensor for human movement monitoring. ACS Applied Materials & Interfaces, 12(37), 42179-42192.

[143] Mehmood, A., Mubarak, N. M., Khalid, M., Walvekar, R., Abdullah, E. C., Siddiqui, M. T. H., & Mazari, S. (2020). Graphene based nanomaterials for strain sensor application—a review. Journal of Environmental Chemical Engineering, 8(3), 103743.

[144] Guo, B., Ji, X., Chen, X., Li, G., Lu, Y., & Bai, J. (2020). A highly stretchable and intrinsically self-healing strain sensor produced by 3D printing. Virtual and Physical Prototyping, 15(sup1), 520-531.

[145] Souri, H., Banerjee, H., Jusufi, A., Radacsi, N., Stokes, A. A., Park, I., & Amjadi, M. (2020). Wearable and stretchable strain sensors: materials, sensing mechanisms, and applications. Advanced Intelligent Systems, 2(8), 2000039.

[146] Hassan, G., Khan, M. U., Bae, J., & Shuja, A. (2020). Inkjet printed self-healable strain sensor based on graphene and magnetic iron oxide nano-composite on engineered polyurethane substrate. Scientific reports, 10(1), 1-12.

[147] Qi, X., Li, X., Jo, H., Bhat, K. S., Kim, S., An, J., & Lim, S. (2020). Mulberry paper-based graphene strain sensor for wearable electronics with high mechanical strength. Sensors and Actuators A: Physical, 301, 111697.

[148] Qingqing, X., Ruiyi, L., & Zaijun, L. (2024). Designing of multifunctional graphene quantum dot-polyvinyl alcohol-polyglycerol luminescent film for fluorescence detection of pH in sweat. Analytica Chimica Acta, 1292, 342224.

[149] Cong, C., Wang, R., Zhu, W., Zheng, X., Sun, F., Wang, X., & Li, X. (2025). Self-powered strain sensing devices with wireless transmission: DIW-printed conductive hydrogel electrodes featuring stretchable and self-healing properties. Journal of Colloid and Interface Science, 678, 588-598.

[150] Tanusha, D., & Badhulika, S. (2024). Comparative analysis of micro patterned PDMS-based piezoresistive pressure sensors with multifunctional strain and health monitoring applications. Sensors and Actuators A: Physical, 369, 115139.

[151] Cui, C., Qin, Y., Zeng, Y., Lu, X., Wei, E., & Xie, J. (2024). A flexible capacitive pressure sensor with dual-layer microstructure for health monitoring. Sensors and Actuators A: Physical, 377, 115709.

[152] Lu, J., Xu, L., Hazarika, D., Zhang, C., Li, J., Wu, J., & Luo, J. (2024). Piezoelectric nanogenerator enabled fully self-powered instantaneous wireless sensor system. Nano Energy, 129, 110022.

[153] Hairi, N. I. I. M., Ralib, A. A. M., Nordin, A. N., Yunos, M. F. A. M., Ming, L. L., Tung, L. H., & Samsudin, Z. (2024). Recent advance in using eco-friendly carbon-based conductive ink for printed strain sensor: A review. Cleaner Materials, 100248.

[154] Cui, X., Guo, J., Araby, S., Abbassi, F., Zhang, C., Diaby, A. L., & Meng, Q. (2022). Porous polyvinyl alcohol/graphene oxide composite film for strain sensing and energy-storage applications. Nanotechnology, 33(41), 415701.

[155] Hu, F., Yao, C., Huang, M., He, S., Liu, H., Liu, W., & Xu, W. (2024). Recyclable, healable, and stretchable thermoset shape memory polythiourethane/carbon nanotube composite with segregated conductive structure for strain sensing. Journal of Polymer Science, 62(22), 5186-5196.

[156] Delkhosh, F., Qotbi, A., Behroozi, A. H., & Vatanpour, V. (2024). Magnetron sputtering in membrane fabrication and modification: Applications in gas and water treatment. Journal of Industrial and Engineering Chemistry.

[157] Mustafa, H. A. M., & Jameel, D. A. (2021). Modeling and the main stages of spin coating process: A review. Journal of Applied Science and Technology Trends, 2(03), 91-95.

[158] Ali, A., Zhang, N., & Santos, R. M. (2023). Mineral characterization using scanning electron microscopy (SEM): a review of the fundamentals, advancements, and research directions. Applied Sciences, 13(23), 12600.

[159] Feng, W., Zheng, W., Gao, F., Chen, X., Liu, G., Hasan, T., & Hu, P. (2016). Sensitive electronic-skin strain sensor array based on the patterned two-dimensional α-In2Se3. Chemistry of Materials, 28(12), 4278-4283.

[160] Wu, J. M., Chen, C. Y., Zhang, Y., Chen, K. H., Yang, Y., Hu, Y., ... & Wang, Z. L. (2012). Ultrahigh sensitive piezotronic strain sensors based on a ZnSnO3 nanowire/microwire. ACS nano, 6(5), 4369-4374.

[161] Ukkunda, N. S., Santhoshkumar, P., Paranthaman, R., & Moses, J. A. (2024). X-ray diffraction and its emerging applications in the food industry. Critical Reviews in Food Science and Nutrition, 1-16.

[162] Baldini, G., Albini, A., Maiolino, P., & Cannata, G. (2022). An atlas for the inkjet printing of large-area tactile sensors. Sensors, 22(6), 2332.

[163] Cerdan, K., Moya, C., Van Puyvelde, P., Bruylants, G., & Brancart, J. (2022). Magnetic self-healing composites: Synthesis and applications. Molecules, 27(12), 3796.

[164] "Reserch Proposal Ultra stretchable Self-Healing Strain Sensor."

[165] Hassan, G., Khan, M. U., Bae, J., & Shuja, A. (2020). Inkjet printed self-healable strain sensor based on graphene and magnetic iron oxide nano-composite on engineered polyurethane substrate. Scientific reports, 10(1), 18234.

[166] Zhang, K., Song, C., Wang, Z., Gao, C., Wu, Y., & Liu, Y. (2020). A stretchable and self-healable organosilicon conductive nanocomposite for a reliable and sensitive strain sensor. Journal of Materials Chemistry C, 8(48), 17277-17288.

[167] Jiang, D., Wang, Y., Li, B., Sun, C., Wu, Z., Yan, H., & Guo, Z. (2019). Flexible sandwich structural strain sensor based on silver nanowires decorated with self-healing substrate. Macromolecular Materials and Engineering, 304(7), 1900074.

[168] Fang, Y., Xu, J., Gao, F., Du, X., Du, Z., Cheng, X., & Wang, H. (2021). Self-healable and recyclable polyurethane-polyaniline hydrogel toward flexible strain sensor. Composites Part B: Engineering, 219, 108965.

[169] Gupta, R., Gupta, P., Footer, C., Stenning, G. B., Darr, J. A., & Pancholi, K. (2022). Tuneable magnetic nanocomposites for remote self-healing. Scientific reports, 12(1), 10180.

[170] Tan, S., De, D., Song, W. Z., Yang, J., & Das, S. K. (2016). Survey of security advances in smart grid: A data driven approach. IEEE Communications Surveys & Tutorials, 19(1), 397-422.

[171] Yan, Y., Qian, Y., Sharif, H., & Tipper, D. (2012). A survey on cyber security for smart grid communications. IEEE communications surveys & tutorials, 14(4), 998-1010.

[172] Shinde, V. V., Wang, Y., Salek, M. F., Auad, M. L., Beckingham, L. E., & Beckingham, B. S. (2022). Material design for enhancing properties of 3D printed polymer composites for target applications. Technologies, 10(2), 45.

[173] PV, N. (2021). Comparative analysis of different control strategies in Microgrid. International Journal of Green Energy, 18(12), 1249-1262.

[174] Zieliński, J. S. (2016). Microgrids and resilience. Rynek Energii, (2), 108-110.

[175] Nishimuko, M. (2009). The role of non-governmental organisations and faith-based organisations in achieving Education for All: the case of Sierra Leone. Compare, 39(2), 281-295.

[176] Ciocarlie, G. F., Lindqvist, U., Nováczki, S., & Sanneck, H. (2013, October). Detecting anomalies in cellular networks using an ensemble method. In Proceedings of the 9th international conference on network and service management (CNSM 2013) (pp. 171-174). IEEE.

[177] Ma, C., Zhou, R., & Xie, L. (2022). Recent advances in flexible pressure/strain sensors using carbon nanotubes. International Journal of Agricultural and Biological Engineering, 15(2), 1-12.

[178] Liao, X., Zhang, Z., Liang, Q., Liao, Q., & Zhang, Y. (2017). Flexible, cuttable, and self-waterproof bending strain sensors using microcracked gold nanofilms@ paper substrate. ACS applied materials & interfaces, 9(4), 4151-4158.

[179] Gao, K., Zhang, Z., Weng, S., Zhu, H., Yu, H., & Peng, T. (2022). Review of flexible piezoresistive strain sensors in civil structural health monitoring. Applied Sciences, 12(19), 9750.

[180] Yang, P. A., Xiang, S., Li, R., Ruan, H., Chen, D., Zhou, Z., & Liu, Z. (2022). Highly stretchable and sensitive flexible strain sensor based on Fe NWs/graphene/PEDOT: PSS with a porous structure. International Journal of Molecular Sciences, 23(16), 8895.

[181] Jili, T., & Xiao, N. (2020, August). DDoS detection and protection based on cloud computing platform. In Journal of Physics: Conference Series (Vol. 1621, No. 1, p. 012005). IOP Publishing.

[182] Hassan, R. U., Khalil, S. M., Khan, S. A., Ali, S., Moon, J., Cho, D. H., & Byun, D. (2022). High-resolution, transparent, and flexible printing of polydimethylsiloxane via electrohydrodynamic jet printing for conductive electronic device applications. Polymers, 14(20), 4373.

[183] Zaheer, M. U., & Chang, S. H. (2024). Recent trend in stretchable composite sensors for wearable robot applications. Advanced Composite Materials, 33(3), 456-477.

[184] Xu, K., & Wang, C. (2024). Recent progress on wearable sensor based on nanocomposite hydrogel. Current Nanoscience, 20(2), 132-145.

[185] Kaushik, N., Singh, P., Rana, S., Sahoo, N. G., Ahmad, F., & Jamil, M. (2024). Self-Healable Electromagnetic Wave Absorbing/Shielding Materials for Stealth Technology: Current Trends and New Frontiers. Materials Today Sustainability, 100828.

[186] Han, P., Liang, S., Zou, H., & Wang, X. (2024). Structure, principle and performance of flexible conductive polymer strain sensors: a review. Journal of Materials Science: Materials in Electronics, 35(11), 775.

[187] An, Y., Wang, D., Wang, S., Xing, K., Chen, Z., Jiang, Z., & Wei, C. (2024). Fabrication and performance of multisensory flexible hydrogel toward strain, temperature, and flame sensing. ACS Applied Polymer Materials, 6(15), 9059-9068.

[188] Khan, M., Shah, L. A., Rahman, T. U., Ara, L., & Yoo, H. M. (2024). Multiple-Language-Responsive Conductive Hydrogel Composites for Flexible Strain and Epidermis Sensors. ACS Applied Polymer Materials, 6(7), 4233-4243.

[189] Chen, H., Zhuo, F., Zhou, J., Liu, Y., Zhang, J., Dong, S., & Fu, Y. (2023). Advances in graphene-based flexible and wearable strain sensors. Chemical Engineering Journal, 464, 142576.

[190] Hu, L., Chee, P. L., Sugiarto, S., Yu, Y., Shi, C., Yan, R., & Huang, W. (2023). Hydrogel-based flexible electronics. Advanced Materials, 35(14), 2205326.

[191] Chen, Y., Lu, K., Song, Y., Han, J., Yue, Y., Biswas, S. K., & Xiao, H. (2019). A skin-inspired stretchable, self-healing and electro-conductive hydrogel with a synergistic triple network for wearable strain sensors applied in human-motion detection. Nanomaterials, 9(12), 1737.

[192] Hassan, G., Sajid, M., & Choi, C. (2019). Highly sensitive and full range detectable humidity sensor using PEDOT: PSS, methyl red and graphene oxide materials. Scientific reports, 9(1), 15227.

[193] Mughal, S., Hassan, G., & Shuja, A. (2025). Fabrication of cost effective flexible resistive temperature sensor based on poly (3, 4-ethylenedioxythiophene) polystyrene sulfonate (PEDOT: PSS) via all printed technologies. Journal of Materials Science: Materials in Electronics, 36(5), 340.

[194] Hassan, G., Bae, J., Hassan, A., Ali, S., Lee, C. H., & Choi, Y. (2018). Ink-jet printed stretchable strain sensor based on graphene/ZnO composite on micro-random ridged PDMS substrate. Composites Part A: Applied Science and Manufacturing, 107, 519-528.

[195] Asif, A., Bibi, M., Hassan, G., Shuja, A., Ahmad, H., Alam, S., & Ibrahim, Z. (2024). Highly sensitive strain sensor based on ZnO nanofiber mat for medical applications. Journal of Materials Science: Materials in Electronics, 35(18), 1227.

[196] Xu, Q., Wu, Z., Zhao, W., He, M., Guo, N., Weng, L., & El-Bahy, Z. M. (2023). Strategies in the preparation of conductive polyvinyl alcohol hydrogels for applications in flexible strain sensors, flexible supercapacitors, and triboelectric nanogenerator sensors: an overview. Advanced Composites and Hybrid Materials, 6(6), 203.

[197] Huang, C., Jia, X., Wang, D., Sun, X., Liang, Q., Tian, R., & Song, H. (2024). Stretchable ionogels: Recent advances in design, toughening mechanisms, material properties and wearable devices applications. Chemical Engineering Journal, 151850.

[198] Sanjanwala, D., Londhe, V., Trivedi, R., Bonde, S., Sawarkar, S., Kale, V., & Patravale, V. (2024). Polysaccharide-based hydrogels for medical devices, implants and tissue engineering: A review. International Journal of Biological Macromolecules, 256, 128488.

[199] Xie, H., Wang, Z., Wang, R., Chen, Q., Yu, A., & Lu, A. (2024). Self-healing, injectable hydrogel dressing for monitoring and therapy of diabetic wound. Advanced Functional Materials, 34(36), 2401209.

[200] Zhu, N., Yang, B., Li, S., Yang, H., Miao, Y., Cong, Y., & Fu, J. (2022). Dynamic and structural studies on synergetic energy dissipation mechanisms of single-, double-, and triple-network hydrogels sequentially crosslinked by multiple non-covalent interactions. Polymer, 250, 124868.

[201] Yang, Y., Yang, Y., Cao, Y., Wang, X., Chen, Y., Liu, H., & Wu, D. (2021). Anti-freezing, resilient and tough hydrogels for sensitive and large-range strain and pressure sensors. Chemical Engineering Journal, 403, 126431.

[202] Li, J., Ding, Q., Wang, H., Wu, Z., Gui, X., Li, C., & Wu, J. (2023). Engineering smart composite hydrogels for wearable disease monitoring. Nano-micro letters, 15(1), 105.

[203] Wang, X., Ji, H., Gao, L., Hao, R., Shi, Y., Yang, J., & Chen, J. (2024). Wearable hydrogel-based health monitoring systems: A new paradigm for health monitoring.Chemical Engineering Journal, 495, 153382.

[204] De Mulatier, S., Nasreldin, M., Delattre, R., Ramuz, M., & Djenizian, T. (2018). Electronic circuits integration in textiles for data processing in wearable technologies. Advanced Materials Technologies, 3(10), 1700320.

[205] Akindoyo, J. O., Ismail, N. H., & Mariatti, M. (2019). Performance of poly (vinyl alcohol) nanocomposite reinforced with hybrid TEMPO mediated cellulose-graphene filler. Polymer Testing, 80, 106140.

[206] Xie, X. L., Mai, Y. W., & Zhou, X. P. (2005). Dispersion and alignment of carbon nanotubes in polymer matrix: a review. Materials science and engineering: R: Reports, 49(4), 89-112.

[207] Chen, Y., Zhang, X., & Lu, C. (2024). Flexible piezoelectric materials and strain sensors for wearable electronics and artificial intelligence applications. Chemical Science.

[208] Liu, P., Yao, D., Lu, C., Gao, X., & Dong, P. (2024). Highly sensitive strain sensors based on PVA hydrogels with a conductive surface layer of graphene. Journal of Materials Science: Materials in Electronics, 35(2), 97.

[209] Jiao, Y., Lu, Y., Lu, K., Yue, Y., Xu, X., Xiao, H., & Han, J. (2021). Highly stretchable and self-healing cellulose nanofiber-mediated conductive hydrogel towards strain sensing application. Journal of Colloid and Interface Science, 597, 171-181.

[210] Zheng, Y., Li, Y., Wang, L., Xu, H., & Han, W. (2024). A wearable strain sensor based on self-healable MXene/PVA hydrogel for bodily motion detection. Microelectronic Engineering, 291, 112197.

[211] Ibrahim, Z., Hassan, G., Alatawi, A. A., Alwageed, H. S., & Asif, A. (2025). Development of wearable self-healable strain sensor utilizing nano-composite materials for advanced sensing applications. Journal of Materials Science: Materials in Electronics, 36(2), 173.

[212] Hassan, G., Khan, M. U., Bae, J., & Shuja, A. (2020). Inkjet printed self-healable strain sensor based on graphene and magnetic iron oxide nano-composite on engineered polyurethane substrate. Scientific reports, 10(1), 18234.

[213] Sun, H., Fang, X., Fang, Z., Zhao, L., Tian, B., Verma, P., & Jiang, Z. (2022). An ultrasensitive and stretchable strain sensor based on a microcrack structure for motion monitoring. Microsystems & nanoengineering, 8(1), 111.

[214] Liu, X., Shi, H., Song, F., Yang, W., Yang, B., Ding, D., & Zhang, F. (2024). A highly sensitive and anti-freezing conductive strain sensor based on polypyrrole/cellulose nanofiber crosslinked polyvinyl alcohol hydrogel for human motion detection. International Journal of Biological Macromolecules, 257, 128800.

[215] Wu, Z., Liu, X., Xu, Q., Zhang, L., Abdou, S. N., Ibrahim, M. M., & Guo, Z. (2024). Poly (vinyl alcohol)/polyacrylamide double-network ionic conductive hydrogel strain sensor with high sensitivity and high elongation at break. Journal of Polymer Science, 62(20), 4599-4611.

[216] Wang, Z., Li, N., Yang, X., Zhang, Z., Zhang, H., & Cui, X. (2024). Thermogalvanic hydrogel-based e-skin for self-powered on-body dual-modal temperature and strain sensing. Microsystems & Nanoengineering, 10(1), 55.

[217] Abbas, Z., Hassan, G., Khan, M. U., Abbas, H., Ahmad, B., Shuja, A., & Choi, C. (2025). Polyurethane packed graphene-coated spider silk by dip-casting for a highly stretchable strain sensor. Journal of Materials Chemistry B, 13(10), 3437-3447.

[218] Alam, S., Asif, A., Bibi, M., Hassan, G., Shuja, A., Shah, I. J., & Ibrahim, Z. (2025). Fabrication of self-healing strain sensor based on AgNWs and Fe2O3

nanocomposite on engineered polyurethane substrate. Applied Physics A, 131(4), 317.

[219] Ghemari, Z., Bendaikha, A., Belkhiri, S., & Saad, S. (2025). Fabrication of Flexible Resistive Pressure Sensors Using Graphene/Polydimethylsiloxane Composites. Transactions on Electrical and Electronic Materials, 1-22.

[220] Zhao, Y., Tao, X., Li, X., & Zhang, T. (2020). Novel self-initiating UV-curable acrylate monomers. Journal of Applied Polymer Science, 137(44), 49356.

[221] Senol, S., & Akyol, E. (2018). Synthesis and characterization of hydrogels based on poly (2-hydroxyethyl methacrylate) for drug delivery under UV irradiation. Journal of materials science, 53, 14953-14963.

[222] Aubry, B., Dumur, F., Lansalot, M., Bourgeat-Lami, E., Lacote, E., & Lalevée, J. (2022). Development of Water-Soluble Type I Photoinitiators for Hydrogel Synthesis. Macromol, 2(1), 131-140.

[223] Cong, C., Wang, R., Zhu, W., Zheng, X., Sun, F., Wang, X., & Li, X. (2025). Self-powered strain sensing devices with wireless transmission: DIW-printed conductive hydrogel electrodes featuring stretchable and self-healing properties. Journal of Colloid and Interface Science, 678, 588-598.

[224] Chen, R., Wang, L., Ji, D., Luo, M., Zhang, Z., Zhao, G., & Zhu, Y. (2025). Highly stretchable, conductive, and self-adhesive starch-based hydrogel for high-performance flexible electronic devices. Carbohydrate Polymers, 352, 123220.

[225] Gu, Z., Ma, R., Chen, X., Lin, Z., Yang, Y., Tan, B., & Chen, T. (2025). Polyvinyl alcohol modified plant fiber hydrogel pressure and strain dual-model sensors for biomedical signal detection. Advanced Composites and Hybrid Materials, 8(2), 1-15.

[226] Zhang, Y., Deng, K., Shen, T., Huang, Y., Xu, Z., Zhang, J., & Wu, D. (2025). Hollow fiber-based strain sensors with desirable modulus and sensitivity at effective deformation for dexterous electroelastomer cylindrical actuator. Microsystems & Nanoengineering, 11(1), 34.